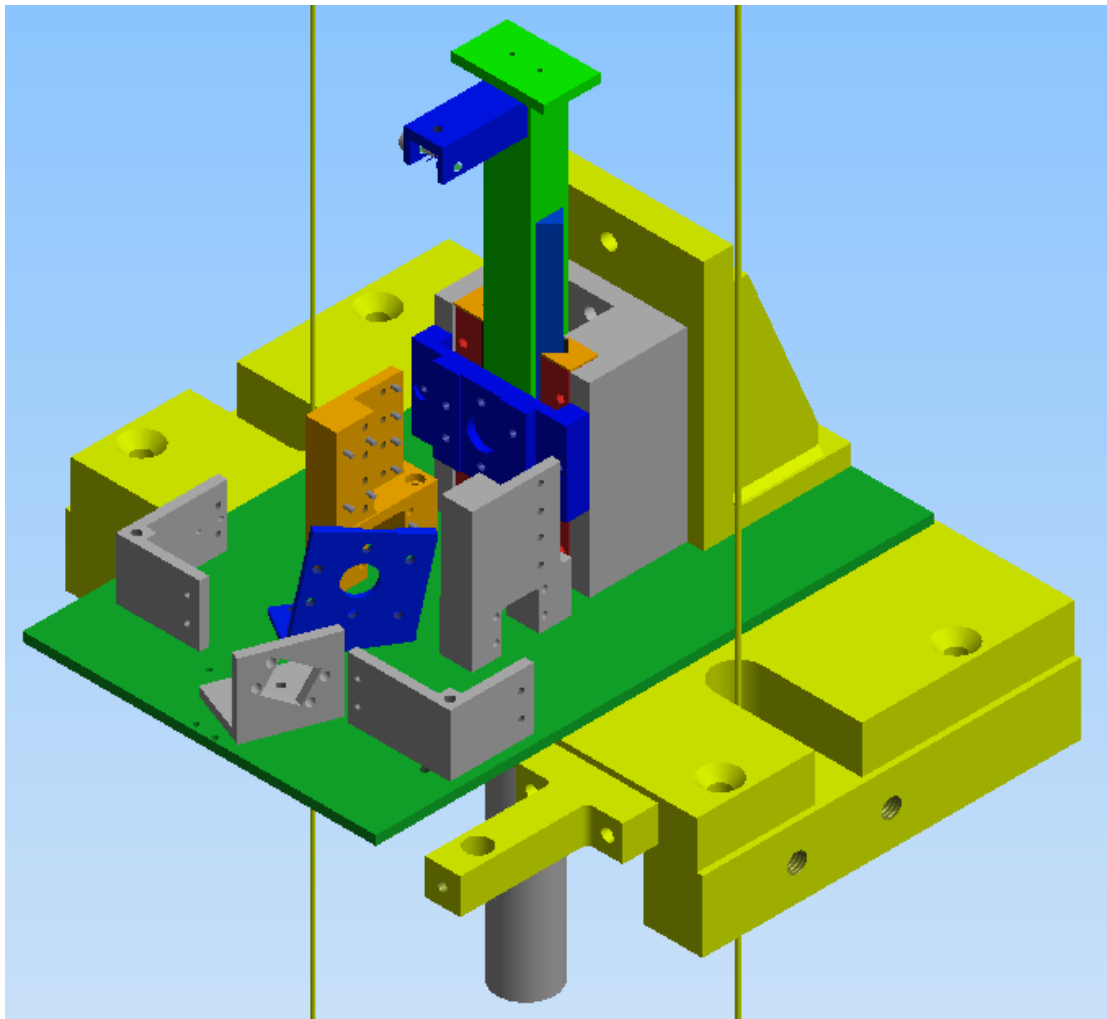


Design of a Dynamic IR-TRACC Test Set-up

A Thesis for Mechanical Engineering



10-01-2019

The Hague University of Applied Sciences, Faculty of Technology, Innovation & Society

Written by Daniël Leffelaar, Mechanical Engineering, 14142600

Internship performed at Humanetics Europe GmbH, Delft Office

Graduation Spervisor: Sarah Panahkhahi

Company Supervisor: Kees Waagmeester

Summary

This document entails the activities performed by Daniël Leffelaar during his graduation period at Humanetics Europe GmbH in Delft. The goal of the project was to create a test set-up with which the behavior of measurement instruments under dynamic circumstances could be evaluated. This was done by first compiling a list of relevant instruments supported by Humanetics. Secondly the circumstances to which the instruments would need to be exposed to were determined by analyzing test results of a test provided by Humanetics, and a means of replicating them was created. Next suggested displacements were formed based on results from certification tests. Lastly interfaces were created for each instrument, which could facilitate the desired movement.

Acknowledgements

Firstly I would like to thank my colleagues at Humanetics, Kees Waagmeester and Bernard Been, for both their assistance and understanding over the course of the project.

My thanks also goes out to my Supervisor Sarah Panahkahi for her willingness to accommodate her students, and her advice over the course of the graduation.

Lastly I would like to thank my parents for being a positive influence over the course of my life, and especially the final year of my education.

List of Abbreviations

Abbreviation	Stands for
IR-TRACC	Infra Red Telescopic Rod for the Assessment of Chest Compression
GmbH	Gesellschaft mit beschränkter Haftung
DAS	Data Acquisition System
THOR	Test Device for Human Occupant Restraint
EUROSID-II	European Side Impact Dummy, second generation
LCS	Local Coordinate System
UTS	Upper Thoracic Spine
LTS	Lower Thoracic Spine
LS	Lower Spine
TCS	Test Coordinate System

List of Figures

Figure 1: Locations of Humanetics' offices around the world (Humanetics ATD, n.d.)	8
Figure 2: Left top: 2D IR-TRACC (Infra-Red deflection measurement sensor), Left bottom: Digital 3D IR-TRACC, Right: Static 3D verification rig suitable for all 3D IR-TRACCs	9
Figure 3: Try-out of a dynamic test set-up. Left: ES2 rib unit with parallel mounted IR-TRACC, Right: Drop tower equipment (total height 6.2 m)	10
Figure 4: Dynamic test set-up for constant velocities (Wahl, 2016)	10
Figure 5: Principle of the spherical coordinate system (Technical Committee ISO/TC 22, 2018)	13
Figure 6: Coordinate system used in 3D IR-TRACCs (Technical Committee ISO/TC 22, 2018)	13
Figure 7: Location of the Lower Thorax 3D-IRTRACC in a THOR dummy	14
Figure 8: Extended IR-TRACC (1D)	15
Figure 9: IR sensor of an IR-TRACC and its mounting components	15
Figure 10: IR LED of an IR-TRACC and its mounting component	15
Figure 11: IR-TRACC calibration output (Been, 2016)	16
Figure 12: Various IR-TRACC models for 1D, 2D and 3D measurements. For the 3D models, first 3 right sided models are shown, followed by a left-sided model for the upper thorax. Finally the digital (476-series) versions of the lower right and upper right are displayed. The left-sided models are obtained by “inverting” the right-sided models in a similar fashion	18
Figure 13: Situation 0. The car has made contact with the pole, but the dummy is not yet undergoing deformation (Euro NCAP, 2015)	20
Figure 14: Situation 1. The dummy has made contact with the airbag and door and is being compressed (Euro NCAP, 2015)	20
Figure 15: Situation 2. The dummy's direction of movement has been reversed and the compression is now decreasing instead of increasing (Euro NCAP, 2015)	20
Figure 16: Euro NCAP Oblique Pole Impact set-up (Euro NCAP, 2017)	20
Figure 17: Excerpt from a crash test, the complete graph can be found in Appendix I: Crash test graph. The dashed box encloses the area of interest	21
Figure 18: In-dummy global coordinate system (ISO 21002)	21
Figure 19: Eurosid-2 Dummy	22
Figure 20: Eurosid-2 rib-unit	22
Figure 21: Velocity and displacement per component of the ES-2 Rib-unit	23
Figure 22: ES-2 rib-unit impact setup	23
Figure 23: In-dummy movement and sinusoid imposed	25
Figure 24: Effects of the impact duration and mass of the system on the spring rate	26
Figure 25: Free body diagram of the set-up	27
Figure 26: Comparison of expected velocities	28
Figure 27: Result of drop height on the displacement for various drop masses	29
Figure 28: Buckle risk of compression springs (Atlas Coevorden, -)	31
Figure 29: Distance between the drop cables, top of the drop tower	34
Figure 30: Sketch of the parallel sliding setup, side view	35
Figure 31: Single sliding bearing, front	36
Figure 32: Single sliding bearing, section view	36
Figure 33: Two M and V guidways in a closed layout, taken out of an EuroSID-2 dummy	37
Figure 34: schematic of an M and V guidway, divided by an angled needle cage (Egis-SA, 2018)	37
Figure 35: Parallelism of the M and V guidways (Egis-SA, 2018)	37
Figure 36: Chosen slider mechanism, extended	38

Figure 37: Chosen slider mechanism, compressed.....	38
Figure 38: Chosen sliding mechanism, on drop tower table.....	38
Figure 39: Location of the UTS, LTS and LS on the spine of a 50M THOR dummy	39
Figure 40: Position of the LCS for a 2D IR-TRACC.....	39
Figure 41: Dimensions of the foot (and LCS) of the IF-367 (above) and IF-368 (below)	41
Figure 42: 2D variant overlap of boltholes	42
Figure 43: 2D adapter lay-out with non-coinciding LCS.....	42
Figure 44: Vertical dual 2D mounting solution	42
Figure 45: Mounting location of the IF-372	43
Figure 46: Adapter for the IF-372, or Q10 variant	43
Figure 47: IR-TRACC reduction to 1D on the 472-3570	44
Figure 48: 472-3570 bottom end	44
Figure 49: 1D reduction concept.....	45
Figure 50: 1D reduction concept with abdomen variant installed	45
Figure 51: 1D reduction concept with 2D variant installed	45
Figure 52: Vertical multi-mounting solution, main part	46
Figure 53: Multi-mounting solution, main part with 2D adapter	46
Figure 54: Vertical multi-mounting solution, opposite part	46
Figure 55: Vertical multi-mounting solution, both parts and central plane	46
Figure 56: Multi-mounting adapter, 2D adapter	46
Figure 57: Positioning of Multi-mounting adapter in the set-up.....	47
Figure 58: One of the opposite walls of the U-shaped adapter.....	48
Figure 59: Apparent fit of a 2D IR-TRACC	48
Figure 60: Collision of a 2D IR-TRACC with a centering pin	48
Figure 61: Mounting of the lower and digital upper thorax variants, the blue line indicates the shared axis of displacement	49
Figure 62: Distance between the LCS and the edge of the foot of digital thorax variants (476-series)	49
Figure 63: 2D vertical adapter mounted on the sliding mechanism.....	49
Figure 64: Compatibility with digital variants	49
Figure 65: Local axis of the IF-369 (left) 472-4730-2 (right) (ISO 21002).....	50
Figure 66: Decomposition of the displacement.....	52
Figure 67: Addition of IR-TRACC length and rotation	52
Figure 68: IR-TRACC placement in the set-up Coordinate System	52
Figure 69: Decomposed approach for an abdomen IR-TRACC	53
Figure 70: Abdomen IR-TRACC adapter, oblique	54
Figure 71: 2-in-1 thorax IR-TRACC adapter	55
Figure 72: Distances between the mounting positions and their shared center	55
Figure 73: Displacement tool: Female Thorax	56
Figure 74: Angular symmetry of the Thorax displacement tool	56
Figure 75: Z-axis rotation for 70mm displacement, 35 mm offsets.....	56
Figure 76: Z-axis rotation for 60mm displacement, 35 mm offsets.....	56
Figure 77: Vertical adapter for oblique displacements.....	57
Figure 78: Slider and baseplate.....	58
Figure 79: 3mm dowel pin	58
Figure 80: Distance between tower mount and impact point.....	59
Figure 81: Available space for the sensor (section view of the slider unit on the table)	59
Figure 82: Position of the UCS origin of the 2D IR-TRACCs and male thorax IR-TRACCs.....	60

Figure 83: Position of the 2D-Oblique adapter (red) and male thorax adapter (Blue) relative to the TCS origin (on the green plate)	60
<i>Figure 84: Vertical displacement adapter and Q10 adapter, mounted</i>	60
Figure 85: Multi-variant adapter with shared coordinate	60
Figure 86: Location of the origin of the Test Coordinate System (TCS).....	61
Figure 87: Left top: 2D IRTRACC (Infra-Red deflection measurement sensor), Left bottom: 3D IRTRACC, Right: Static 3D verification rig suitable for all 3D IRTRACCs.	70
Figure 88: Try-out dynamic test set-up, Left: ES2 rib unit with parallel mounted IRTRACC, Right: Drop tower equipment (total height 6.2 m).....	71

Table of Contents

Summary	1
Acknowledgements.....	1
List of Abbreviations	2
List of Figures	3
1 Introduction	8
1.1 Company background	8
1.2 Problem definition	9
1.3 The goal.....	11
1.4 List of requirements.....	11
1.5 Research questions	12
2. The IR-TRACC.....	13
2.1 Operation of the IR-TRACC.....	13
2.2 IR-TRACC variations.....	16
3. Desired behavior	19
3.1 Crash test behavior	19
3.2 In-dummy movement	21
3.3 Drop tower behavior.....	22
3.4 General behavior of the system.....	24
3.5 Achieving the desired behavior	27
3.6 Spring design.....	30
4. Measurement of movement.....	32
4.1 Reference measurement	32
Eurosid-2 Linear Potentiometer.....	32
4.2 Spring/guidance setup	34
4.2.1 Double spring/sliding bearing.....	35
4.2.2 Single spring, sliding bearing.....	36
4.2.3 Needle roller bearing	37
5. IR-TRACC placement	39
5.1 Differences between the variations.....	39
5.1.2 2D-variant unification	41
5.2 Vertical displacement	44
5.2.1 Reduction to 1D	44
5.2.2 Multi-adapter mounting	46

5.2.3	Mirrored adapters.....	48
5.3	Oblique displacement.....	50
5.3.1	Thorax IR-TRACC placement.....	55
5.3.2	2D IR-TRACCs.....	57
6.	Final concept.....	58
6.1	Complete design.....	58
6.2	Impact conditions.....	62
7.	Conclusion.....	64
8.	Recommendations.....	66
9.	Competences.....	67
	References.....	69
	Appendix I: Original assignment.....	70
1.	The Assignment: Design of a dynamic IRTACC test setup.....	70
1.1	Background.....	70
1.2	Thesis objective.....	71
1.3	Issue and Goal.....	72
1.4	Boundaries.....	72
1.5	The final product:.....	72
	Appendix II: Crash test graph.....	73
	Appendix III: Eurosid-2 test data.....	74
	Appendix IV: Mounting dimensions.....	77
	Appendix V: Excerpt from a manual from Atlas Coevoerden.....	82
	Appendix V: Displacement tools.....	83
	Appendix VI: IR-TRACC Origin locations.....	84
	Appendix VII: Competentie-niveaus.....	85

1 Introduction

This chapter explains some of the background of the project. Firstly, some information about the company at which the internship was conducted will be given, subsequently the background of the assignment will be given, and afterwards the goals of the assignment will be listed.

1.1 Company background

Humanetics is the world's leading supplier in the design and manufacture of sophisticated crash test dummies, associated technical support and laboratory services, development and supply of finite element software dummy models for computerized crash test simulations and specialties in static and dynamic strain measurements. Figure 1 shows the location of all offices and factories of Humanetics.



Figure 1: Locations of Humanetics' offices around the world (Humanetics ATD, n.d.)

Humanetics Europe was founded in 2001 in order to provide a better presence and support for the European market of the car safety area. Humanetics Europe is considered to be one of the most important suppliers of the automotive industry in the car safety area with products like crash-test dummies (ATD) and sensors as well as special instrumentations for ATD's.

Humanetics Europe is not only responsible for the products of the Humanetics group but also for a range of selected products of other manufacturers within the crash-test and corresponding product support market. The products and services are readily available to the European suppliers and manufacturers of the car safety industry within most European countries.

Humanetics Europe also supports the Humanetics distributors in their respective countries with an extensive service package. This includes service, training and technical support for crash-test dummies, force sensors and accelerometers as well as further measures.

1.2 Problem definition

In Crash dummies the deformation of the ribs and the abdomen is commonly measured with an IR-TRACC (Infra-Red Telescopic Rod for the Assessment of Chest Compression). These sensors are often used in combination with one or two angular potentiometers to obtain 2D or 3D measurements results. Besides the current static calibration (ISO/PRF TS 21476) and the 2D or 3D zero-position verification (ISO 21002 and Figure 2), there is a need for a dynamic verification test that mimics the in-dummy measurement conditions. These voices originate not only from Humanetics, but also from the International Organization for Standardization (ISO). This due to more alternatives to IR-TRACC entering the market recently with no standards available to compare them according to.



Figure 2: Left top: 2D IR-TRACC (Infra-Red deflection measurement sensor), Left bottom: Digital 3D IR-TRACC, Right: Static 3D verification rig suitable for all 3D IR-TRACCs.

Previously a try-out of a dynamic IR-TRACC verification test was created by mounting the IR-TRACCs on a linear guided ES-2 rib unit that is impacted by the drop tower with a guided impactor mass (Figure 3).

In 2016 a preliminary test set-up was created which used a linear impactor to displace 3 rib deflection measurement devices with a constant velocity (Figure 4). This set-up however it was found to have multiple issues (Wahl, 2016).

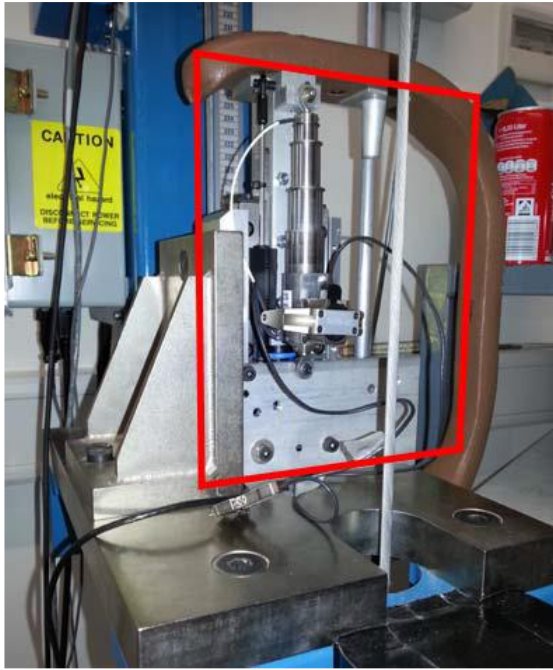
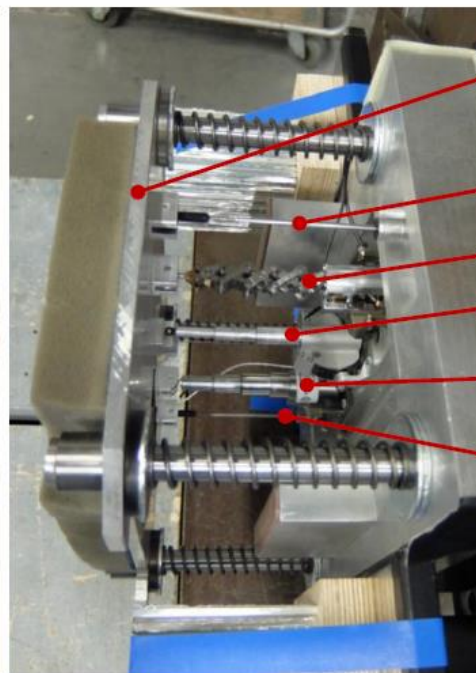
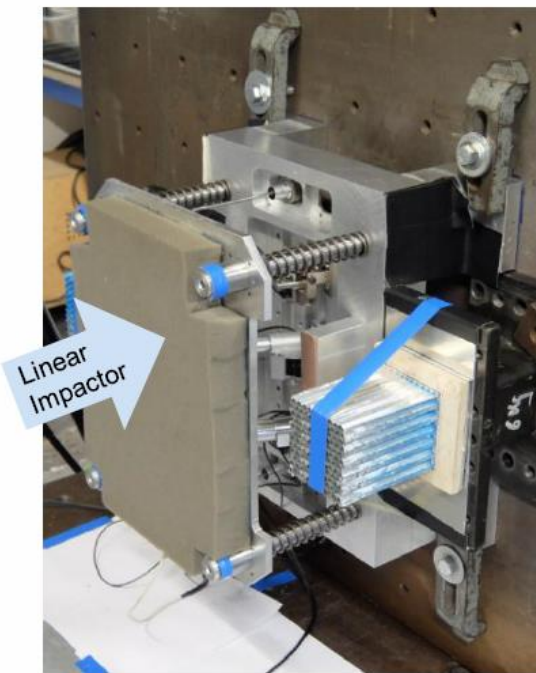


Figure 3: Try-out of a dynamic test set-up. Left: ES2 rib unit with parallel mounted IR-TRACC, Right: Drop tower equipment (total height 6.2 m).



- Ball bearing guided Impactor Plate
- Upper Linear Potentiometer
- S-Track
- Multi-dim. RDS
- 2D-IRTRACC
- Lower Linear Potentiometer

Figure 4: Dynamic test set-up for constant velocities (Wahl, 2016)

1.3 The goal

The objective of this research is to design a dynamic test set-up that can be used on the Thorax drop tower test equipment to test several IR-TRACCs. This set-up will need to be detachable from the drop rig, guarantee the safety of the IR-TRACC being tested and be suitable for use with the commonly used IR-TRACCs by Humanetics.

The basic principle of the test set-up is that it will be impacted by a mass from a predetermined height, which in turn will induce a displacement on the mounted IR-TRACC. By comparing the measurements made by the IR-TRACC to a build-in reference measurement device the accuracy of the IR-TRACC in a dynamic situation can be determined. The dynamic situation in which it is desirable to verify the behavior of the IR-TRACCs will need to be defined, as well as how this situation will be simulated within the drop tower.

1.4 List of requirements

Below in Table 1 the list of requirements are detailed. These requirements have been taken as guidelines of the design of the test-setup. When it is necessary to deviate from these requirements for technical or practical reasons, this decision will need to be made in deliberation with the client.

Table 1: List of Requirements

Nr.	Name	Description	Critical value	Validation method
1	Deceleration	The IR-TRACC needs to be able to experience the same acceleration as if it were used in an actual test	100 G	Calculations
2	Impact speed	The impactor of the drop tower with which the test set-up will be used can achieve a certain impact speed. Therefore the test set-up should be capable of withstanding this speed	8 m/s	Calculation based on the required drop height & occurring forces on impact
3	IR-TRACC stroke	Due to the impact the IR-TRACC will be displaced. The amount of required displacement will vary with each test and sensor, but the test set-up should be capable of providing a certain range of movement.	>100 mm	Measurement in the CAD-model
4	Compatibility	Humanetics has a wide range of IR-TRACCs, and the test set-up should be compatible with most of these	Yes	Verification of interfacing compatibility by the client

Nr.	Name	Description	Critical value	Validation method
5	Security	An IR-TRACC is an expensive instrument that requires a lot of time to be calibrated. Therefore it is imperative that any test the IR-TRACC is subjected to does not risk any damage to it.	Yes	Mechanical stop provision
6	Removability	The drop tower will not be used solely for the IR-TRACC verification test. As such the set-up will need to be easily removable from the drop-tower and capable of being stored on a shelf.	Yes	Analysis of (dis)mounting procedures
7	Accuracy	The test set-up will be moved and impacted often. In order to preserve the validity of the performed tests the set-up will need to be resistant to bumping and small drops. Also no meaningful deformation may occur between the origin of the IR-TRACCs internal coordinate system and the measured point.	<0.1mm	Review of Design

1.5 Research questions

In order to come up with a proper solution, it is important to realize the extent of the question being asked. To this purpose the following main- and sub-questions have been formed:

Main question:

- **How can Humanetics verify the accuracy of their IR-TRACCs in a dynamic situation?**

Sub questions:

1. What are the basic operating principles of an IR-TRACC?
2. What variations of IR-TRACC are in use and what are the differences between them?
3. What is the characteristic behavior of an in-dummy IR-TRACC during a car crash test?
4. How can this behavior be simulated in a controlled environment?
5. What will the movement of an IR-TRACC be compared to?
6. How can the different IR-TRACCs be mounted on the test set-up?
7. What further research can be done in order to improve both the accuracy and usability of the proposed test set-up?

2. The IR-TRACC

This chapter is dedicated to the IR-TRACC. It explains what it is, how it works, and how it is currently used. It also contains a list of variants currently supported by Humanetics.

2.1 Operation of the IR-TRACC

IR-TRACC is an abbreviation for Infra-Red Telescoping Rod for the Assessment of Chest Compression. It is an instrument used by the automotive industry in order to measure the deformation of crash test dummies. It is capable of high precision measurements ($\pm 0.1\text{mm}$ with a sample frequency up to 40000 Hz) in both car crash tests and sled tests. When used in conjunction with angular sensors the deformation can be determined in either 2D or 3D by using a (local) spherical coordinate system. In the figures below this is shown for a 3D IR-TRACC. 2D and 1D IR-TRACCs operate under the same principle but with either 1 or no angular rotations.

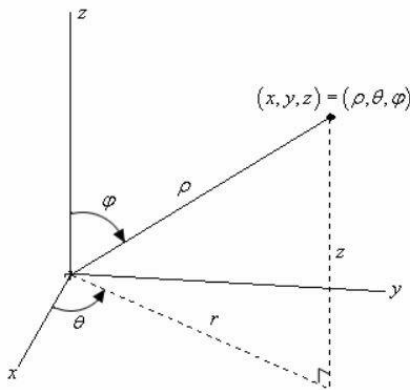


Figure 5: Principle of the spherical coordinate system (Technical Committee ISO/TC 22, 2018)

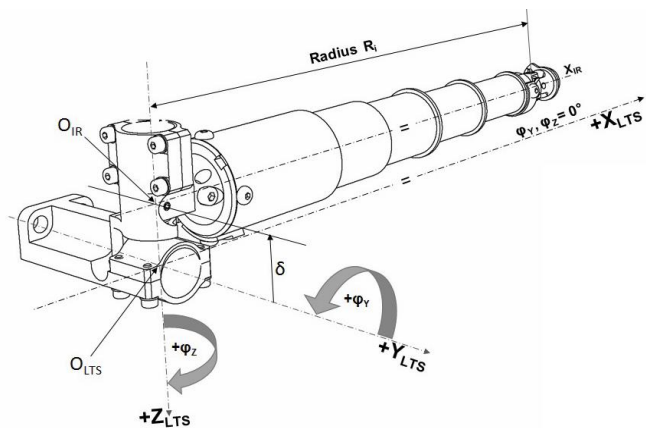


Figure 6: Coordinate system used in 3D IR-TRACCs (Technical Committee ISO/TC 22, 2018)

The coordinate system with which the IR-TRACC determines its position is known as the Spherical Coordinate System or 3D Global Coordinate System. It is defined by an initial rotation about the Y-axis, followed by a second rotation along the new Z-axis (or Z') (measured by the angular potentiometers in the IR-TRACC), and finalized by a distance R, measured from the origin by the IR-TRACC. The difference between the initial and compressed position, or deformation, can then be used to assess the risk of injury to the car occupant during an actual crash. In Figure 7 the location of a lower thorax IR-TRACC in a male THOR dummy is shown. This dummy has been designed for use in frontal crash tests, hence the orientation of the IR-TRACC. The conventions for working with multiple coordinate systems in a THOR-dummy are defined in ISO 21002.

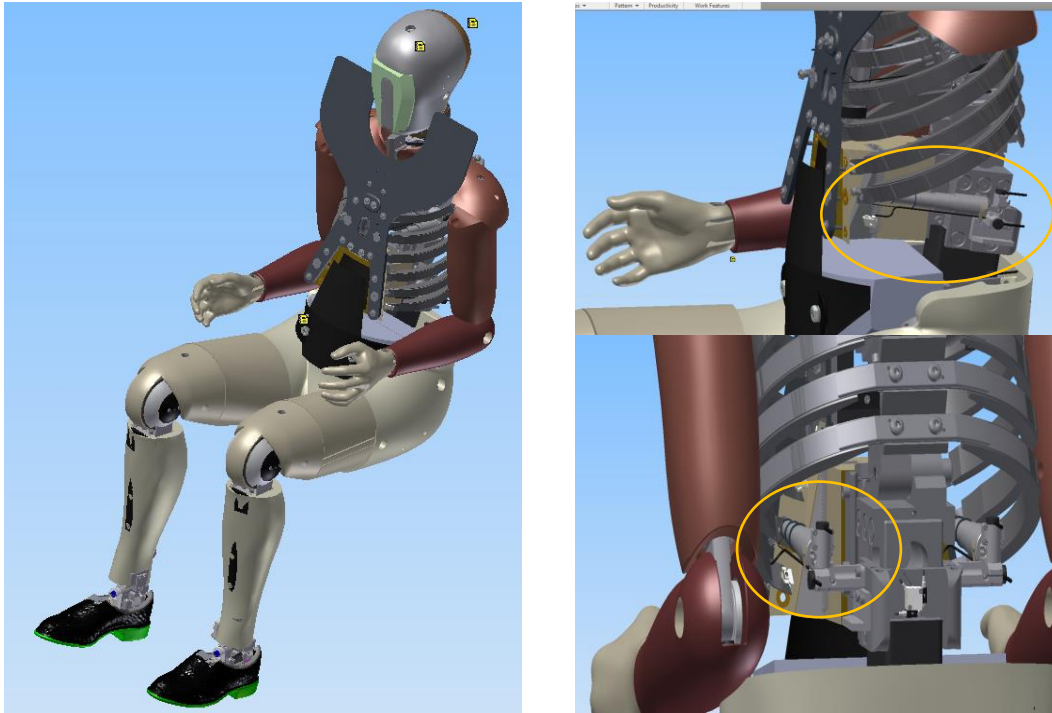


Figure 7: Location of the Lower Thorax 3D-IRTRACC in a THOR dummy

The IR-TRACC itself consists of a telescopic rod (**Error! Reference source not found.**Figure 8) with an infrared phototransistor on the inside of the larger base (Figure 9) and an infrared LED on the inside at the smaller tip (Figure 10).



Figure 8: Extended IR-TRACC (1D)

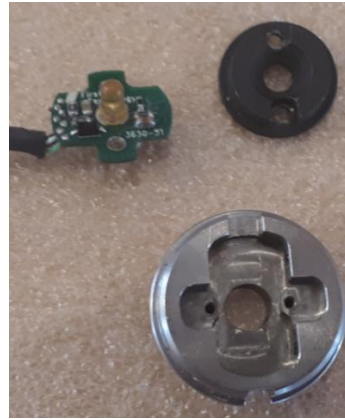


Figure 9: IR sensor of an IR-TRACC and its mounting components



Figure 10: IR LED of an IR-TRACC and its mounting component

When the instrument is in use, the LED will continuously emit infrared radiation which the phototransistor will detect. Based on the distance between the LED and phototransistor the intensity of the beams reaching the phototransistor will become either stronger (compression) or weaker (elongation):

The distance between the emitter and transistor is inversely proportional to the intensity of the beams reaching the transistor. The intensity of the beams reaching the transistor in turn are proportional to the conductivity of the transistor. Combining these two relationships tells us that the distance between the sensor and transistor is proportional to the inverse of the square root of the strength of the electrical signal. This translates to the following equation:

$$d = C * U_{IR}^{-0.5} \quad (1)$$

Where d stands for the distance in millimeters, U_{IR} the phototransistor output voltage and C the calibration factor, which is determined during calibration and is expressed in mm/V. With this equation a linear output (the distance d) can be obtained from a non-linear signal (the voltage U_{IR}). The effect of this can be seen in Figure 11.

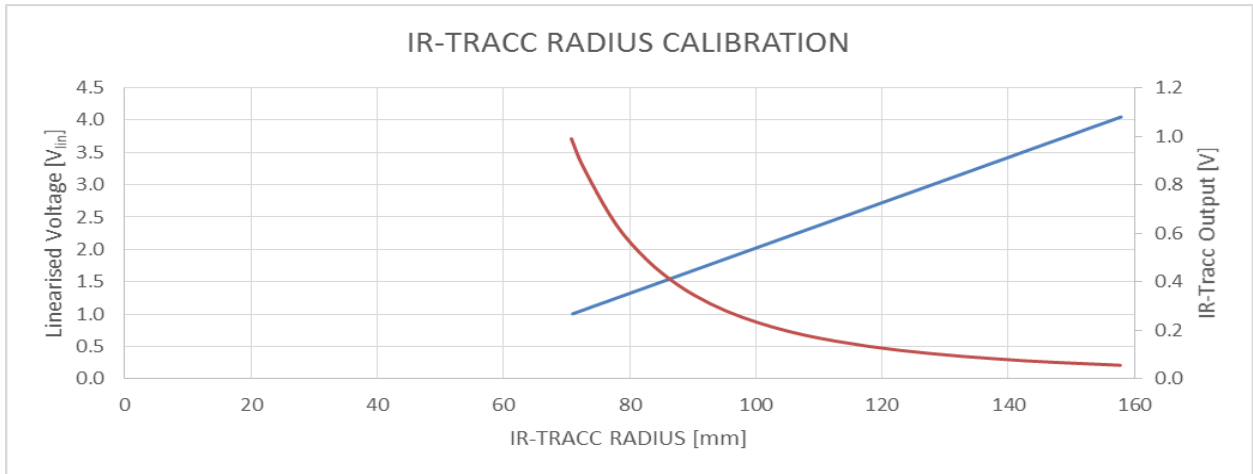


Figure 11: IR-TRACC calibration output (Been, 2016)

In practice it has been found that the linearization exponent, with a theoretical value of -0.5, can be modified alongside the calibration factor in order to increase the linearity of the output. When this is done the exponent is closer to -0.42857 (ISO/PRF TS 21476), meaning the original formula becomes:

$$d = C * U_{IR}^{-0.42857} \quad (2)$$

Both the linearization exponent and calibration factor can change over the lifecycle of the IR-TRACC. For this reason, all IR-TRACCs are recalled for recalibration annually. The dummy's in which they are mounted are also recertified regularly (3-10 tests). This is done in order to verify the behavior of the mechanical components and involves subjecting parts of the dummy to a controlled impact. By comparing the observed output to the expected output (since the test is done in a controlled environment) of the instruments, the mechanical properties of the dummy can be verified.

For detailed information about the calibration process, see ISO TS 21476.

2.2 IR-TRACC variations

Compatibility with both existing and future IR-TRACCs is a priority for the test set-up. While only 3 types of IR-TRACCs are currently supported by Humanetics, both the 2D and 3D models sport a total of 3 different mounting systems each. Here an overview of these models is given, as well as their respective applications. Figure 12 shows the differences per variant.

Table 2: List of compatible sensors

Model nr	Dummy application	Dummy Locations	Radius fully collapsed – extended [mm]	Type
6510	Hybrid III 6YO	Thorax	65-129	1D
IF-362	Q3	Thorax	63-153	1D
IF-367	WorldSID 50M	Thorax and Abdomen ribs	43-132	2D
IF-368	WorldSID 50M	Shoulder ribs	43-132	2D
IF-372	Q10	Center	43-132	2D
472-3550; 476-3550	THOR 50M	Thorax Upper Left	70-164	3D
472-3560; 476-3560	THOR 50M	Thorax Upper Right	70-164	3D
472-3570; 476-3570	THOR 50M	Thorax Lower Right	70-164	3D
472-3580; 476-3580	THOR 50M	Thorax Lower Left	70-164	3D
472-4730-1	THOR 50M	Abdomen Left	69-192	3D
472-4730-2	THOR 50M	Abdomen Right	69-192	3D
IH-11608	THOR 5F	Thorax Lower Right	65-140	3D
IH-11609	THOR 5F	Thorax Lower Left	65-140	3D
IH-11621	THOR 5F	Thorax Upper Left	65-140	3D
IH-11622	THOR 5F	Thorax Upper Right	65-140	3D



Figure 12: Various IR-TRACC models for 1D, 2D and 3D measurements. For the 3D models, first 3 right sided models are shown, followed by a left-sided model for the upper thorax. Finally the digital (476-series) versions of the lower right and upper right are displayed. The left-sided models are obtained by “inverting” the right-sided models in a similar fashion.

3. Desired behavior

In this chapter a car-test in which the dummy returned a high total chest deflection will be analyzed. The total chest deflection in this test exceeded the legal threshold, and is to be considered as the maximum deflection an IR-TRACC is expected to accurately register. The goal of of this chapter is to define the behavior to which we wish to subject the IR-TRACCs to, and find a way to replicate this behavior.

3.1 Crash test behavior

As specified before, the IR-TRACC applications most relevant to the test set-up are crash tests. Crash tests are performed in order to assess the safety of the occupant in a car during a collision. During such a test a car with one or more dummies inside is forced into collision with either a different car or an object simulating a car, heavy vehicle, wall or pole. In these tests the role of occupant is performed by a crash test dummy.

The collision is achieved by accelerating either both or one of these objects towards each other with a winch along a track. Here the dynamics during a crash will be briefly detailed using a “side pole impact test” as an example. Figure 16 shows the orientation of the car and pole in this test.

For this test a vehicle with dummy is placed on a carriage which will be accelerated towards a fixed pole at an angle of 75°. In order to obtain repeatable results, the vehicle will be at constant speed before it is within 10m of the pole. At the moment of collision ($t = 0$ s, Figure 13), the dummy’s inertia will still be moving the dummy in the initial direction while the vehicle is rapidly decelerated towards a velocity of 0. This means the dummy will experience no significant deformation until it comes into contact with something in the direction it is moving. This is typically an airbag, seat belt or interior part.

Once the dummy has made contact with the airbag (Figure 14) it will be decelerated towards a standstill and a subsequent rebound (Figure 15). It is during this initial deceleration towards a (temporary) standstill that the largest forces in the dummy occur, as they would in an actual human in a car-crash. It is during this time period of “internal impact”, henceforward also referred to as T_i , that the largest deformations occur, which are used to determine the risk of injury to the occupants during a collision. Therefore is it the dynamic behavior during this time period that we will seek to emulate in the test set-up. The relevant parameters of this behavior are: impact duration, peak deflection, velocity and acceleration.



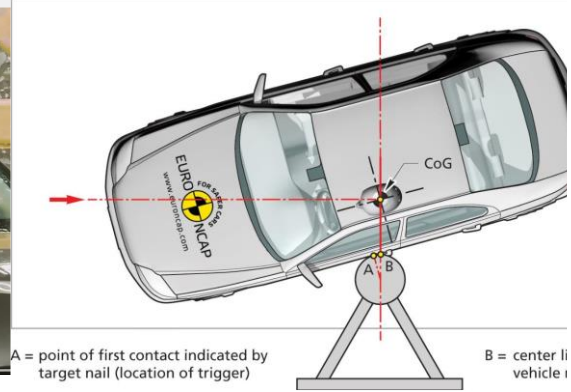
Figure 13: Situation 0. The car has made contact with the pole, but the dummy is not yet undergoing deformation (Euro NCAP, 2015)



Figure 14: Situation 1. The dummy has made contact with the airbag and door and is being compressed (Euro NCAP, 2015)



Figure 15: Situation 2. The dummy's direction of movement has been reversed and the compression is now decreasing instead of increasing (Euro NCAP, 2015)



A = point of first contact indicated by target nail (location of trigger)

B = center of vehicle

Figure 16: Euro NCAP Oblique Pole Impact set-up (Euro NCAP, 2017)

3.2 In-dummy movement

Now that the interval of interest has been determined, the behavior of the dummy during this interval can be analyzed.

After analyzing a pole impact report the time interval in which the IR-TRACCs reach their maximum deflection in a test was determined to be around 0.025 seconds, or 25 ms. Figure 17 shows an excerpt on which this interval was chosen. In this figure the red line shows the displacement of the IR-TRACC in mm, with a positive value indicating a displacement towards the center of the dummy. The green line shows the deflection of the IR-TRACC in degrees, with a negative value indicating a counter-clockwise rotation, seen from top (see Figure 18). Please note the offset between the two vertical axis. This offset was created merely to prevent the green line representing the deflection from touching the bottom of the graph and does not indicate an actual offset.

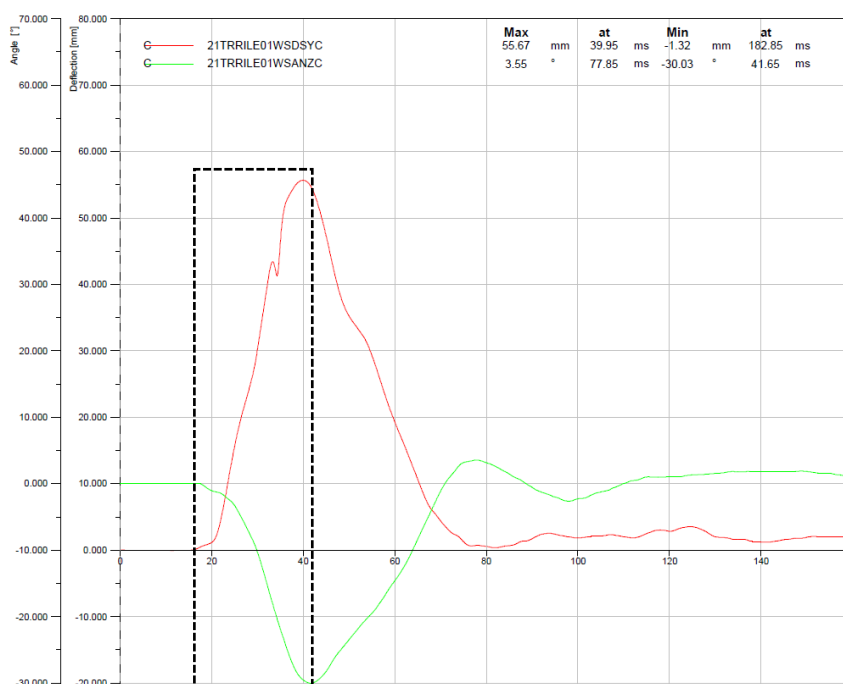


Figure 17: Excerpt from a crash test, the complete graph can be found in Appendix II: Crash test graph. The dashed box encloses the area of interest.

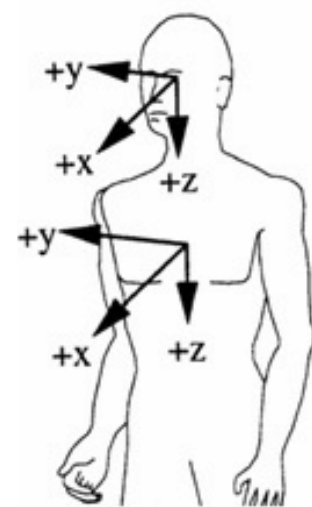


Figure 18: In-dummy global coordinate system (ISO 21002)

Furthermore, the report also shows that occurring forces as well as accelerations after 42 ms (after the “rebound”) are significantly lower than during the interval. This confirms the earlier claim that the further deformations are extremely unlikely to cause further injury. The data beyond this point is therefore of little interest and will be disregarded from here on out.

Examining the marked area in Figure 17 reveals the displacement in the area of interest to be sinusoidal in nature, except for the initial acceleration, which lasts until $t \approx 22$ ms. This means that in order to accurately simulate in-dummy movement, the test set-up should be designed to be capable of mimicking this behavior.

3.3 Drop tower behavior

The drop tower that the test set-up is to be used in conjunction can impose an impact on a test set-up by dropping a guided mass of predetermined weight from a predetermined height (Figure 22). In the past the drop tower has been used for amongst others, certification tests for the rib-units of the Eurosid-2 dummy.

This type of dummy has been designed to measure deformation due to impacts on the side of a car. Figure 19 shows the position of the rib-units in the dummy and Figure 20 the rib-unit itself. These tests are performed in order to verify the behavior of the rib-unit after several crash-tests. These so-called certification tests involve impacting the rib-unit with a mass at multiple velocities, quite like the dynamic tests the test set-up will have to perform.

A Eurosid-2 rib-unit (or ES-2 rib-unit) is designed to mimic the behavior of (a part of) the human ribcage and consists of:

- The rib itself (shown in yellow and magenta), which redirects the impact energy in the same way a human ribcage would when impacted from the side. The rib is covered with foam on the impacted side for increased biofidelity as well as to reduce wear and tear.
- A damper/spring combination with another spring serially connected (colored green and blue respectively), which simulate the reaction counterforce created by the ribcage and internal tissue during the collision.
- A static unit (colored grey) containing a guided linear sliding unit connected to the impacted side (right-front) and the guide itself which is connected to the other side (left-back). This sliding unit is used by the build in linear potentiometer in order to measure the deformation of the rib-unit. This part has been designed to act as rigid during impact in order to ensure the point which is measured by the potentiometer only moves in the desired direction. It also serves to connect the rib-unit to the spine of the dummy.

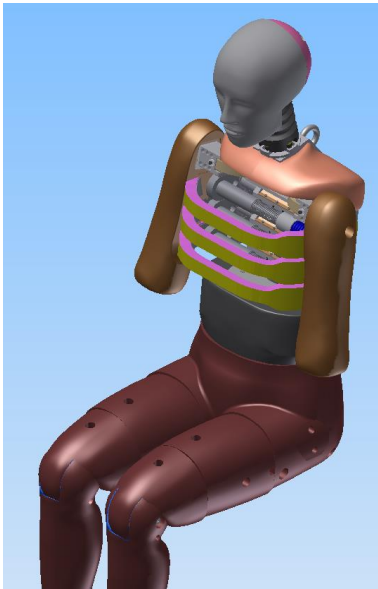


Figure 19: Eurosid-2 Dummy

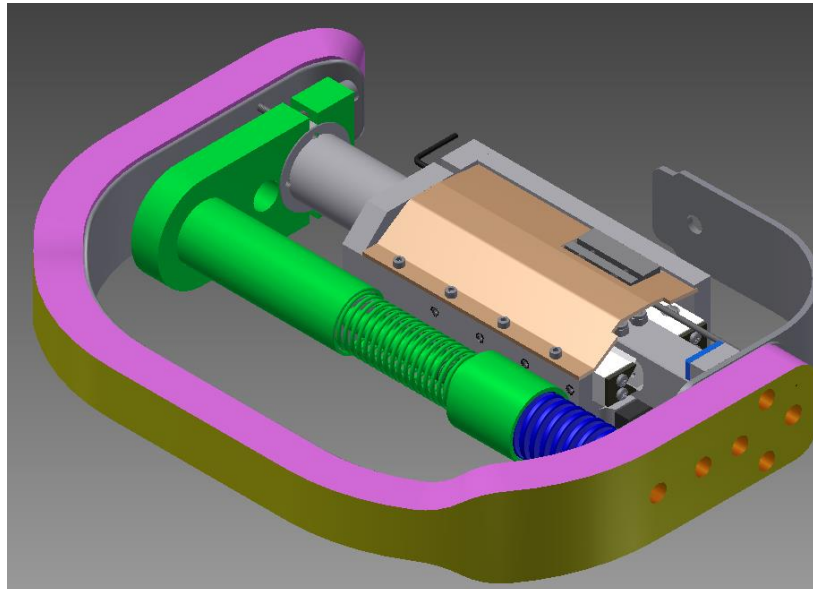


Figure 20: Eurosid-2 rib-unit

The data shown in Figure 21 was obtained during research into the effects of different types of damper oil on the ES-2 rib-unit behavior. The second graph in Figure 21, detailing the movement of the rib unit, shows a remarkable similarity to the graph detailing the movement of an IR-TRACC during a crash test. The test was performed by having by mounting the rib-unit in a drop rig (as shown in Figure 22) and impacting it with a mass of 7.78 kg at 4 m/s, after which the following happens:

1. The foam is compressed and the rib accelerated towards the same speed as the impactor over a very short time interval (± 0.004 seconds). This slows down the impactor to some extent. This step starts at the left line of the box in the graph and ends at the dashed line in Figure 21.
2. When the rib and foam combined have the same velocity as the impactor the damper/spring combination starts to accelerate. Now that the damper has a velocity, it starts to generate resistive force. This causes a further increase of the impactor deceleration. This step starts at the dashed line in the velocity graph in Figure 21 and ends at $t=0.01$ seconds)
3. The resulting deceleration continues until the peak displacement is reached, after which the combined force of the damper/spring combination and rib will be in balance with the inertia of the impactor and the rebound starts. This step continues from the end of step 2 and lasts until the right line of the box.

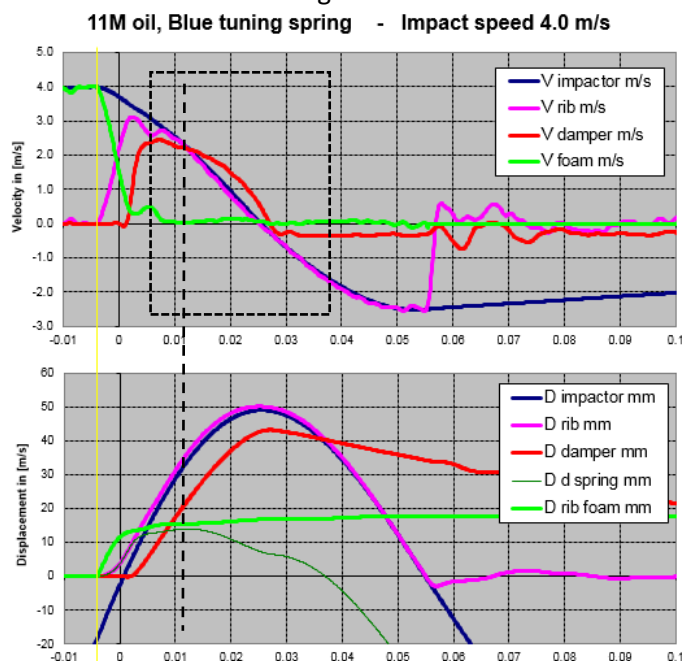


Figure 21: Velocity and displacement per component of the ES-2 Rib-unit

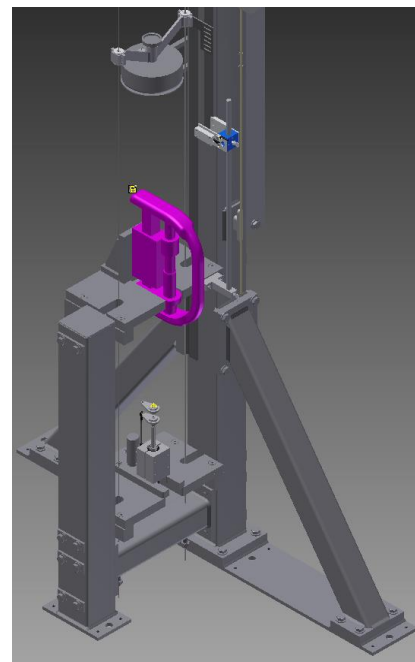


Figure 22: ES-2 rib-unit impact setup

There is however a small “bump” in the velocity of the rib right between $t=0$ and $t=0.01$. This sudden decrease in velocity of the rib-unit coincides with the initial increase in velocity of the damper. The subsequent temporary recovery of the rib velocity is mirrored by an equally temporary increase of foam velocity. This bump can be attributed to the damper being activated after the rib has traveled a small initial distance (10 mm) that exists between the rib and the damper. This distance is in fact the blue spring in Figure 20 being compressed before the damper is activated. Further investigation revealed the same trend displaying in the other data-sets of the same research as well.

Overall this data shows the behavior a displacement sensor exhibits during a drop tower test is very similar to that which an IR-TRACC exhibits during a vehicle collision test. Therefore, it can be concluded that the drop tower is indeed suitable for use in conjunction with the to-be-designed set-up for the verification of the dynamic behavior of IR-TRACCs.

3.4 General behavior of the system

Now that the movement of an IR-TRACC during a test has been determined to be sinusoidal in nature, this movement can be analyzed. In order to do so the movement will be approached as part of a harmonic motion. The general equation for the position of the mass as a function of time is:

$$x(t) = A * \sin(\omega t) \quad (3)$$

Where ω is the angular frequency of the system, calculated with the formula $\omega = \sqrt{\frac{k}{m}}$, k stands for the spring rate of the system and m for the mass that is being moved. This formula will be used to approximate the behavior of the system later on.

$$\omega = \sqrt{\frac{k}{m}} \quad (4)$$

Differentiating equation (3) over time gives us a formula for the velocity of the mass:

$$v(t) = \omega * A * \cos(\omega t) \quad (5)$$

This function can be differentiated over time again in order to obtain a function for the acceleration of the mass, but this is not necessary at this point.

Solving for A requires us to have knowledge of a point the mass goes through, which luckily we do. By defining $t=0$ as the time in which the spring is set into motion with an initial speed v_0 , we obtain that

$$A = \frac{v_0}{\omega} \quad (6)$$

from equation 5. Since this initial velocity is also the maximum velocity of the system, and a harmonic motion goes from maximum velocity to a zero velocity in 0.5π radians, we can deduce that the 0.025s it takes for the mass to reach zero velocity is equal to 0.5π radians, or a quarter of a harmonic circle. Writing this in the form of an equation we get:

$$T_s = 4 * T_i = 0.1 \text{ s} \quad (7)$$

Where T_s stands for the time it takes for the system to complete a complete harmonic circle, and T_i the time the internal impact lasts for.

Also, with A being equal to the amplitude of the motion, this gives us a relation between the displacement of the spring, the spring rate, displaced mass and the initial, maximum velocity of the mass-spring system:

$$u * \sqrt{\frac{k}{m}} = v_0 \quad (8)$$

Where u stands for the spring displacement in meters. This equation will be very useful in determining the operational parameters.

Comparing the crash test behavior with a quarter sinusoid we can see the resemblance. Due to how acceleration due to impact works this is not completely correct, but it is nonetheless an accurate representation as can be seen in Figure 23. This figure consists of a zoomed-in Figure 17, a blue line representing the quarter sinusoid and a black dashed line indicating the effect of the initial impact. The black line will get further attention in Chapter 0

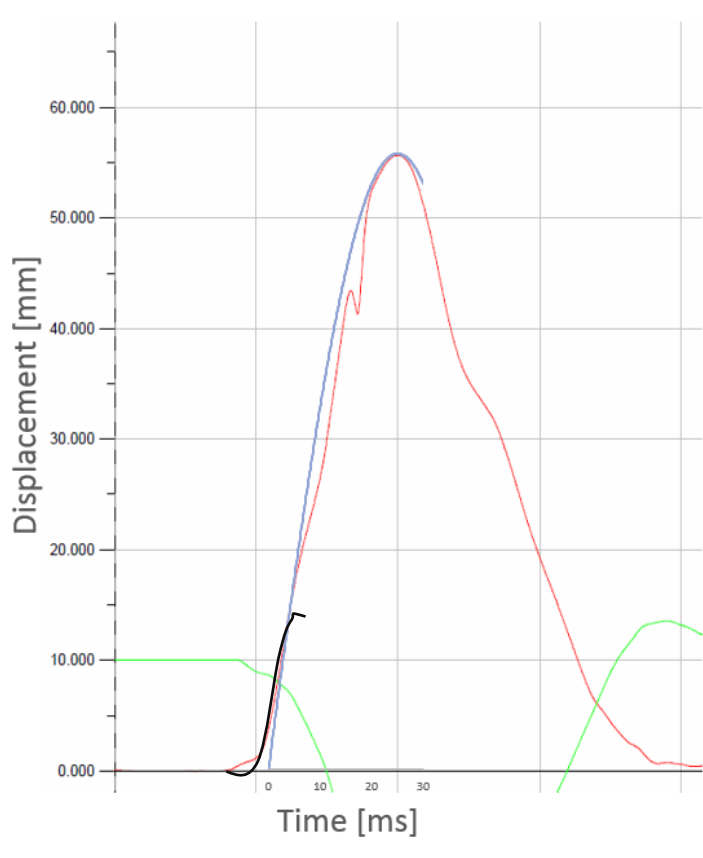


Figure 23: In-dummy movement and sinusoid imposed

Now that the basic operating principle of the test has been determined, the actual parameters of the system can be established, namely the drop height (h), drop mass (m_d), initial velocity (v_o), impact velocity (v_i) and the spring rate (k). Currently the angular frequency ω , the amount of vibrations the system experiences per second, can already be calculated by using the following equation:

$$\omega = \frac{2\pi}{T} \quad (9)$$

Where T represents the duration of a single vibration, or time period. Entering $T_i = 0.1$ into the equation gives us $\omega = \frac{2\pi}{0.1}$ which returns $\omega = 62.831 \text{ rad/s}$. As can be observed by combining equations (4) and (9), the impact duration T_i has a profound impact on the required stiffness of the spring. The effects of a different impact time over a varying mass against the stiffness can be seen in figure 24.

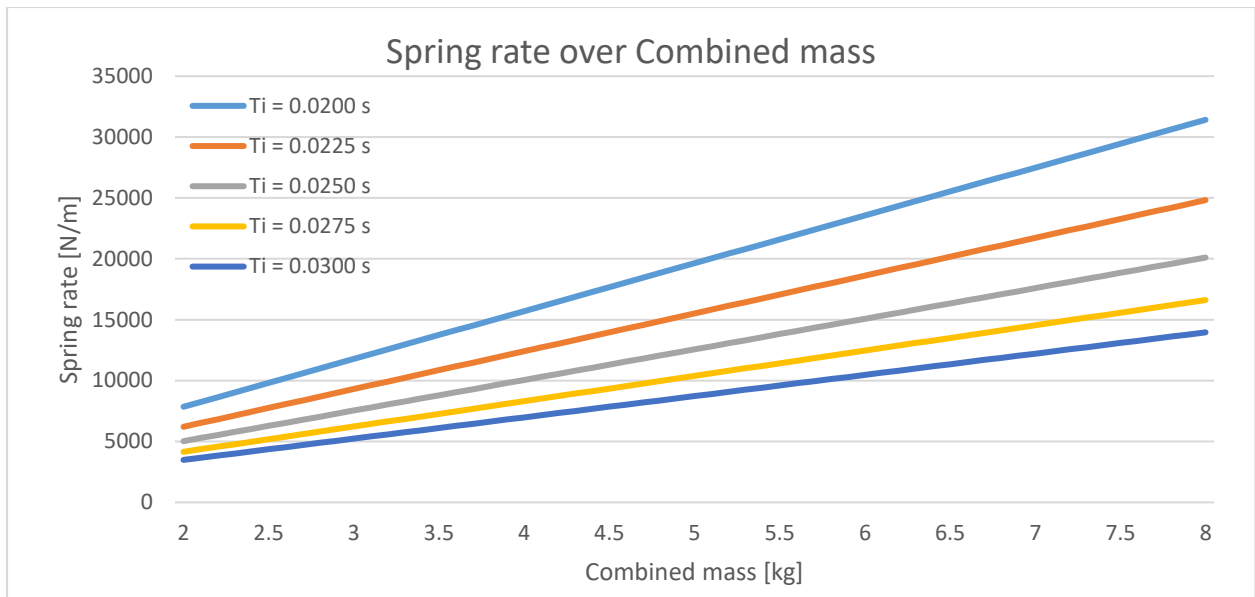


Figure 24: Effects of the impact duration and mass of the system on the spring rate

The graph above clearly shows the required spring rate increases when the combined mass increases and the impact duration decreases, with impact duration being the stronger influencer of the two. The effect is significant enough that even a 10% deviation in spring rate has a significant effect on the dynamic behavior. This graph also illustrates that in the event of a follow-up design the impact duration should be re-evaluated first, due to the effect it has on the rate (and therefore size) of the spring. This effect is even greater when the combined mass increases.

To this end we conclude that, in order to fit the spring in the slith (where the pink rib-unit is mounted in Figure 22), the combined mass should be kept as low as possible.

Assuming the only changing variable in the system is the spring rate, we can calculate its effect on the impact duration by combining equations (3) and (7).

Table 3: Effect of spring rate deviation of 10% on impact duration

Mc	5	5	5	2	2	2
Ti	0.02	0.025	0.03	0.02	0.025	0.03
k	30842.5	19739.21	13707.78	12337.01	7895.684	5483.114
k-	27758.25	17765.29	12337	11103.31	7106.116	4934.803
k+	33926.75	21713.13	15078.56	13570.71	8685.252	6031.425
Ti-	0.021082	0.026352	0.031623	0.021082	0.026352	0.031623
Ti+	0.019069	0.023837	0.028604	0.019069	0.023837	0.028604
%diff	4.65372	4.653744	4.653728	4.653758	4.653744	4.653745

Table 3 shows us that while a 10% spring rate deviation does result in a measurable difference in behavior, this difference is limited to <5%, and therefore acceptable.

3.5 Achieving the desired behavior

Let us approach the drop tower set-up as a spring with a mass on top (M_s) getting impacted by another mass (M_b), after M_b falls from height h . Neglecting air resistance, we can define 4 distinct positions:

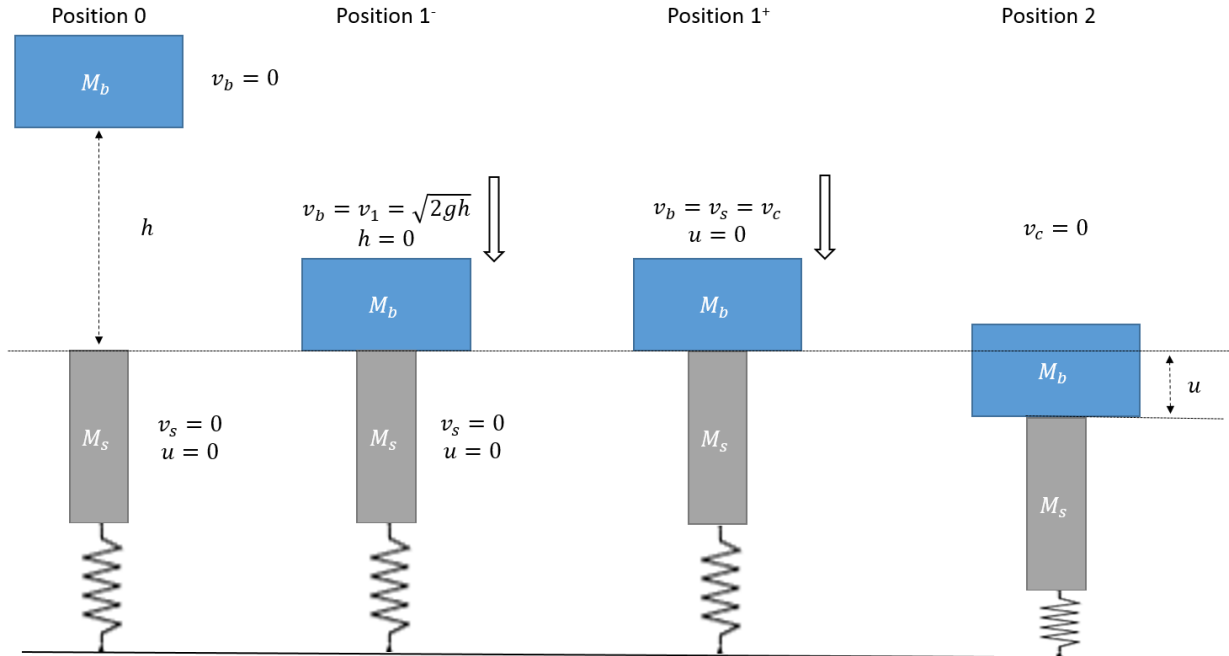


Figure 25: Free body diagram of the set-up

In position 0 the drop mass (M_b) is at rest at a height h above the spring mass (M_s), which is at rest as well. The rest position of the spring mass is the point at which the spring completely counteracts the force due to gravity on the spring mass.

At position 1⁻, the moment just before collision, the drop mass has a velocity of $v_1 = \sqrt{2 * g * h}$ (neglecting air resistance) and the spring mass is still assumed to be at rest.

Position 1⁺ is defined as the moment right after the collision of the drop and spring masses, meaning both blocks are assumed to have achieved the same speed, v_c , while the spring is still at rest. Since the conservation of energy always applies it may seem obvious to calculate the resultant velocity with the formula:

$$\frac{1}{2} * m_s * v_1^2 = \frac{1}{2} * (m_s + m_b) v_c^2 \quad (10)$$

However, the above formula only applies for perfectly elastic collisions, which this collision is not, due to both masses sticking together (until at least position 2) and it being a macroscopic collision in general (Beer, 1996). In fact, by utilizing the formula for the ratio of the kinetic energies after an inelastic collision the amount of kinetic energy lost in the collision can be determined.

$$\frac{KE_f}{KE_i} = \frac{m_1}{m_1 + m_2} \quad (11)$$

The correct formula for calculating the resultant velocity in a (perfectly) inelastic collision is:

$$v_2 = \frac{m_1 * v_1}{m_1 + m_2} \quad (12)$$

With $v_2 = v_c$, $m_1 = m_d$ and $m_2 = m_s$ in our situation as shown in Figure 25. Using equations (10) and (12) we can visualize the speed loss as has been done in Figure 17. Note that the left y-axis corresponds with the gray line, and the right y-axis with the others.

Let us assume a mass ratio of 0.8. In this case, using only the conservation of energy (equation (8)) over conservation of impulse (equation (9)) gives us a deviation of 10.6% before even getting started on analyzing the movement itself.

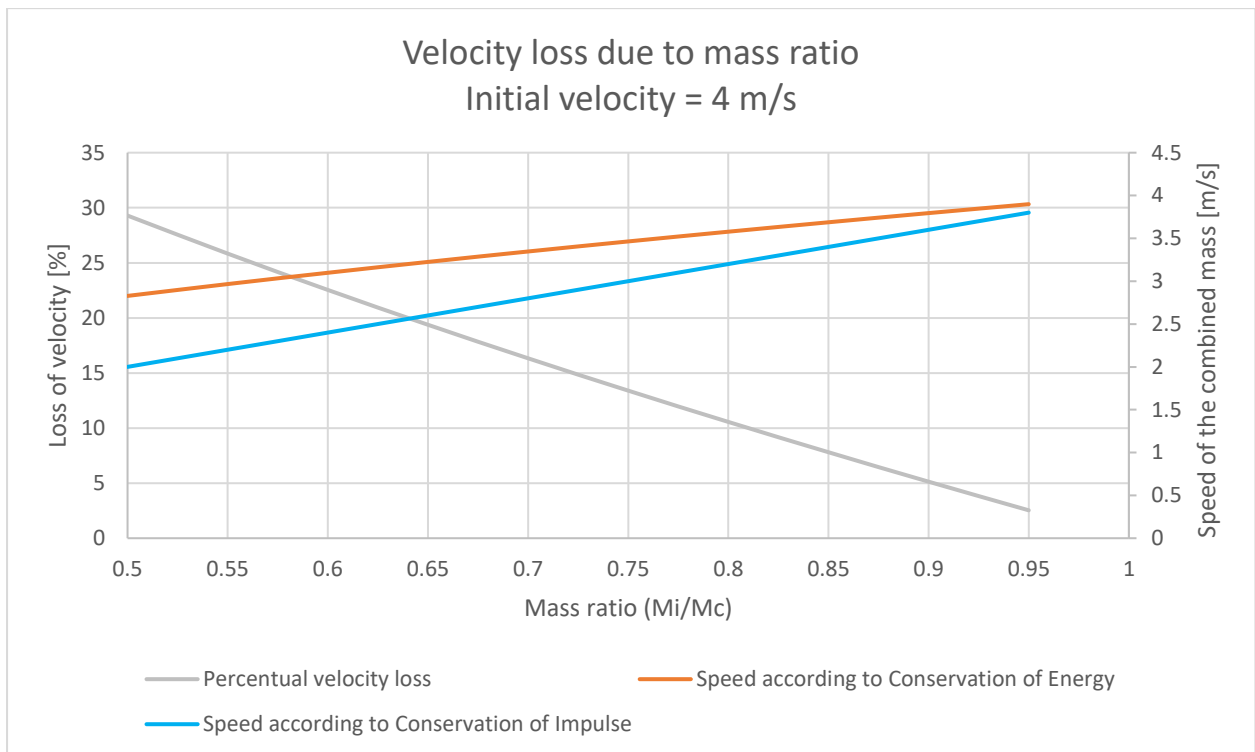


Figure 26: Comparison of expected velocities

As the figure shows, a high mass ratio is preferable for the set-up since it will require a lower impact speed to achieve the same end velocity. This is important because the formula for the impact velocity

$$v_1 = \sqrt{2 * g * h} \quad (13)$$

still stands, and height is a limiting factor in the drop tower.

In reality this collision, as well as nearly all other collisions, will be neither perfectly elastic nor perfectly inelastic. The collision can be made more elastic by adding an impact layer on top of the impacted mass, but the formula for inelastic collision is the more accurate one, and will thus be used.

At the final position, position 2, the spring is as far compressed as the downwards force of the masses allow, and the velocity of the masses 0. Since no collision is taking place between positions 1+ and 2, we could still use the law of conservation of energy to write the spring constant as a function of the masses and velocity:

$$\frac{1}{2} * k * u^2 - (m_b + m_s + \frac{1}{2} * m_k) * g * u = \frac{1}{2} * (m_b + m_s) * v_c^2 \quad (14)$$

Where k equals the spring rate in $\frac{N}{mm}$, u stands for the compression of the spring relative from the resting point in m , positive upwards and m_k for the mass of the spring in kg . The difference in potential energy as a result of the movement of the masses of the blocks and the spring itself should not be neglected, since their contribution to the energy equation is more than 1% of the end result. This does however make this formula unsuitable if we want to plot the displacement against the drop height.

We can however achieve this by combining equations (8) (11) and (13), resulting in

$$u_{max} = \frac{(\sqrt{(2 * g * h)} * \frac{m_1}{m_c})}{(\omega)} \quad (15)$$

Where $\omega = 62.831 \text{ rad/s}$ for an impact duration of 0.025 s.

Assuming the mass on the spring (or displaced mass) is 1kg, we obtain the graph shown in Figure 27. In this figure the displacement requested by the customer is denoted by the green area. The drop heights achievable in a low-ceiling laboratory blue area and drop heights achievable in yellow areas respectively.

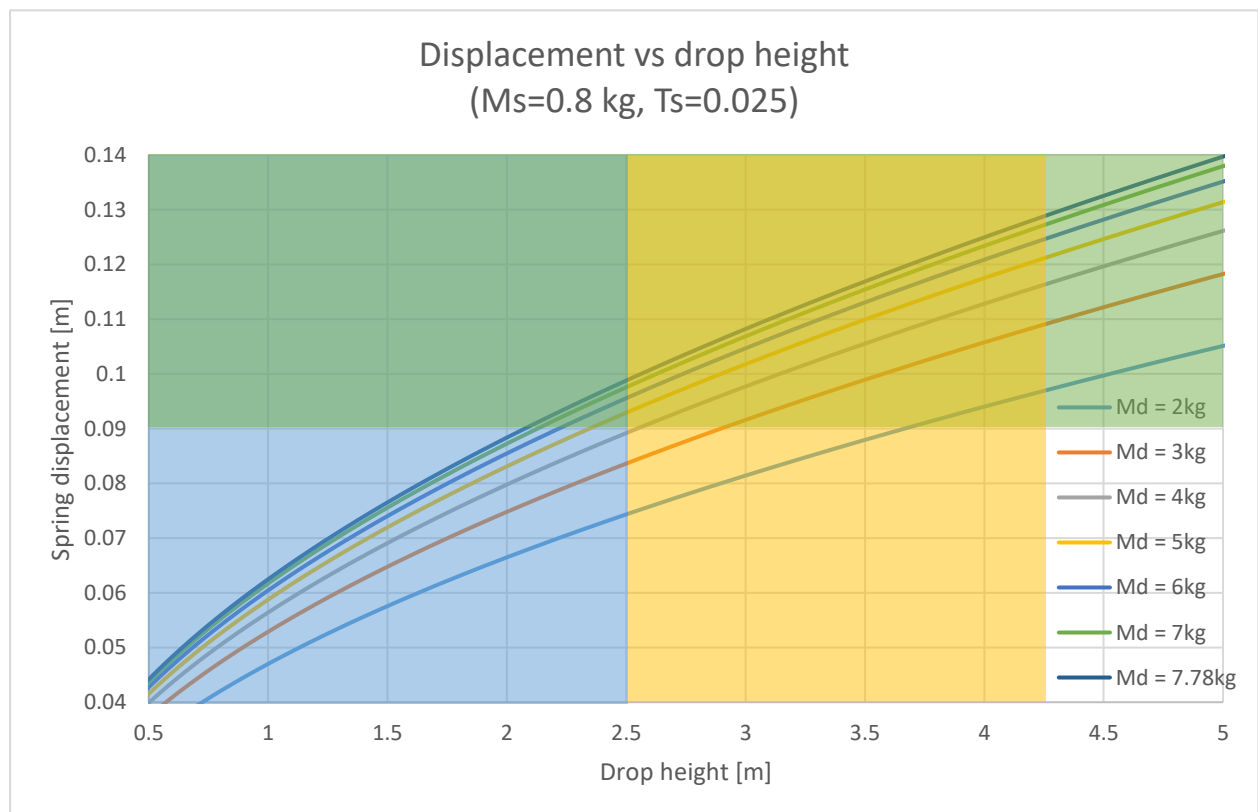


Figure 27: Result of drop height on the displacement for various drop masses

As Figure 27 shows, the desired displacement in a low-ceiling laborator can only be achieved by a very large drop mass, necessitating a very large spring. Ignoring the drop height limit of 2.5 m, a drop mass of only 2 kg is required, drastically decreasing the spring rate required (as per Figure 24). Considering this data and the fact that only 1 IR-TRACC variation can be subjected to a displacement of more than 90 mm, the following parameters for the system were determined:

- The total mass of the slider would be limited to 0.8 kg, and that of the drop mass to 2.0 kg
- The rate of the spring would be 11 kN/m, and its maximum displacement 100 mm

3.6 Spring design

With both the desired spring rate (11 kN/m) and stroke (100 mm) known, and a strong desire to keep the spring diameter ≤ 50 mm, a spring could be selected. Digging through the catalogue of Amatec yielded very few relevant springs. Due to these disappointing results, it was decided that a custom spring would be ordered from Globe BV. Using an Atlas Coevoerden manual in the possession of Humanetics this process was initiated. Using the equation:

$$n = \frac{s * G * d^4}{8 * F * D^3} \quad (16)$$

Where n stands for the number of coils [-], s for the occurring stroke [m], G for the shear modulus [Pa], d for the wire thickness [m], F for the required force [N] and D for the heart-to-heart diameter. The required number of coils for a compression spring can be calculated. This number can then be used to determine the length of the desired spring. For the complete list of formula's and used graphs, see Appendix V: Excerpt from a manual from Atlas Coevoerden.

Below in Table 4 the properties from three standard springs from Amatec are listed, along with two custom springs from Globe (formerly known as Atlas Coevoerden), one with a wire ratio of 8, and another with a wire ratio of 5.

Table 4: Comparison of various springs

Designation	Drop mass [kg]	Drop height [m]	Impact velocity [m/s]	Spring rate [kN/m]	Spring diameter [mm]	Free length [mm]	Deformation [mm]
DH24210	3	1.6	7.3	11.2	54.5	250	90
D13860	3	2.1	6.5	15.8	37	160	80
DH14050	3	3.4	6.1	16.1	37	380	135
Globe Custom W8	2	2.36	6.8	11	53.6	220	100
Globe Custom W5	2	2.36	6.8	11	26.5	356	100

While the custom springs are better suited than the standard springs, they are still not useable. Choosing a wire ratio of 8 causes the diameter of the spring to be too big to fit in the slith, causing the set-up to be very high. Choosing a wire ratio of 5 allows for insertion in the slith, but requires the spring to have a free length of 356 mm, causing the set-up to still be rather large. Analysis of a spring

used in the Eurosid-2 yielded some very interesting results: while both the occurring torsion stress and deflection exceeded factory specifications, they were still known to be performing as desired after thousands of tests. Therefore in order to make the required spring more compact, it was decided to “shrink” the spring until just before stresses comparable to the Eurosid-2 spring occur. Table 5 shows a comparison between some properties of the Eurosid-2 spring and the chosen spring and the earlier custom springs.

Table 5: Optimization of the spring

	Eurosid-2 spring	Selected spring design	Custom W8	Custom W5
Wire diameter [mm]	3.75	4	6.7	5.3
Wind ratio [mm/mm]	5.186667	5	8	5
Outer diameter [mm]	23.2	24	60.3	31.8
Stroke [mm]	60	100	100	100
Spring ratio [N/mm]	19	11	11	11
Effective winds [-]	13.00	29.64	12.12	39.27
Torsion stress [N/mm ²]	1392	1134	565	648
Bottom out length [mm]	59.81	137.00	100.37	237.68
Play (% of stroke)	5	10	20	20
Free length [mm]	124.81	247.00	220.37	357.68

As can be seen, by almost doubling the occurring torsion stress and halving the amount of play, but only up to a level where spring failure is known not to occur within an acceptable amount of cycles. This results in a spring as long as the earlier Custom W8, and even thinner than the Custom W5. With a free length of 247mm, diameter of 24mm and stroke of 100mm, Figure 28 indicates the spring is at extreme buckling risk (the blue mark lies outside of the graph). In order to remove this risk the blue mark must be “moved” to the left (onto the green mark) by reducing the ratio of free length to diameter to 6. Solving

$$\frac{L_0}{D} = 6 \quad (17)$$

For $D = 24 \text{ mm}$ yields $L_0 = 144 \text{ mm}$. Subtracting that number from the original free length gives us the length of the spring that can be unsupported before buckling occurs, 103 mm. In order to be on the safe side the spring will be supported by an internal rod 120 mm from below, and a casing of 70 mm from above.

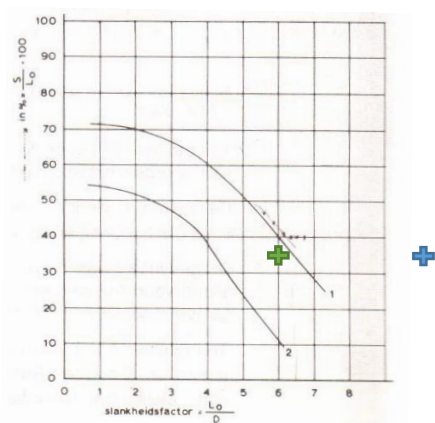


Figure 28: Buckle risk of compression springs (Atlas Coevorden, -)

4. Measurement of movement

This chapter describes how the choices for the measurement instrument and means of guiding the displacement (or slider type) were made.

4.1 Reference measurement

In order for the test to be meaningful, the output values of the tested IR-TRACC will need to be compared to another obtained value that is known (or assumed) to be correct. Since the set-up contains both a mechanical spring whose stiffness may change over time, and a mass that is manually raised by an operator before release, there are too many variables for a calculation to be accurate.

To this end the set-up should include a reference measurement device. ISO 6487 specifies that a distance measurement device used in road vehicle impact tests, i.e. the IR-TRACC, should have an uncertainty of <1% (ISO, 2015). In order to guarantee this measure of accuracy the reference measurement will need to have an uncertainty of <0.1% (since it is being used to measure a measurement).

Eurosid-2 Linear Potentiometer

Since the Eurosid-2 Linear Potentiometer has already been heavily used in the drop-tower, it is a logical step to first compare alternatives to it. The supplier claims this product has a linearity of 1% and has a measurement range of 13 mm - 152 mm. More importantly it has a starting force of only 0.28 N and is rated for an acceleration of 50 g over 11 ms half sine (moving from rest to maximum displacement and back in 11ms with a peak acceleration of 50 g). The 50g 11 m/s condition however applies to any direction, and this instrument is known to have been subjected to accelerations of well over 100g for a very short period of time without loss of performance. This indicates that the acceleration limitations suppliers provide need not be considered as critical, provided they are 50g or above.

With these specifications as a starting point alternatives were sought after, several of which have been gathered in Table 6.

Ultrasonic sensors were also investigated as a potential alternative, but these were found to often have an accuracy of only 1%, and poor repeatability. This in tandem with the possibility of the set-up being used in proximity with other ultrasonic sensors, which can cause interference as well, resulted in the conclusion that ultrasonic sensors would not be considered for use in this dynamic environment.

Table 6: Overview of reference sensors, all are linear potentiometers except for the ILD2300, which is a laser based sensor

Sensor	Eurosid-2 Potentiometer	Novotechnik TE1-0150	NovoTechnik T-0150	NovoTechnik TEX 0100	NovoTechnik LZW1S-125	optoNCDT ILD2300-100
Minimum distance [mm]	38,10	25	10			70
Measurement range [mm]	13-152	150	150	125	125	100 (+)
Measurement frequency	Analog	Analog	Analog	Analog	Analog	30kHz
Linearity	1%	0.15%	0.075%	0.1%	0.05%	$\leq 20\mu/0.02\%$ FSO
Price	\$600					
Size	9.53	33x18	27.6x18	18	19x26	97x75x30
Compressed length	183	230	230	250	174.5	-
Maximum velocity [m/s]	9 m/s	11 m/s	11	10	10	-
Special constraints	Initial force of 0.28 N	Initial force of 0.30 N	Initial force of 0.30 N	Initial force of 3.0N	Initial force of 0.5N	40k lx max (2x daylight)

The ILD2300-100, a light-based sensor, is the most accurate and smallest of the alternatives, but requires an offset of 70mm for accurate measurements. With the restriction to ambient light easily accounted for it may seem like the best solution at first, but the goal of the test set-up is to verify the accuracy of a sensor that is optically based itself. Since verifying the dynamic behaviour of a sensor with a sensor of the same type yields little validation, the

4.2 Spring/guidance setup

Perhaps the most important part of a displacement-based test is the control over the displacement. Since a high precision ($\pm 0.1\text{mm}$) is demanded of the set-up, the positioning of the spring(s) will require extra attention as well. As concluded in 3.5 Achieving the desired behavior, it is desired to keep the mass of the slider low.

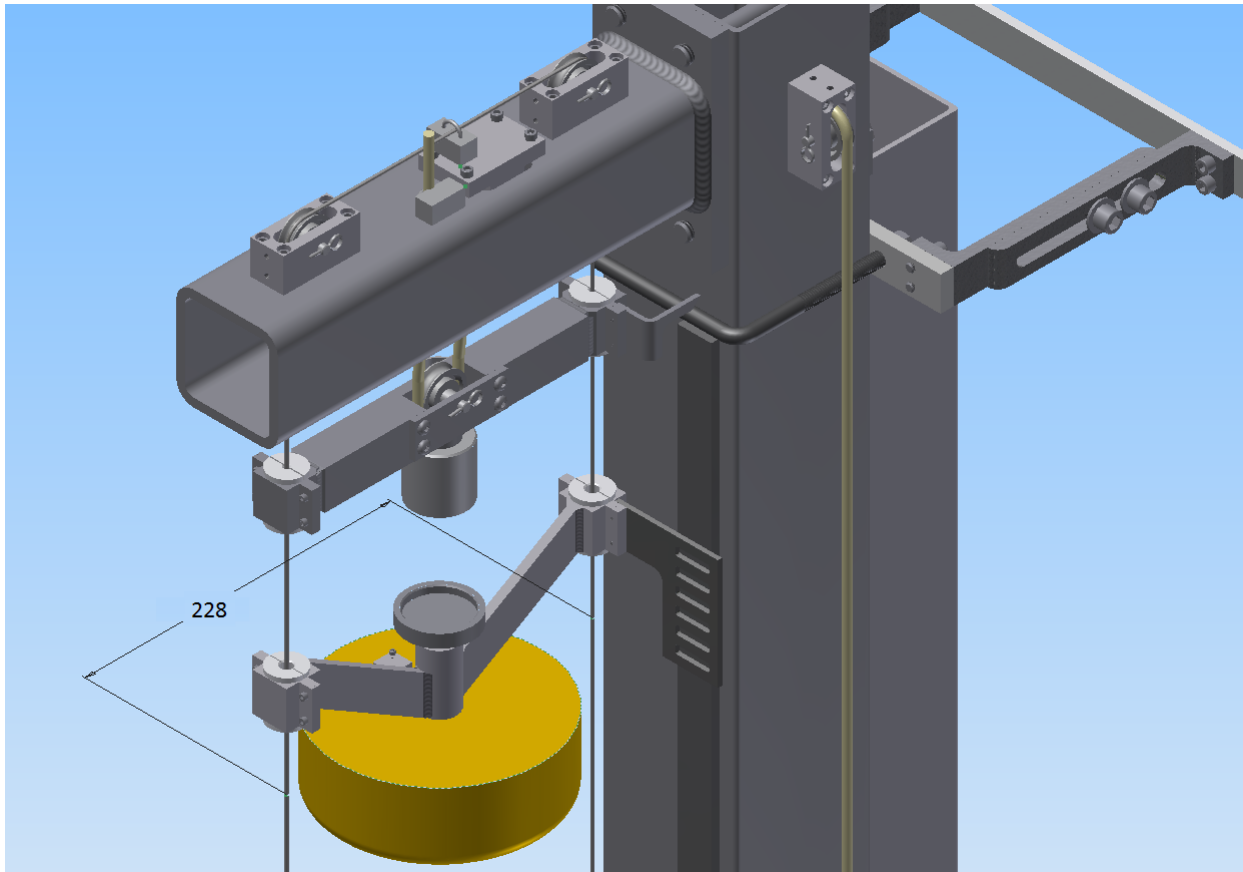


Figure 29: Distance between the drop cables, top of the drop tower

Going into this decision the only known parameters are the distance between the cables (228 mm, see Figure 29) and weight of the impact mass (2 kg). After some research into different sliding solutions several options were considered, these are detailed below.

4.2.1 Double spring/sliding bearing

In an effort to allow for the maximum amount of room for the IR-TRACCs and reference instrument, a design based on the quasi-static test set-up was created. Taking into account the lessons learned from the first set-up (Figure 4), several improvements were made.

As a start the amount of bearings were reduced from four to two, decreasing the amount of springs required as well (Figure 30). The remaining springs, bearings, IR-TRACC and reference instrument would be rearranged so that they would occupy a single line.

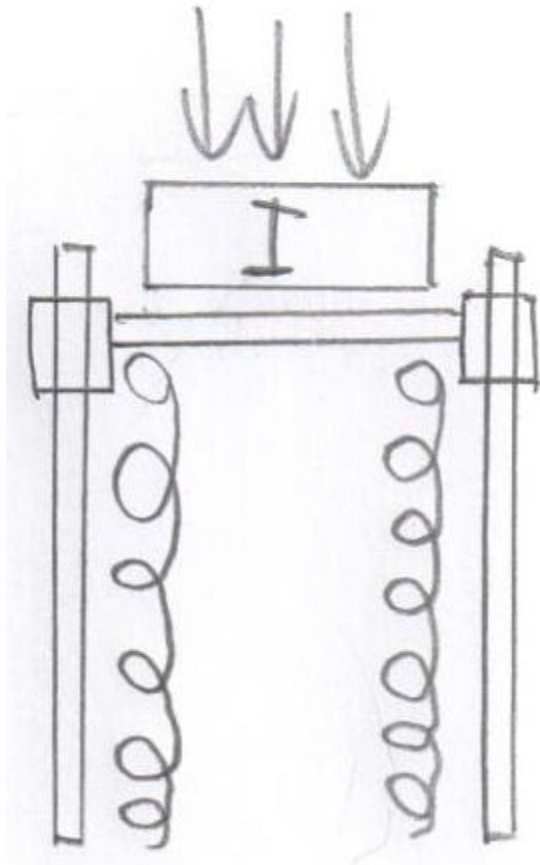


Figure 30: Sketch of the parallel sliding setup, side view

By positioning every component on the same line, the set-up becomes more or less one-dimensional. This is extremely useful, as a lot of interfering forces are greatly diminished. Due to the inexactness of compression springs however, there is a risk of the plane obtaining a slant during compression. In order to make this design work, the guiding components will need to consist of lightweight sliding bearings, which typically do not handle velocities over 5 m/s well. Their ability to carry transversal loads is also weaker, since these would cause a very small area of the bearing to experience a lot of friction.

While this solution would provide ample room for the attachment of IR-TRACCs, the risk of the bearings jamming due to either an off-center impact or a difference in the spring rates caused this concept to be dropped in favor of more reliable alternatives, along with any other potential designs which would require two springs to be positioned parallel to each other.

4.2.2 Single spring, sliding bearing

In an effort to have as little moving mass as possible, this concept is much like a piston. Instead of having the bearing move, in this concept the bearing is fixed in place, and the slider moves through the bearing (Figure 31). With the spring coiled around the main rod, the rod would feature a small mantle around the spring on the top (the section view of Figure 32 was made just below the “pistonhead”). Rather than encased in a tube, the idea is to have the slider sunk in a hard material like metal. This was done so that, in the case of potential overshoot, be it due to a mass that is too heavy, or dropped from too high, the slider would only be able to move downward until the drop mass makes contact with the material. This does mean that this concept will be more heavy altogether, but damage to the instruments would be extremely unlikely.

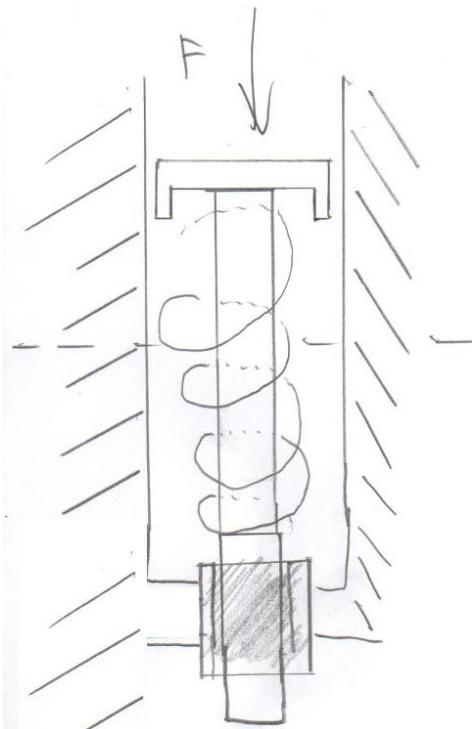


Figure 31: Single sliding bearing, front



Figure 32: Single sliding bearing, section view

Since the only moving component (discounting the spring) in this concept can be made very small, there would be little difficulty in conforming to the weight limit. As with the previous concept however, the inclusion of a sliding bearing would require the drop mass to be guided relatively precise. If the required level of accuracy can not be maintained over time, the increased stress on the bearing could very well lead to failure, resulting in at least the set-up to be inoperable until repaired, and potentially damaging the instrument as well. Also concerning is the fact that the spring would coil part of the sliding mechanism.

The high amount of mass still available does however mean a sizeable area would be available, potentially allowing multiple IR-TRACCs to be tested at the same time.

While this concept could potentially offer the ability of getting absolute comparisons between different types of instrument, attempting to do so is perhaps a bit too ambitious for the first iteration of the project.

4.2.3 Needle roller bearing

Already referred to earlier in this report, the needle roller bearing was first applied by Humanetics in the Eurosid-2 dummy. It was introduced in order to prevent displacement sensors from moving in unwanted directions, causing inaccurate measurement and an increased risk of damage. Also known as M and V guideways, this bearing consists of two hard, smooth surfaces separated by a multiple steel needles, held together by a plastic cage.



Figure 33: Two M and V guideways in a closed layout, taken out of an EuroSID-2 dummy

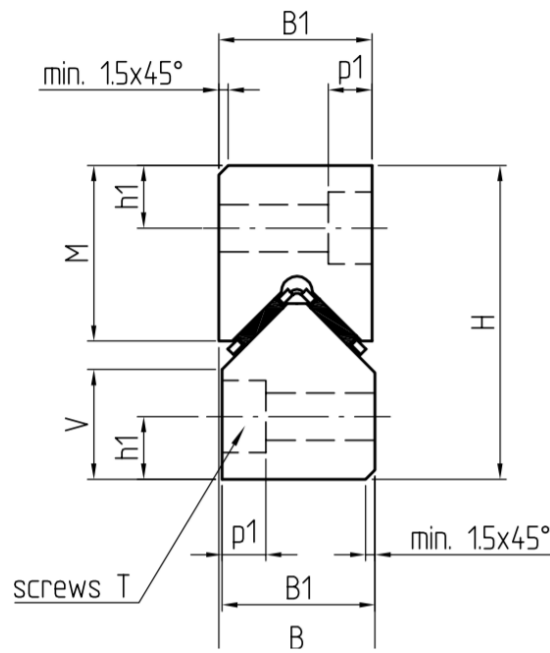


Figure 34: schematic of an M and V guideway, divided by an angled needle cage (Egis-SA, 2018)

In the configuration in which they are present in the Eurosid-2, they have been used during hundreds of tests without failure, can withstand high lateral forces and have very high parallelism (Figure 35).

- Q10: normal quality for general machine construction
- Q6: precise quality for machine tool construction
- Q2: particularly precise quality for exceptionally demanding structures

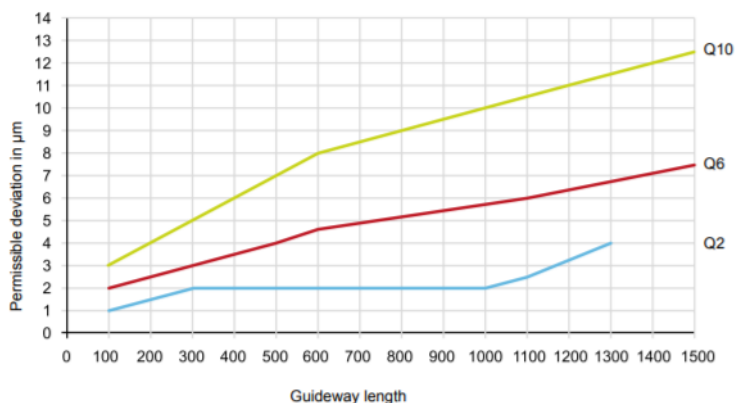


Figure 35: Parallelism of the M and V guideways (Egis-SA, 2018)

While the steel parts do make any concept featuring it rather heavy, with a 60 mm long V component weighing 260 gram, this is not insurmountable. With no promising alternatives found after researching, and the Eurosid-2 system already being a proven concept, the closed M and V sliding bearing with needle roller system was chosen to guide the displacement.

In order to achieve the desired 100 mm displacement while keeping the total mass of the slider itself under 0.8 kg, the sliding mechanism was designed as follows (Figure 36, Figure 37 and Figure 38):

- Two V3015 guideways (blue) of 100 mm each (weighing 0.167 kilograms each)
- Two E-HW10 F needle roller cages of 40 mm each (black, inbetween the guideways)
- Two M3015 guideways of 100 mm each (red) with stoppers (orange)
- An aluminum case (light green), which will house the V guideways, IR-TRACC connector, impact absorber and a plastic spring foot (black, at the bottom of Figure 36 and Figure 37)
- An aluminum hull (gray), on which the M guideways will be mounted, and will be connected to the baseplate (dark green in Figure 38) and spring cone (Gray, below the drop tower table in Figure 38)

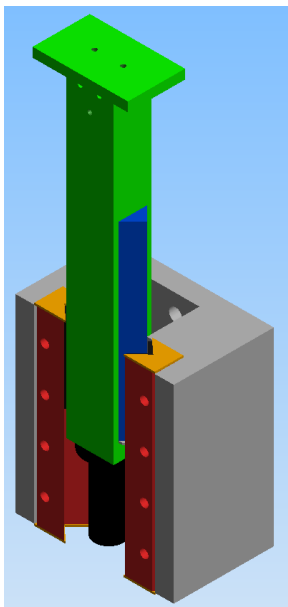


Figure 36: Chosen slider mechanism, extended

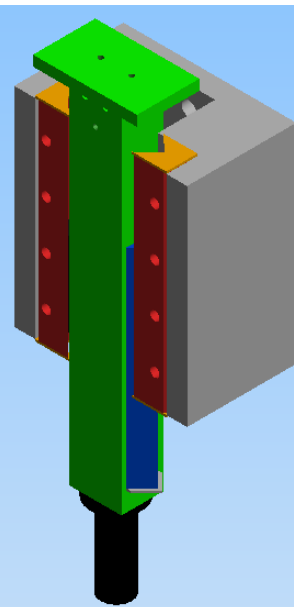


Figure 37: Chosen slider mechanism, compressed

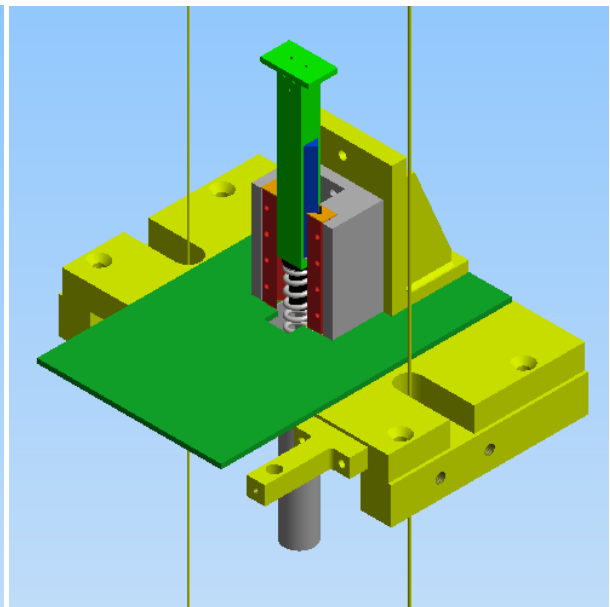


Figure 38: Chosen sliding mechanism, on drop tower table

The (estimated) total mass of the slider can be found in Table 7. Note that only half of the mass of the spring is counted, since only half of it will move.

Table 7: Total mass of the slider

Component	Total mass [kg]
2x V guideways	2 x 0.167
2x Needle roller cages	2 x 0.012 (Estimated)
1x Spring foot	1 x 0.013
1x Spring	0.5 x 0.154
1x Case	1 x 0.147
Total	0.595

5. IR-TRACC placement

Since the IR-TRACC will already have been statically calibrated before it gets tested in a dynamic situation, the set-up is only designed to keep track of the displacement of the IR-TRACC. To this end it is important for the starting positions of the IR-TRACCs to be documented as possible. This chapter details the various possibilities explored by which this would be possible.

5.1 Differences between the variations

For the vertical displacements, it is highly preferred that the IR-TRACCs are positioned as close as possible to the displacer. This means that for all different variations the means of mounting (or alternatively: IR-TRACC foot) must be checked per position. Table 8 offers an overview of the differences per means of mounting (or: IR-TRACC foot), as well as the distance from the origin of the coordinate system inside of the IR-TRACC, the LCS (Local Coordinate System) to the interface plane. LCS will be used as a unifying term for the Upper Thoracic Spine (UTS), Lower Thoracic Spine (LTS) and Lower Spine (LS) coordinate systems. Figure 39 shows the locations of these coordinate system relative to the spine of a 50M THOR dummy. Figure 40 shows the location of the LCS for a (or any) 2D IR-TRACC.

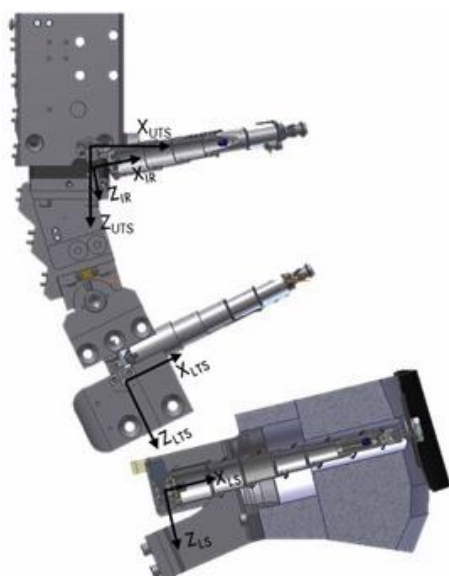


Figure 39: Location of the UTS, LTS and LS on the spine of a 50M THOR dummy

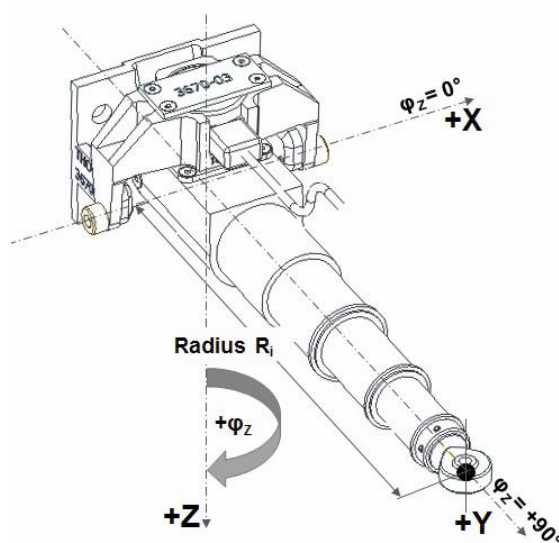
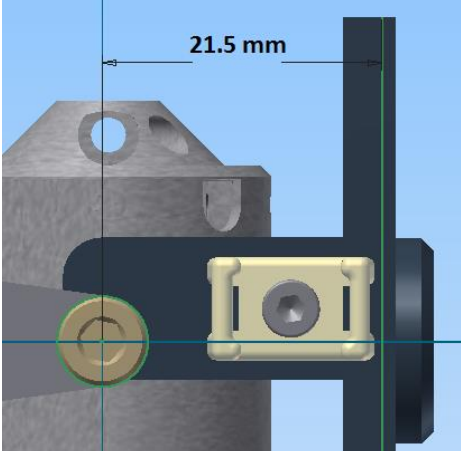
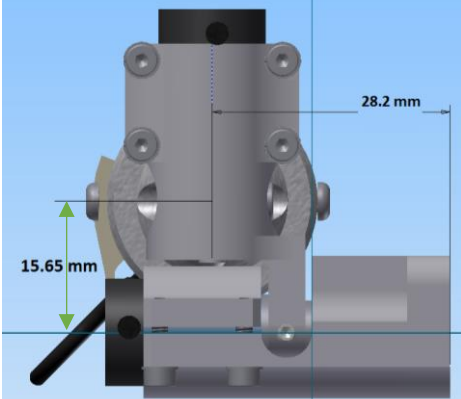
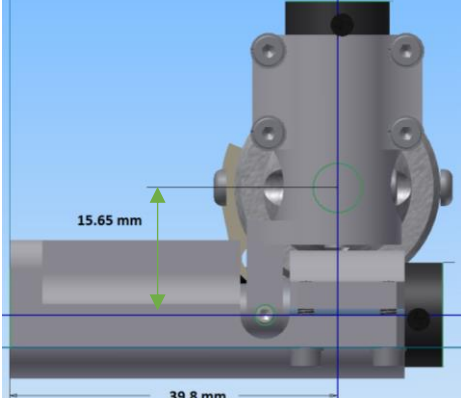
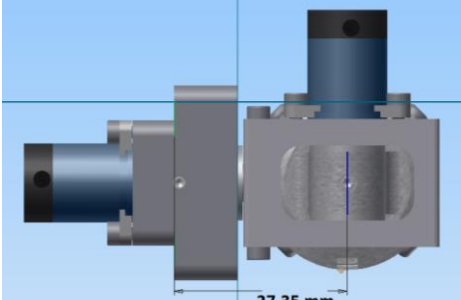


Figure 40: Position of the LCS for a 2D IR-TRACC

Table 8: Distance from LCS to interface plane

Variant	Unique properties	Picture
2D	LCS to interface: 21.5 mm	
Upper thorax	LCS to interface: 28.2 mm $\delta=15.65$ mm	
Lower thorax	LCS to interface: 39.8 mm $\delta=15.65$ mm	
Abdomen	LCS to interface: 27.35 mm Part of the instrument goes through the interface plane	

5.1.2 2D-variant unification

With the desired displacements for these IR-TRACCs being identical, not to mention to increase the ease of use, it was found to be preferable for the 2D variations to share the same origin. Initially it was deemed impossible for the IF-367 and IF-368 to be mounted on the same plate, since it would mean their bolt holes would overlap (Figure 41 and Figure 42 **Error! Reference source not found.**).

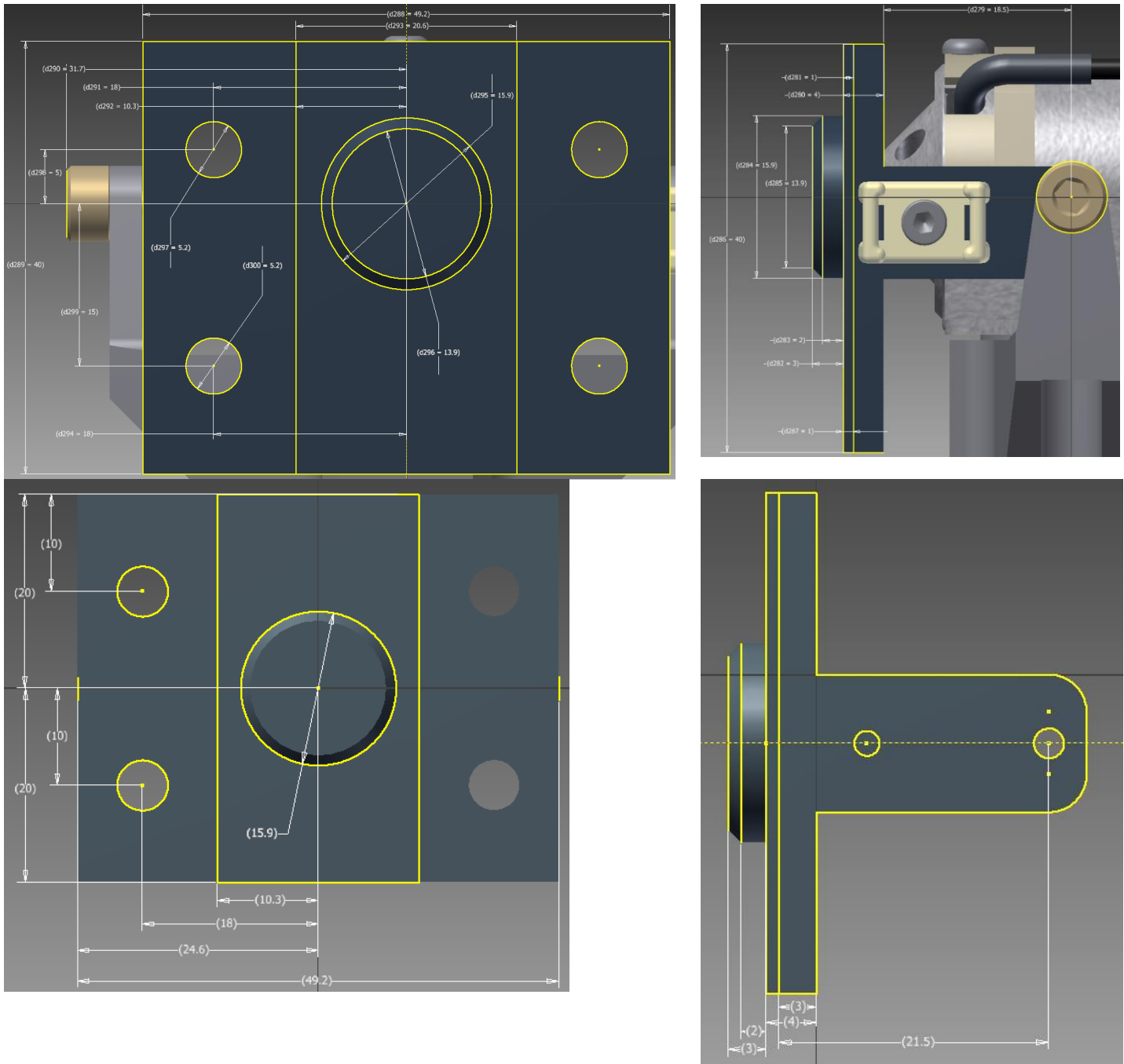


Figure 41: Dimensions of the foot (and LCS) of the IF-367 (above) and IF-368 (below)

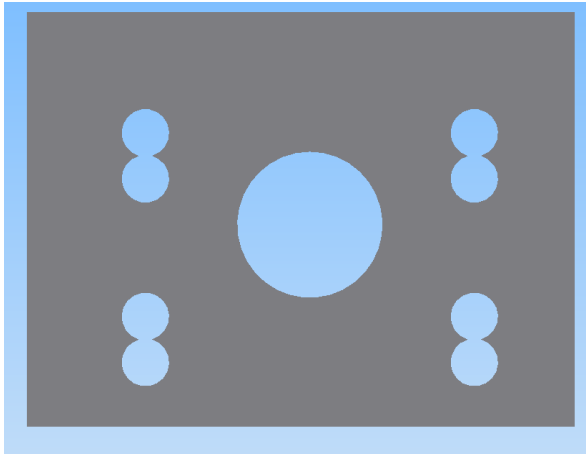


Figure 42: 2D variant overlap of boltholes

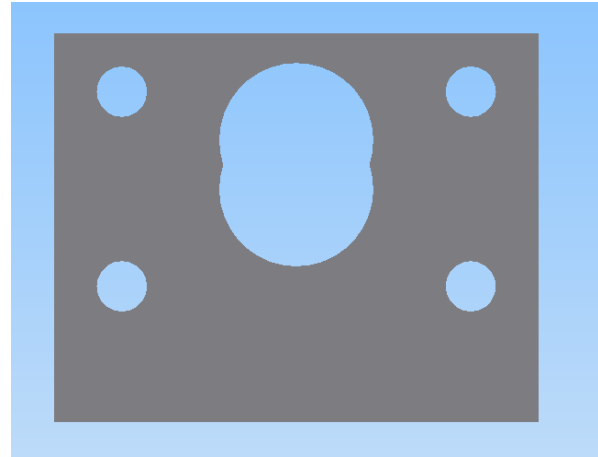


Figure 43: 2D adapter lay-out with non-coinciding LCS

One solution to this problem was to use the same bolt holes for both variations, which would cause a slight offset in the origin, and subsequently the centering hole (Figure 43). This solution however could compromise the accuracy of the set-up. Furthermore the offset in the local starting point would result in a small but significant difference in displacements, which can easily lead to confusion in the future.

With the desire for a uniform displacement being paramount, it was deemed that for a non-moving test set-up not all mounting holes were needed for mounting. By using 2 diagonal mounting holes (blue for the IF-368, red for the IF-367) sufficient stability can be provided to the IR-TRACC, resulting in the setup shown in Figure 44.

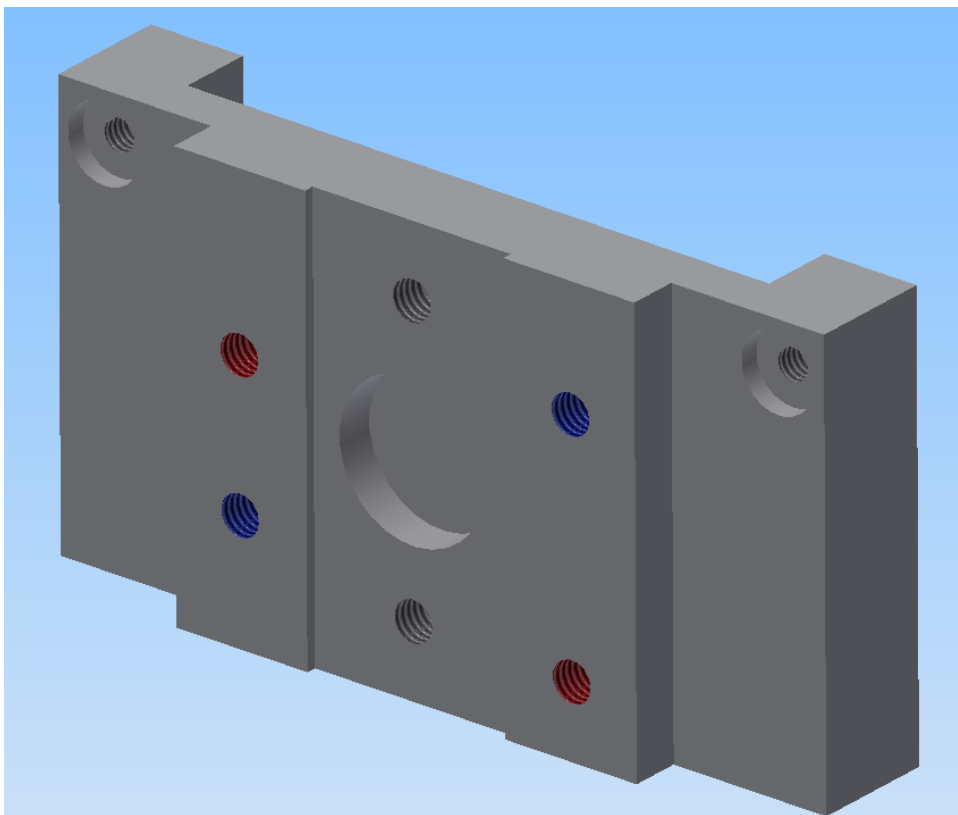


Figure 44: Vertical dual 2D mounting solution

The mounting system of the IF-372 presented a unique challenge to the other variations, due to it being not only different in nature, but also perpendicular to the mounting system of the IF-367 and IF-368 (see Figure 45). After creating several concepts it was determined that creating an adapter that would essentially morph it into a IF-367 or IF-368 would offer the easiest means of compatibility with the existing 2D-adapter (see Figure 46). The decision of adding separate bolt holes for the adapter was made so that the operator could more easily mount the IF-372 in its “personal” adapter, before mounting it to the set-up.

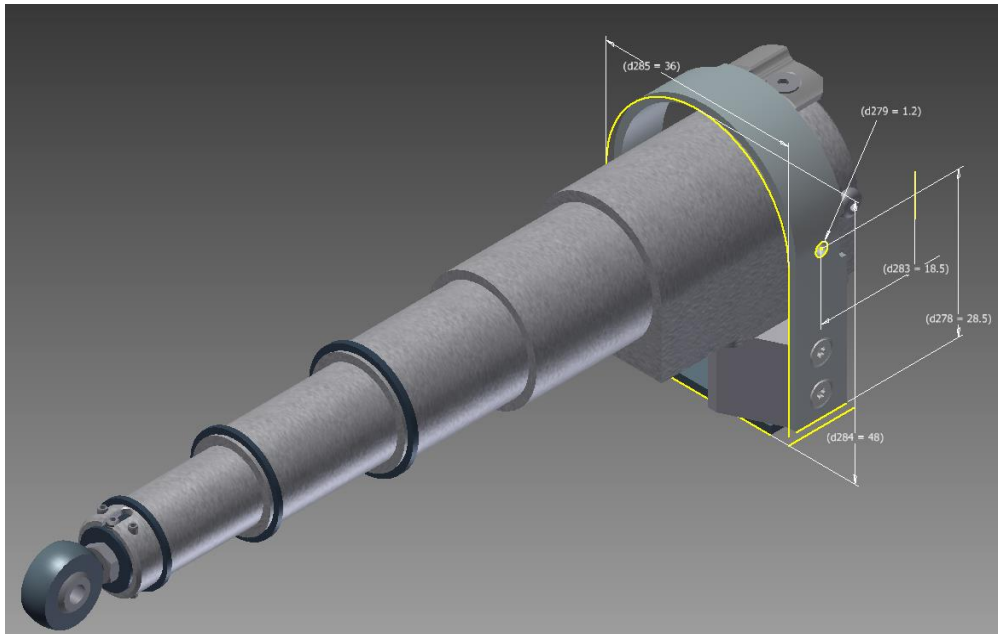


Figure 45: Mounting location of the IF-372

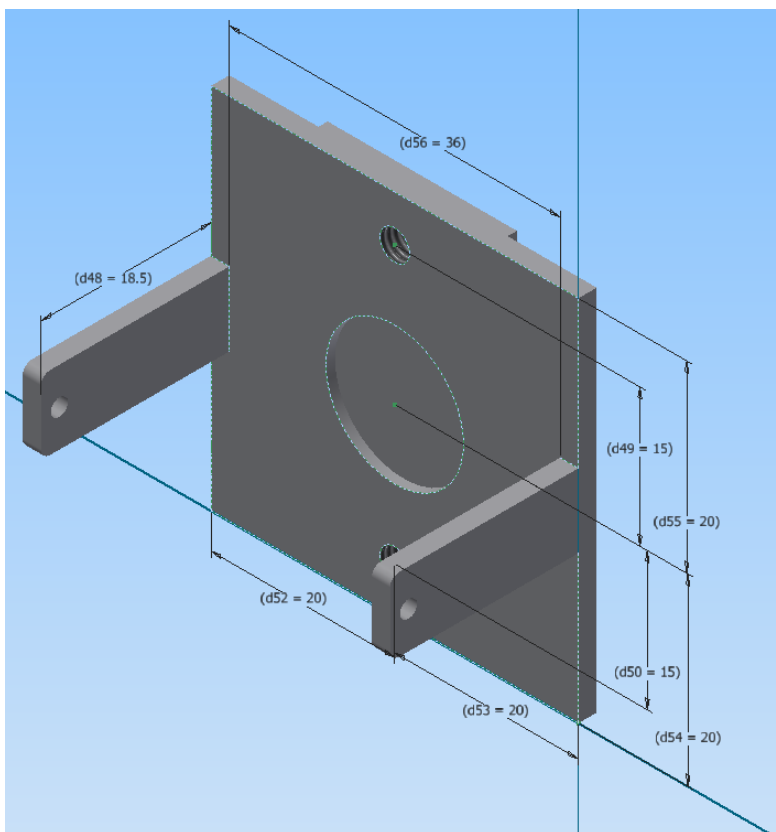


Figure 46: Adapter for the IF-372, or Q10 variant

5.2 Vertical displacement

5.2.1 Reduction to 1D

The vertical displacement tests are meant to test only the IR emitter/receiver combination of each IR-TRACC. This means that one option is to remove the angular rotation components from each IR-TRACC for this test (in Figure 47 this process is shown for the 472-3570, a lower thorax IR-TRACC, it merely involves removing the bolt (blue) connecting the rod to the rotating parts). Doing so will greatly simplify the design needed in order to mount all different IR-TRACCs, as there will effectively be fewer mounting systems.

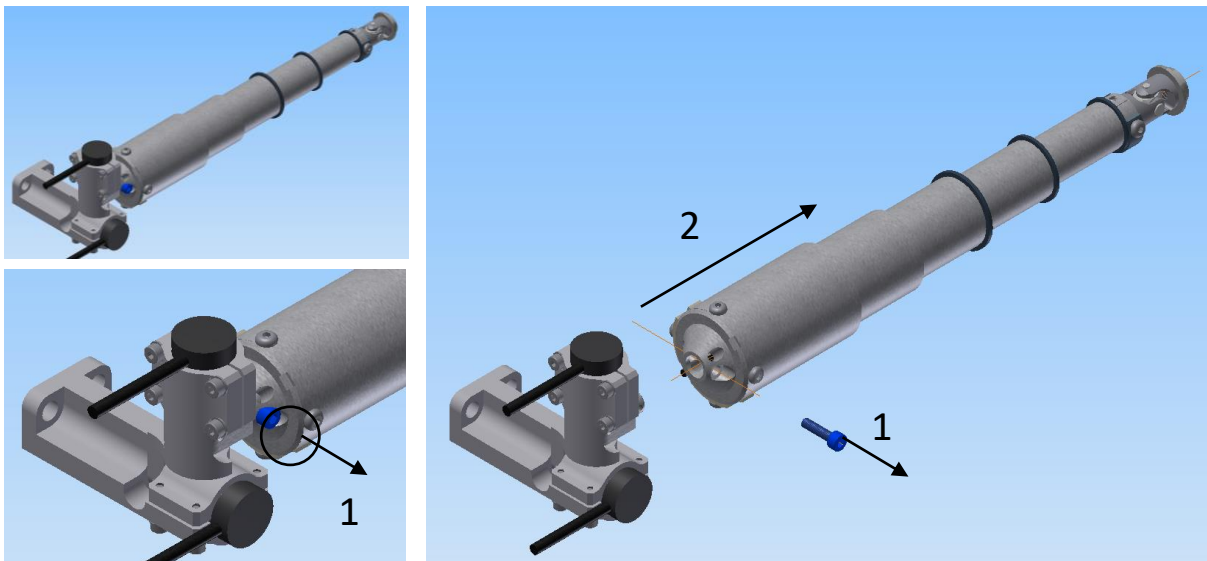


Figure 47: IR-TRACC reduction to 1D on the 472-3570

This is however only applicable to the 3D Thorax IR-TRACCs. The rods of the 3D abdomen IR-TRACCs have a different bottom end (Figure 48) and the 2D variants don't allow for reduction.

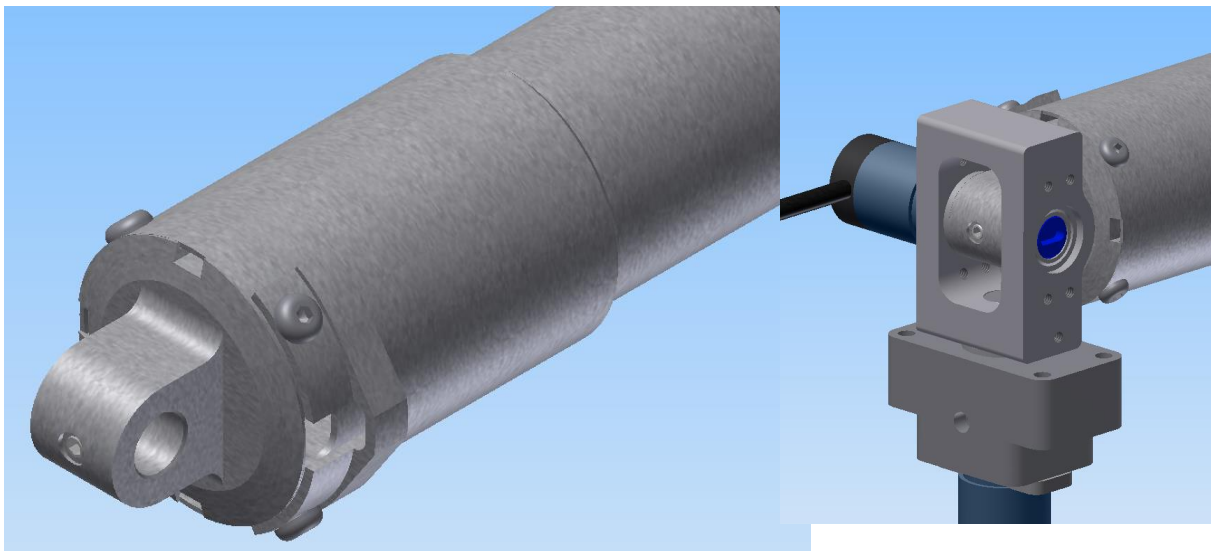


Figure 48: 472-3570 bottom end

Reduction of the variants that allow for it results in four different starting lengths (125 mm for the 2D variants, 135 mm and 160 mm for the 3D thorax variants, and 185 for the abdomen variants).

Figure 49 shows a simple adapter in which the IR-TRACCs could be mounted (figure 34 shows this process with a (reduced to) 1D variant, figure 35 with a non-reduced 2D).

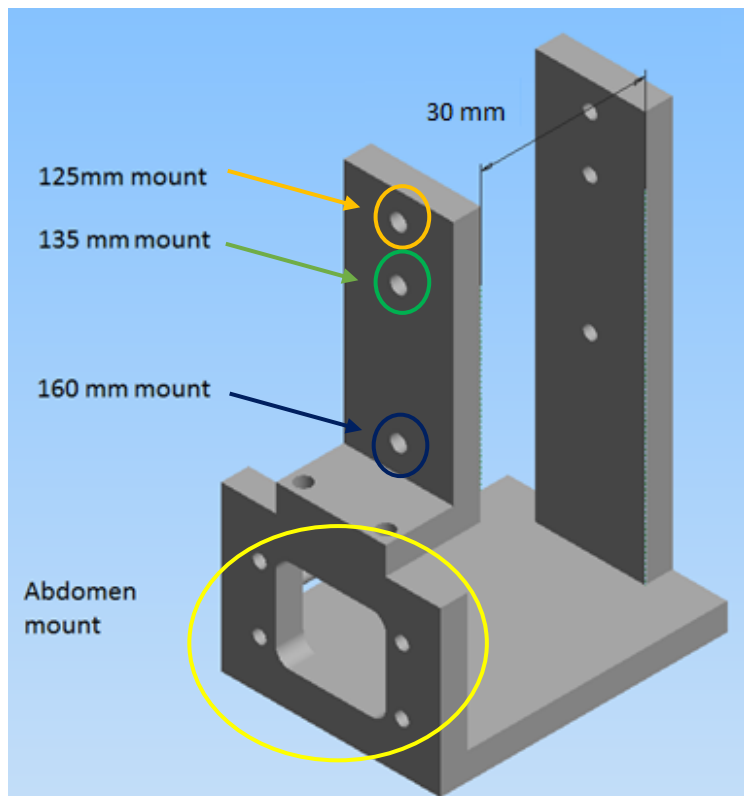


Figure 49: 1D reduction concept

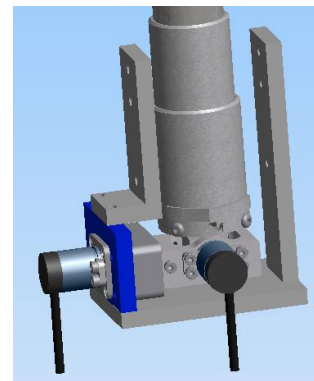


Figure 50: 1D reduction concept with abdomen variant installed

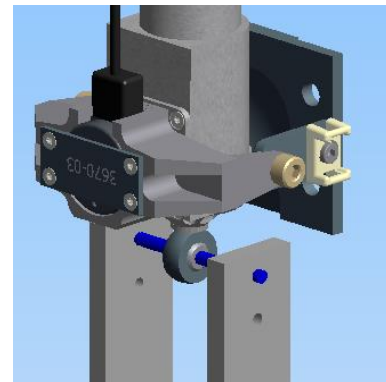


Figure 51: 1D reduction concept with 2D variant installed

While this concept does appear to offer a compact means of mounting all IR-TRACCs, it does so at cost. Firstly over half of the IR-TRACC variants will need to be disassembled in order to fit in this concept, while the goal of the set-up is to validate the behavior of the IR-TRACC as a complete system. Secondly in order for the abdomen variant to be actually mountable, either the 30 mm gap would need to be enlarged, or the or the mounting position will need to be opened from below. Increasing the gap would lead to more distance between the displacement axis and slider, and making the abdomen mount accessible from below would either limit the accessibility of the mount itself (by placing it in the slith, putting the mount under the table) or require an increase of height in the point of impact.

For these reasons this concept was not developed further.

5.2.2 Multi-adapter mounting

In an effort to prevent disassembly being required, a different concept was created in which all mounts would fit on either a single adapter, or an extension of the adapter. Keeping the same starting distances as stated before, eventually the design shown in Figure 52 through Figure 57 Figure 52 was created.

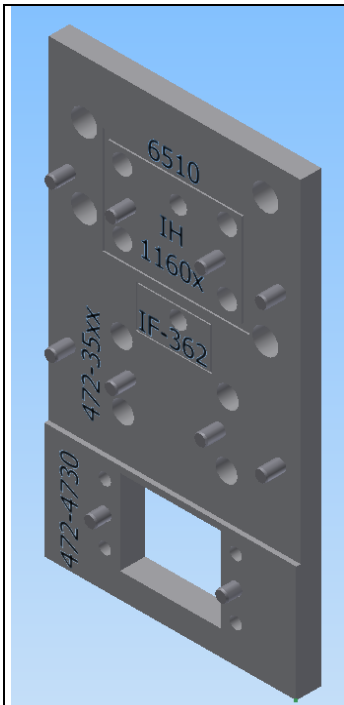


Figure 52: Vertical multi-mounting solution, main part

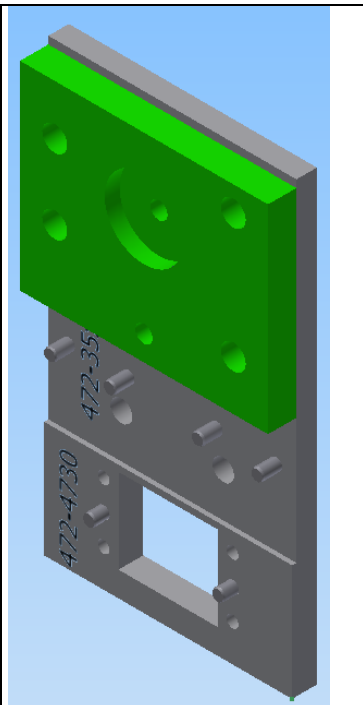


Figure 53: Multi-mounting solution, main part with 2D adapter

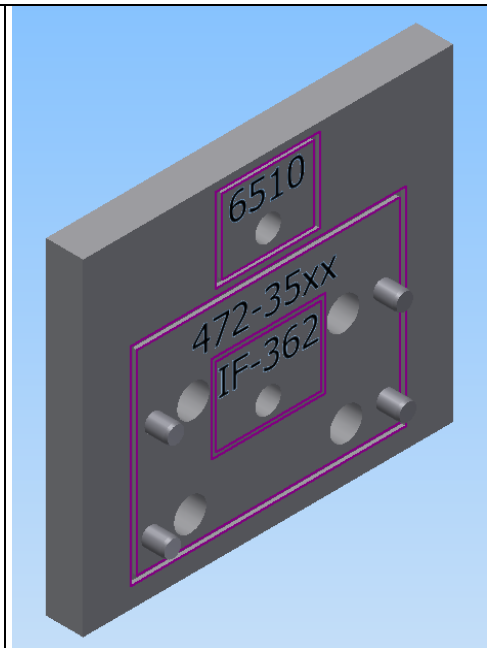


Figure 54: Vertical multi-mounting solution, opposite part

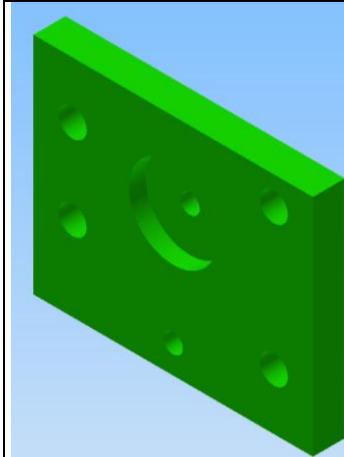


Figure 56: Multi-mounting adapter, 2D adapter

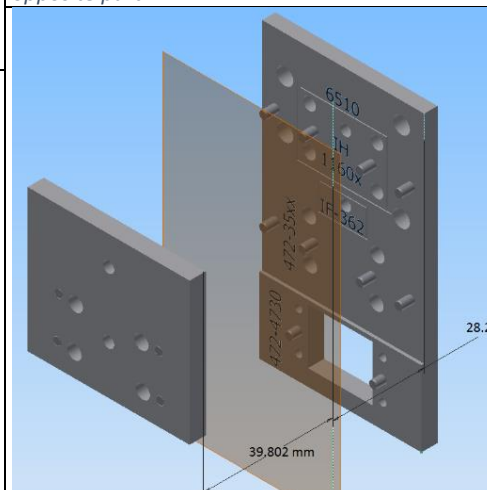


Figure 55: Vertical multi-mounting solution, both parts and central plane

This design consists of a main part (Figure 52) onto which the abdomen and thorax variants can be mounted, as well as the adapter for the 2D variants (green in Figure 51, Figure 53 and Figure 56). A second part (Figure 54) can be used to mount the lower thorax variants, and is placed opposite of the main part, as shown in Figure 55. This second part was necessary due to the abdomen variants having a larger LCS-to-mount distance than the thorax variants (39.8 mm and 28.2mm respectively), as well as to provide additional support for the large pin which would be used to mount the 1D variants.

This concept could however only be placed perpendicular to the slider (Figure 57), since the abdomen IR-TRACCs need to be bolted from the other side than the rest of the variants. Furthermore the opposite part in Figure 54 greatly reduces the accessibility of the main part, and vice versa. While this could be addressed by making this part removable, this would not make efficient use of the space below the part. With the main part being very crowded by pins, boltholes and markings (added in an effort to promote the overview) on top, this design direction was abandoned as well.

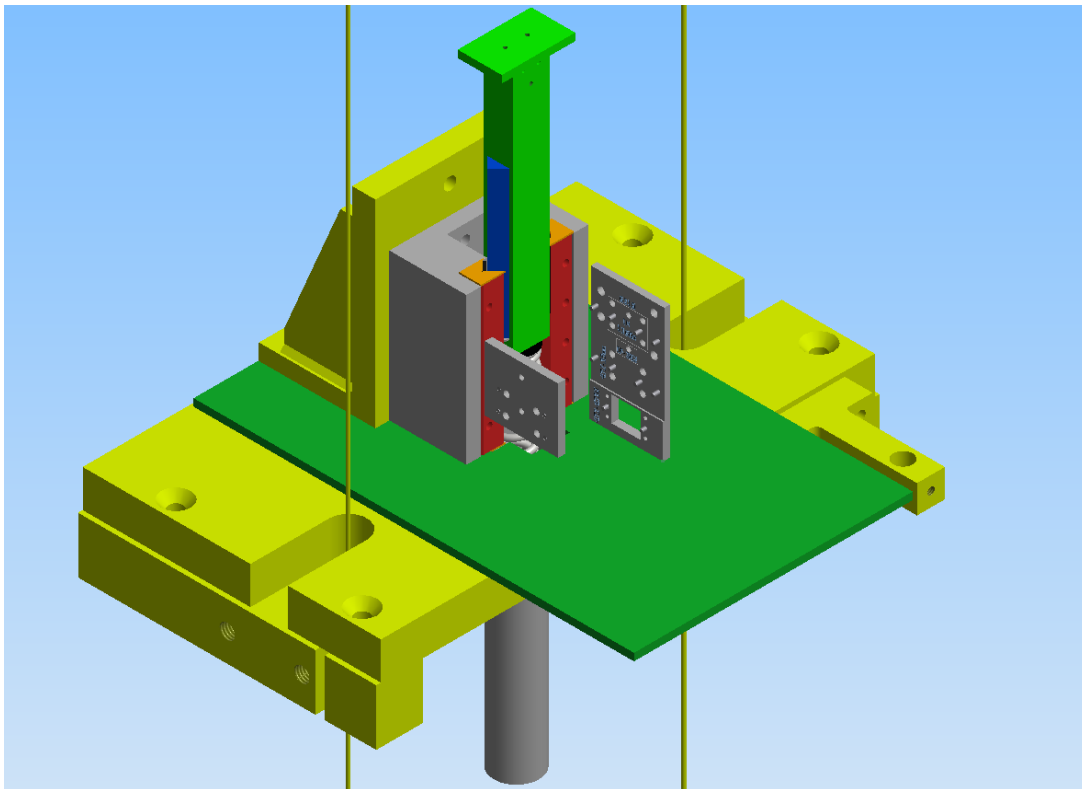


Figure 57: Positioning of Multi-mounting adapter in the set-up

5.2.3 Mirrored adapters

Looking back on the previous concepts, it became apparent that, while the mounting for the 3D-variants could be achieved with little difficulty, attempting to mount them on the same component resulted in a loss of overview. In order to reduce this problem, a design with two opposite adapters was considered. By dividing the mounts equally over the two adapters, the clutter could be halved. By having each component sport both two upper thorax, two lower thorax and one abdomen mount, the adapters could be designed to mirror each other (see Figure 58 **Error! Reference source not found.** for one of the adapters). Both of the adapters need to be positioned perpendicular to the slider due to the opposite fastening direction of the abdomen IR-TRACCs. This means a decision needs to be made regarding whether to put the upper or lower thorax mounts closest to the slider. To make this decision, attention was finally given to the placement of the vertical 2D adapter. With two adapters already left and right of the displacement, and the 2D IR-TRACCs requiring fastening from the front, the only place left for the vertical 2D adapter was behind the displacement axis, or adjacent to the slider. With the 2D IR-TRACC being 31.7 mm wide on either side of the displacement axis, it was initially thought that placing the lower thorax mounts (which are 39.8 mm “wide”) closest to the slider would allow the 2D IR-TRACC to fit between both side adapters (as per Figure 59).

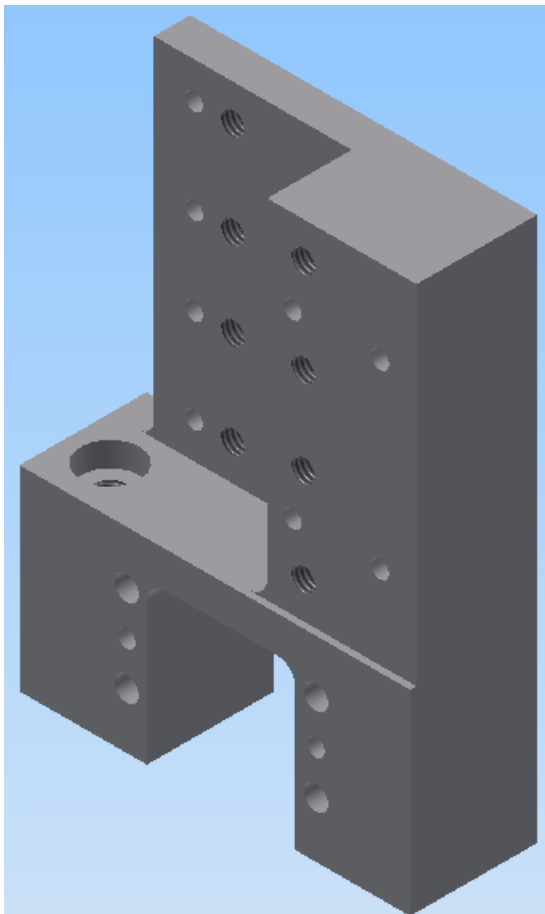


Figure 58: One of the opposite walls of the U-shaped adapter

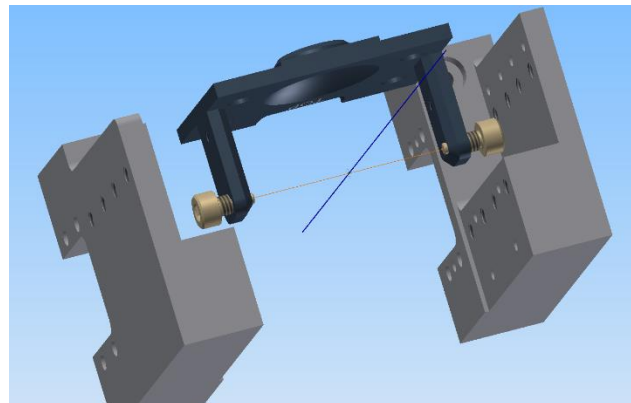


Figure 59: Apparent fit of a 2D IR-TRACC

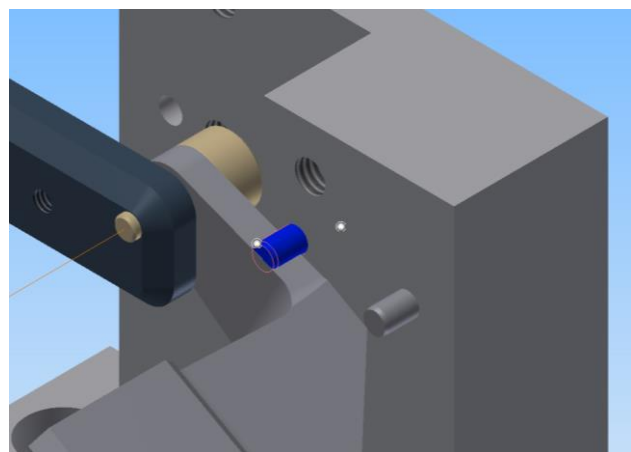


Figure 60: Collision of a 2D IR-TRACC with a centering pin

After using Inventor to install a complete 2D IR-TRACC into the design however, it was found that the 2D IR-TRACC collided with the centering pins of the upper thorax mounts (Figure 60). Observing this issue, the decision was made to make no further attempts to make the vertical 2D adapter compatible with the existing vertical mounting system. In order to still allow for 2D variants to be tested vertically, an adapter was designed to be mounted on the setup with 2 bolts, after both the mirrored adapters had been detached (Figure 63). This adapter will cause the 2D variants to still share the axis of displacement as any variant mounted on the mirrored adapters. This allows the same attachment point to the slider to be used, decreasing the amount of actions between tests of different IR-TRACCs. This set-up is also compatible with digital IR-TRACCs (Figure 61 and Figure 64).

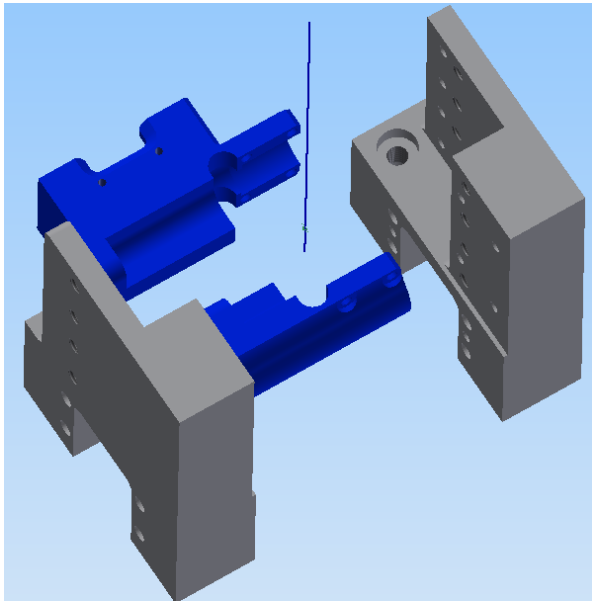


Figure 61: Mounting of the lower and digital upper thorax variants, the blue line indicates the shared axis of displacement

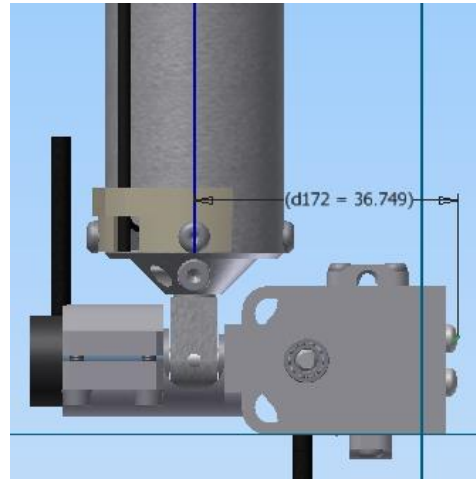


Figure 62: Distance between the LCS and the edge of the foot of digital thorax variants (476-series)

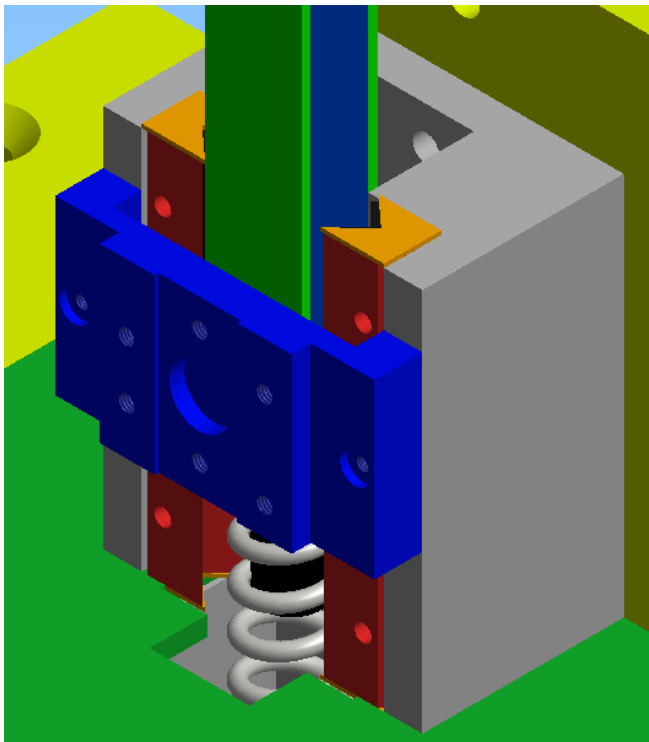


Figure 63: 2D vertical adapter mounted on the sliding mechanism

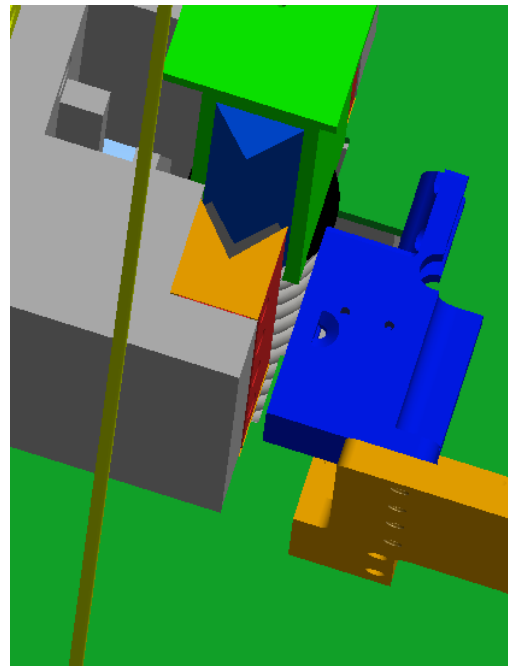


Figure 64: Compatibility with digital variants

5.3 Oblique displacement

The first question to occur when determining the starting positions for the oblique displacements, is what kind of displacement we want to simulate.

One option was to take the displacement of the IR-TRACC over the local Y-axis and Z-axis (see Figure 65) as a requirement, as well as the rotations over these axis as the determining factor. In this case the displacement the IR-TRACC undergoes during the test would be nearly identical to the displacement during a vehicle test. Since this would result in an explicit proof of accuracy of the IR-TRACCs, this option was investigated thoroughly.

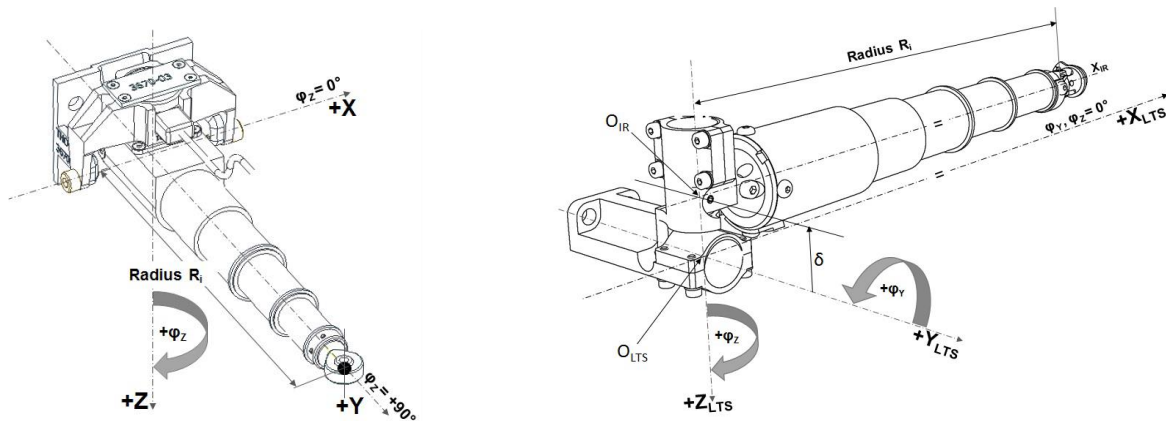


Figure 65: Local axis of the IF-369 (left) 472-4730-2 (right) (ISO 21002)

For this research individual data from both the angular and distance sensors was required, as it would give complete understanding of the IR-TRACC movement during a vehicle test. With this kind of data from an actual vehicle test being unavailable, the choice was made to evaluate data from certification tests instead. The maximum data from these tests could be deemed equivalent to data from a vehicle test for our purpose, as these tests are used to verify their performance under maximum operational circumstances.

Manual review of this data was performed and resulted in Table 9. This table contains per model (blue):

- The maximum displacements from the test (green)
- The suggested movement (yellow)
- The corresponding starting location (orange)

Table 9: Observed and suggested displacements

Properties	Test-Data						Suggested movement					Starting position			
Model	Total Disp. [mm]	X_disp [mm]	Y_disp [mm]	Z_disp [mm]	Y_rot [deg]	Z_rot [deg]	R0 [mm]	R1 [mm]	Disp. [mm]	Rotation Y [deg]	Rotation Z [deg]	Y [mm]	Z [mm]	H0 [mm]	H1 [mm]
IF-367	70	70	-	-	-	25	125	67.3	70	-	25	36.935	-	119.4	78.666
IF-368	70	70	-	-	-	25	125	67.3	70	-	25	36.935	-	119.4	78.666
IF-372	70	70	-	-	-	25	125	67.3	70	-	25	36.935	-	119.4	78.666
472-3550/ 476-3550	51	-42.5	2.5	29	7	5	155	100	64.1	15	5	15.243	61.545	141.483	77.329
472-3560/ 476-3560	52	-42	5	31	12	3	155	100	64.1	15	5	15.243	61.545	141.483	77.329
472-3570/ 476-3570	47.5	-47	-7	-4	10	155	100	64.1	15	5	15.243	61.545	141.483	77.329	155
472-3580/ 476-3580	47.5	-47.5	4	4	5	155	100	64.1	15	5	15.243	61.545	141.483	77.329	155
472-4730 - 1	78	-	-	-	3.5	4	180	129	74.5	20	10	105.01	42.107	140	65.5
472-4730 - 2	76	-	-	-	3	4	180	129	74.5	20	10	105.01	42.107	140	65.5

The suggested movement and corresponding starting positions were obtained by taking the displacements from the test data and inserting them in a newly developed tool. The purpose of this tool was to visualize and decompose the in-test displacements, and rotate the total displacement in such a manner that it becomes suitable for the test set-up. This process will be briefly explained here for a 2D scenario, and complete drawings can be found in Appendix V: Displacement tool. The use of this tool was necessary due to (amongst others) the Thorax variants having an offset between the rotation axes, and the rotation along the Y-axis being limited to 25°. This made calculating a starting position unfeasible, since any equation would be left with 2 or 3 goniometric components. These formulas are displayed in Table 10.

Table 10: Formulas for the coordinates of the IR-TRACC end

$x = X_{IR} + X_1 = \delta * \sin(\varphi_Y) + R * \cos(\varphi_Z) * \cos(\varphi_Y)$
$y = Y_{IR} + Y_1 = R * \sin(\varphi_Z)$
$z = Z_{IR} + Z_1 = \delta * \cos(\varphi_Y) - R * \cos(\varphi_Z) * \sin(\varphi_Y)$

While the rotation axes of the abdomen variants do not have an offset, their construction only allows for ± 15° of rotation along the Z-axis.

Using Inventor first two perpendicular lines representing the displacement along the X- and Z-axes were drawn (orange in Figure 66). Regarding these displacements as the catheti of a triangle, said

triangle was completed by drawing the hypotenuse (blue in Figure 66). This hypotenuse is the displacement we would like the IR-TRACC to experience in the set-up, and would subsequently be regarded as the translation along the X-axis (vertical) of the test set-up. Next two additional lines (also blue) are drawn from the origin to the edges of the hypotenuse, representing the tubes of the IR-TRACC (Figure 67). By defining the length of the IR-TRACC before the displacement (125 mm) and the Z-axis rotation during the displacement, the length after the displacement is obtained (67mm). Now that the IR-TRACC has been fully constrained, a new coordinate system is drawn in the figure. This system consists of a line coincident with the hypotenuse of the triangle as the new X-axis, and a second line perpendicular to the new X-axis from the origin as the new Y-axis (the red lines in Figure 68).

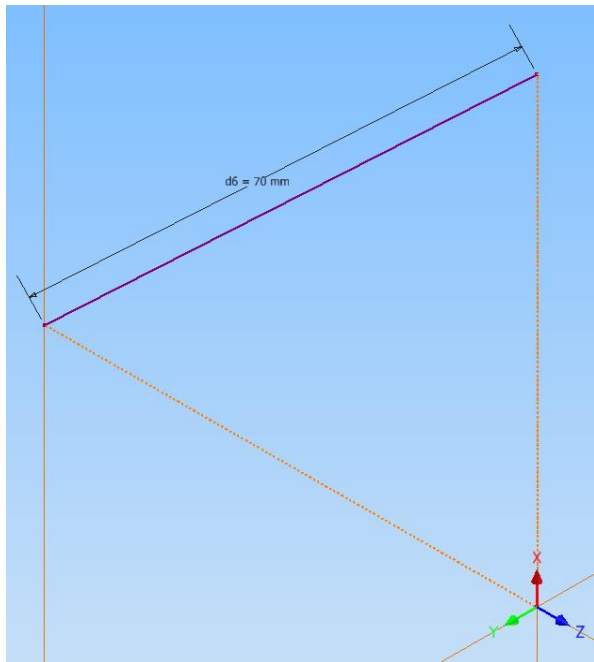


Figure 66: Decomposition of the displacement

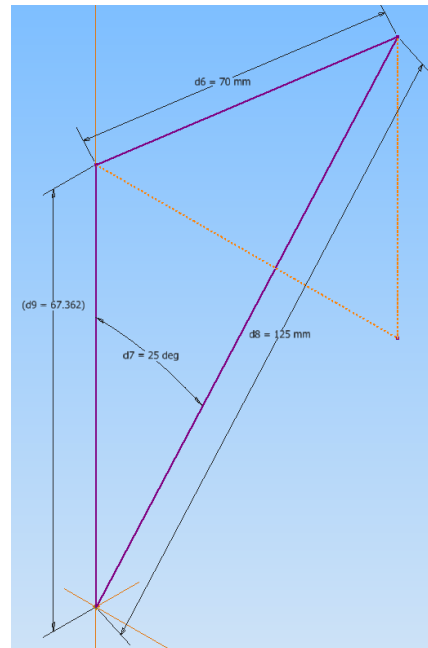


Figure 67: Addition of IR-TRACC length and rotation

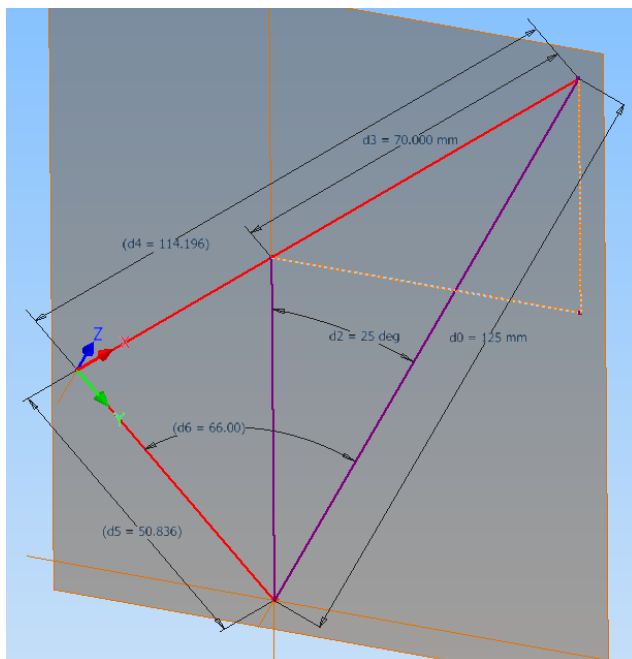


Figure 68: IR-TRACC placement in the set-up Coordinate System

While this approach may be exorbitant for the 2D variant, this is not the case for the 3D variants, as detailed earlier. This can also be seen in Figure 69, where the same approach as above has been performed, but this time for an abdomen IR-TRACC.

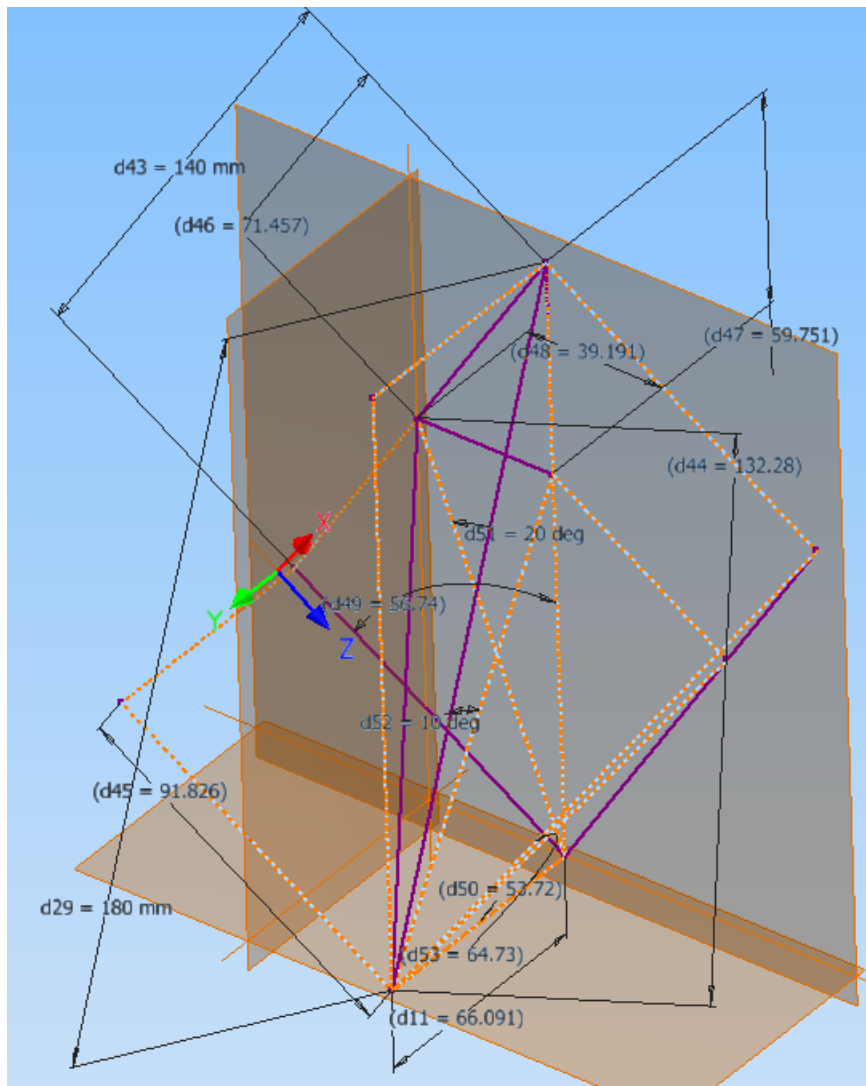


Figure 69: Decomposed approach for an abdomen IR-TRACC

While the development of this tool required considerable time, the main advantage of it is the ability to fully control each component of the displacement. This gives us the ability to completely specify the movement of the IR-TRACC in 3D, and realize this movement with a single one-dimensional stroke.

The tool not only returns the required position relative to the slider, but also the rotational offsets of the IR-TRACC origin. This is especially important to the 3D and Q10 IR-TRACCs, since they suffer from rotation limitations. Below in Figure 70 the adapter for the movement specified for the Abdomen IR-TRACCs (472-4730) in Table 9 can be seen.

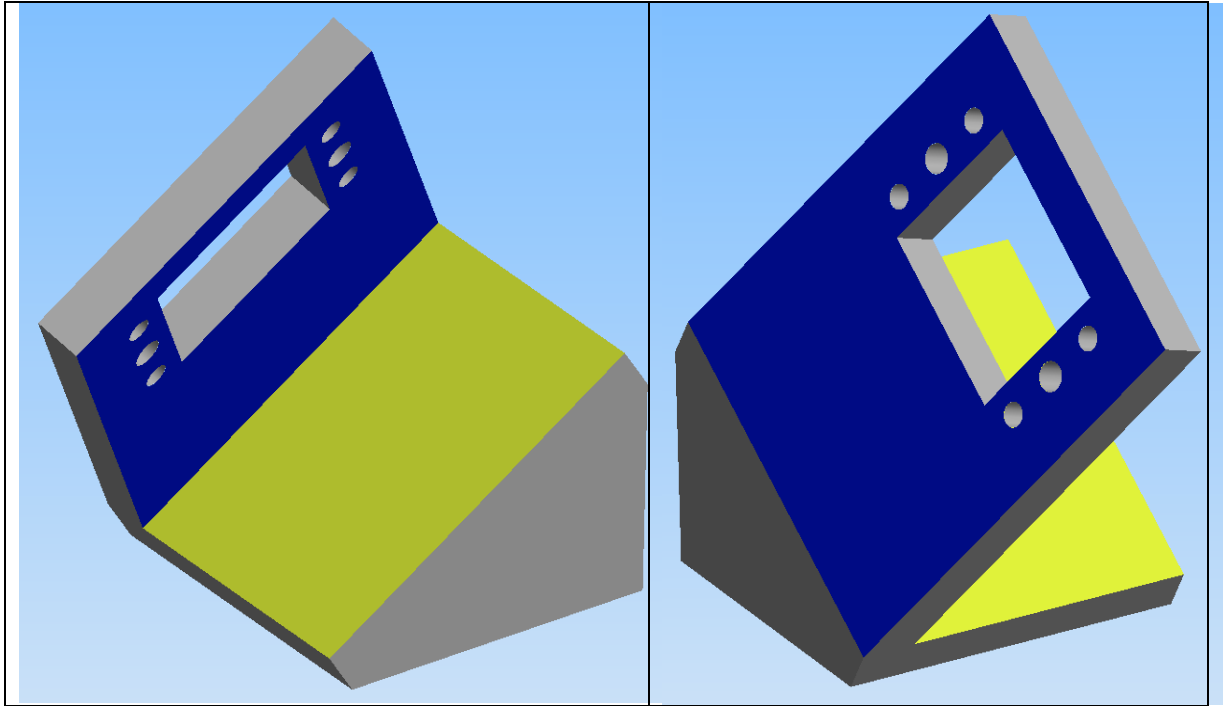


Figure 70: Abdomen IR-TRACC adapter, oblique

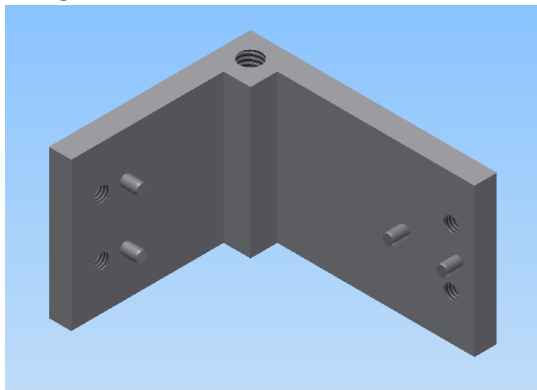
While this option adapter would allow us the desired displacement, production would be quite complicated. This is mainly due to a requirement of high flatness of the blue surface. The angle between the yellow surface and ground plane, as well as the angle between the blue and yellow plane would also have to be produced very precise ($\pm 0.1^\circ$), since considerable effort has been spent in order to obtain them.

5.3.1 Thorax IR-TRACC placement

While all Thorax variations within a model have a comparable range of motion, their differences in orientation (left- and right-handed) and mounting still force a separate mounting point for each variation. Faced with the prospect of four individual adapters and mounting points, a means to reconcile their differences (see Table 8) were explored.

Since the movement of the lower thoracic sensor overlapped that of the upper thoracic sensor, subjecting them both to the movement of the lower variant would prove the accuracy of both. In order for this to be meaningful in-use however, the local coordinate systems of the IR-TRACCs would have to coincide. This would result in the displacement data of different variations mimicking each other, rather than one “lagging” behind the other.

With accessibility to the boltholes being a necessity, and opposing mounting positions therefore being ruled out, the decision was made for the mounting positions to be perpendicular (Figure 71



). In order for the coordinate systems to coincide, the mounting points for the upper and lower variations were positioned at a specific distance from each other. This distance is equal to the length from the base of the foot to the internal Z-axis of the opposite variant (39.8 and 28.2 mm). This effectively creates a square as shown in Figure 72.

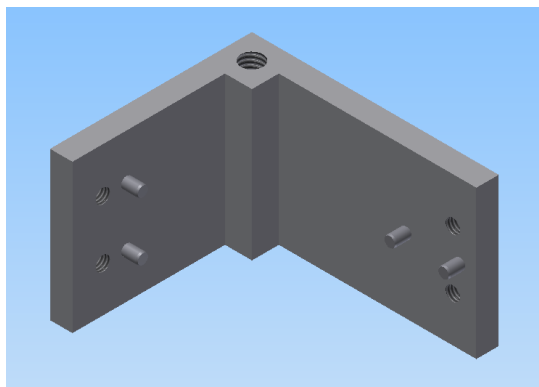


Figure 71: 2-in-1 thorax IR-TRACC adapter

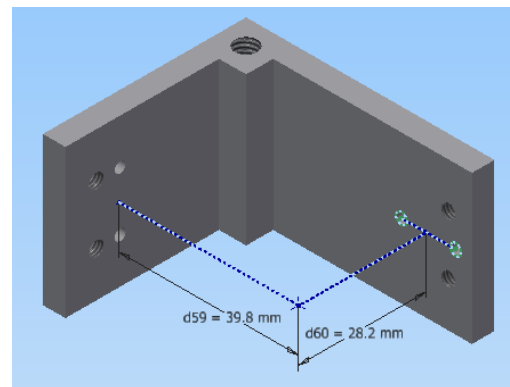


Figure 72: Distances between the mounting positions and their shared center

With an adapter for both the upper and lower thoracic variants finished, the next step was to determine the displacement. Since the complete behavior of the tubes alone can already be verified with the vertical test, the oblique test was chosen to seek to maximize the angular displacement in combination with a tube reduction comparable to a car-test. With a Y-axis rotation limit of 30° in either direction, and a Z-axis rotation limit of 60° or more, a new 3D-sketch was made along the same principles as previously described (Figure 73 and Figure 74).

Keeping the need for simplicity in mind, a choice was also made to keep the Y and Z offset equal to each other. This would allow both mounting points of the adapter to be used without adjustment being necessary. By once again creating a 3D-sketch with CAD-software, and taking care in defining the angles, a different limitation became apparent. With the set-up being capable of displacements up to 100mm, any IR-TRACC other than the Abdomen variants will be at a high risk of damage due to overshoot of the displacement. Keeping with the current example: a displacement of 70mm at a dual offset of 35mm for the Female Thorax variants would result in a maximum φ_Z of $\approx 20^\circ$, which is within the operational range of, but a compressed length of the tubes of only ± 68 mm (Figure 75). This would result in a 3 mm safety margin of the tubes, without accounting for any amount of potential overshoot. Reducing the displacement by 10 mm to 60 mm (Figure 76) improves the margin of safety of course, and a displacement of 60 mm will thus be the recommended value.

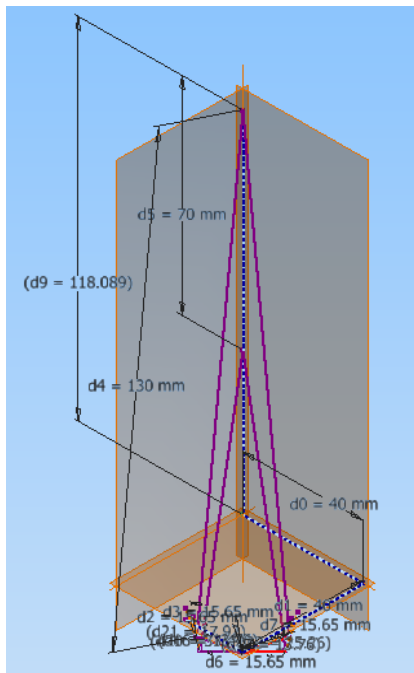


Figure 73: Displacement tool: Female Thorax

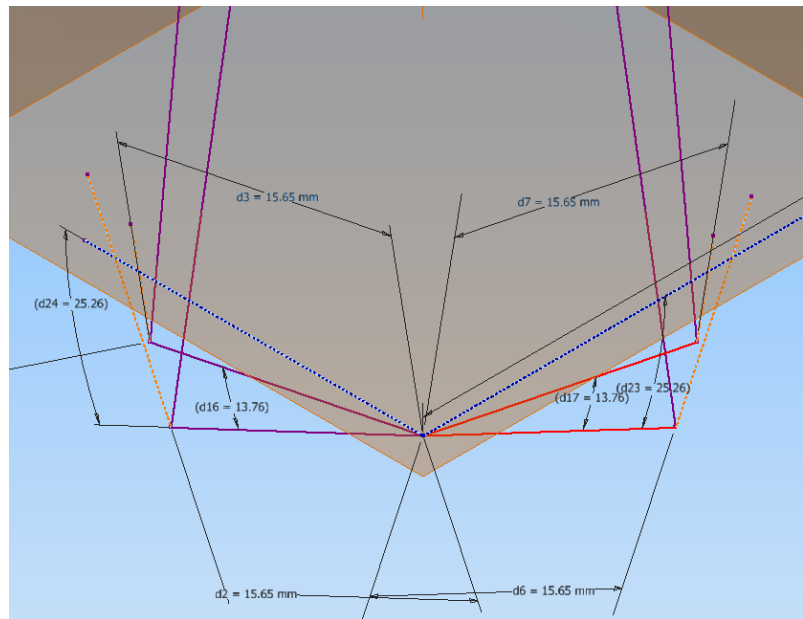


Figure 74: Angular symmetry of the Thorax displacement tool

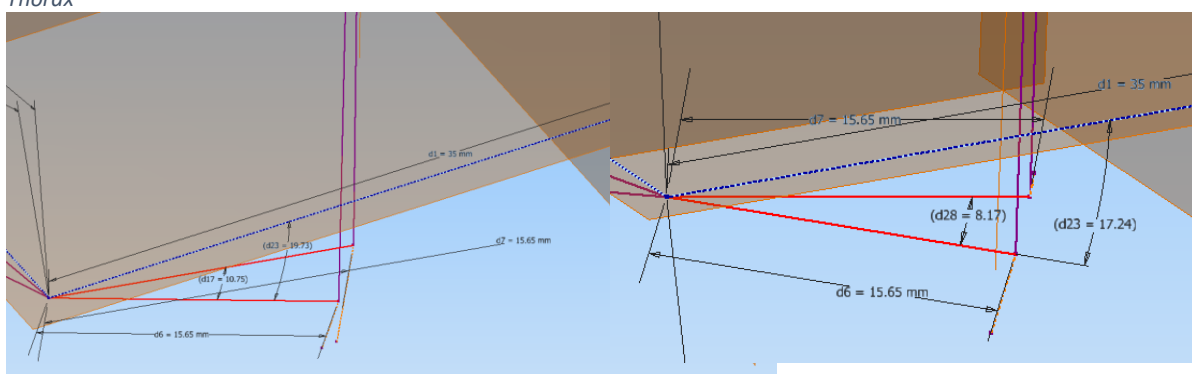


Figure 75: Z-axis rotation for 70mm displacement, 35 mm offsets

Figure 76: Z-axis rotation for 60mm displacement, 35 mm offsets

It is for this reason the offset between the center of the UTS of the Female IR-TRACCs (the IH-11608, IH-11609, IH-11621 and IH-11622) and the joint attachment should be 40mm in both the X and Y direction of the Set-up Coordinate System. Table 11 below contains complete information of the projected start and end positions of the UTS and Joint Center.

Table 11: 3D Thorax displacements

Model	IH-11621 & IH11622		Thor Male	
Value	Begin	End	Begin	End
X_0	125	65	150	60
Y_0	35	-	40	-
Z_0	35	-	40	-
R_i	133.5	80.2	160	81
φ_z	8.7	16.1	9.2	21.2
φ_y	15.2	25.9	14.5	29.6

5.3.2 2D IR-TRACCS

With the desired displacements for these IR-TRACCS being identical, and an option being available to “make” the adapters identical, the set-up shown in Figure 77 was created.

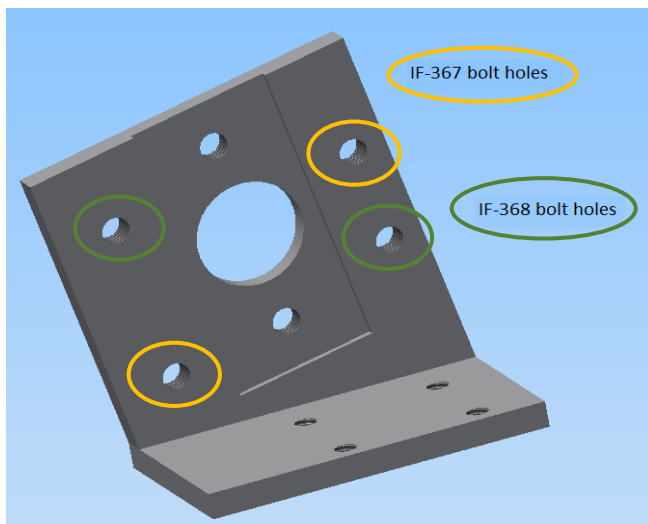


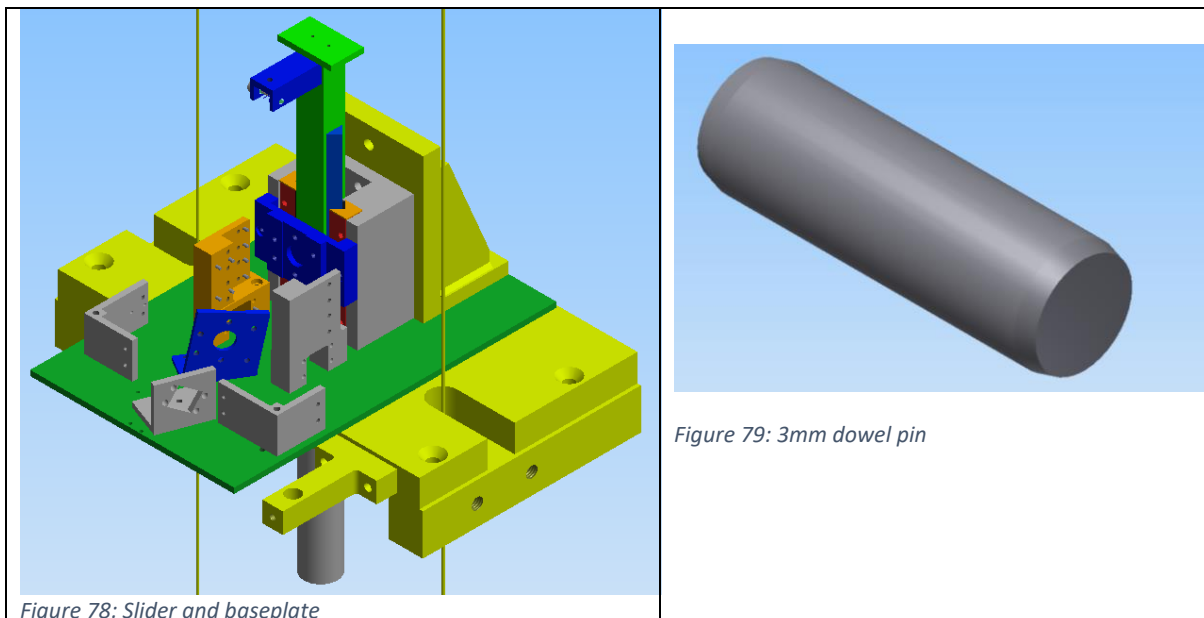
Figure 77: Vertical adapter for oblique displacements

6. Final concept

With the individual components all chosen and the displacements known, the final step in the design process is integrating them into a single solution. This chapter will present the result of this integration, as well as compare the result to the original specifications.

6.1 Complete design

The obvious place to start with a complete design is the placement of the slider (grey in Figure 78) on a plate (green in Figure 78). The plate also has holes on the back, which fit the boltholes on the back of the table, and a recess through which the slider can move and the spring will be connected to the slider. On the bottom of the slider the spring container is mounted with bolts and positioned with the help of 3mm dowel pins (Figure 79).



The first real choice to be made is the position of the displacement sensor. Ideally we would like this sensor to move both parallel to the displacement and as close to the slider as possible for the most accurate readings.

Keeping in mind that the IR-TRACC adapters still need to be placed, and the fact that the set-up will spend a considerable time being stored, the optimal location for the sensor would be in between the sliding unit and the vertical mount (Figure 80). After placing the heartline of the sliders on the on the

impact line, we can see there is 25mm of space available for the sensor to be placed (Figure 81), although this can be increased by decreasing the thickness of the base of the slider unit (10mm).

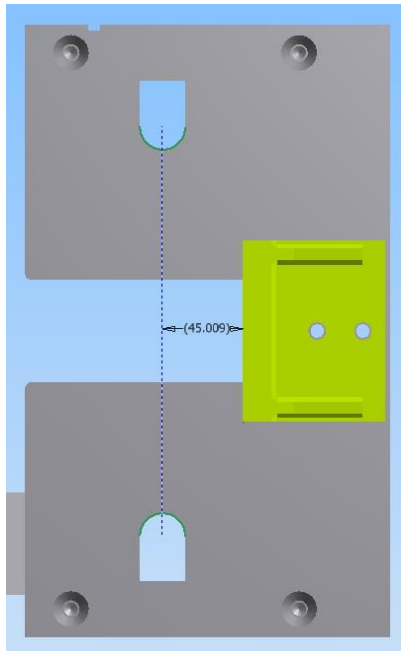


Figure 80: Distance between tower mount and impact point

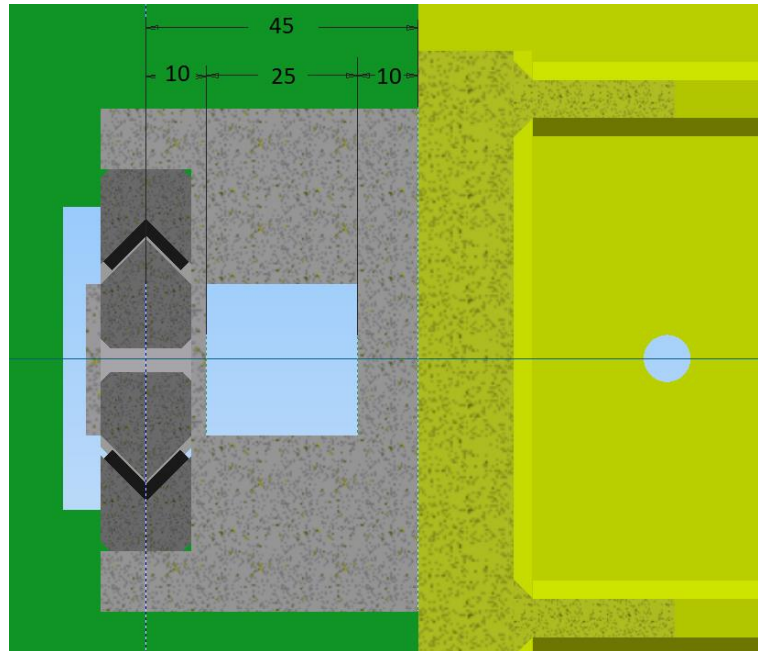


Figure 81: Available space for the sensor (section view of the slider unit on the table)

Earlier in this report, displacements have been specified for each IR-TRACC, which are repeated in Table 12 below. While these coordinates have been calculated with a high precision, these were rounded to the nearest half mm (0.5 mm) upon request for the client. These rounded coordinates were inserted into the same tool with which they were originally created in order to verify these changes in starting position would not endanger the IR-TRACCs. The final coordinates with which their position on the plate has been determined can be found in the same table.

Table 12: Starting positions for each IR-TRACC

Properties	Starting position (Calculated)			Rounded/Final starting position		
	Y [mm]	Z [mm]	H0 [mm]	Y [mm]	Z [mm]	H0 [mm]
IF-367	36.935	-	119.4	37	-	120
472-3550	24.831	67.6	137.254	25	67.5	137.5
472-3560	24.831	67.6	137.254	25	67.5	137.5
472-3570	24.831	67.6	137.254	25	67.5	137.5
472-3580	24.831	67.6	137.254	25	67.5	137.5
IH-11608	29.248	54.493	120	29	54.5	120
IH-11609	29.248	54.493	120	29	54.5	120
IH-11621	29.248	54.493	120	29	54.5	120
IH-11622	29.248	54.493	120	29	54.5	120
472-4730 -1	66.091	91.826	140	66	92	140
472-4730 -2	66.091	91.826	140	66	92	140

These coordinates however apply to the origin of the UCS of each IR-TRACC, not the adapters themselves. In order to account for this, the distance from the UCS origin of each IR-TRACC (when mounted) to the mounting holes on the adapters were attached to the coordinates of the starting positions, and subsequently placed in the same drawing. With 11 different coordinates this drawing does not offer much insight in the process, so therefore the process will be demonstrated with the coordinates of the 2D IR-TRACCs in Figure 82 and shown in-assembly in Figure 83. An image of Inventor sketch can be found in Appendix VI: IR-TRACC Origin locations.

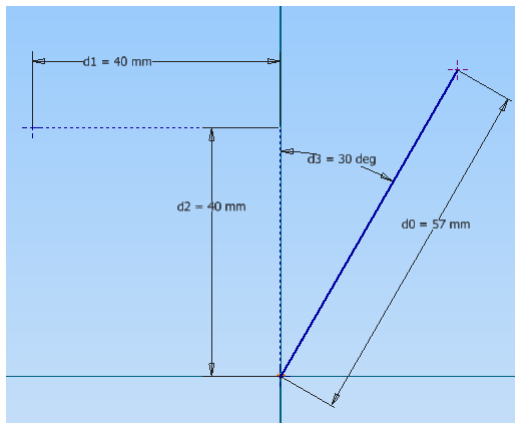


Figure 82: Position of the UCS origin of the 2D IR-TRACCs and male thorax IR-TRACCs

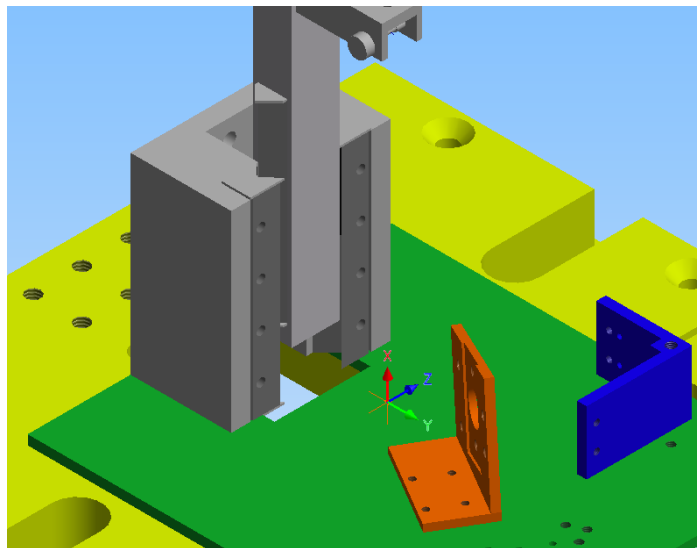


Figure 83: Position of the 2D-Oblique adapter (red) and male thorax adapter (Blue) relative to the TCS origin (on the green plate)

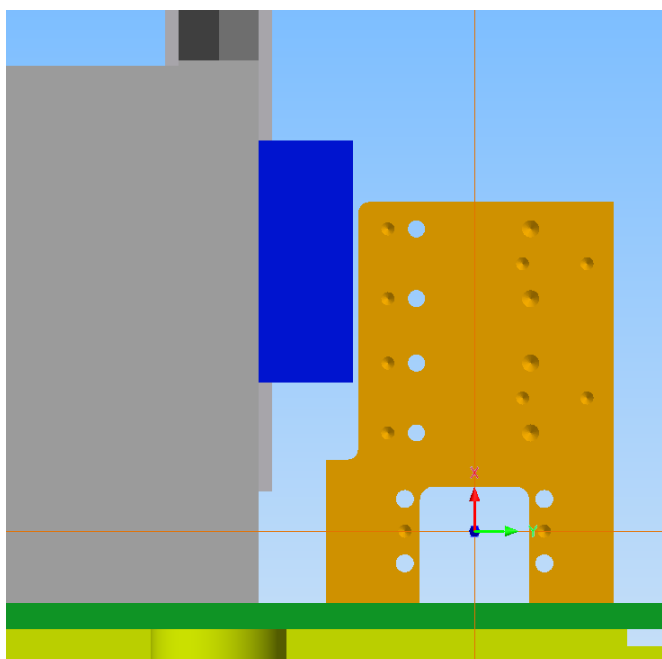


Figure 84: Vertical displacement adapter and Q10 adapter, mounted

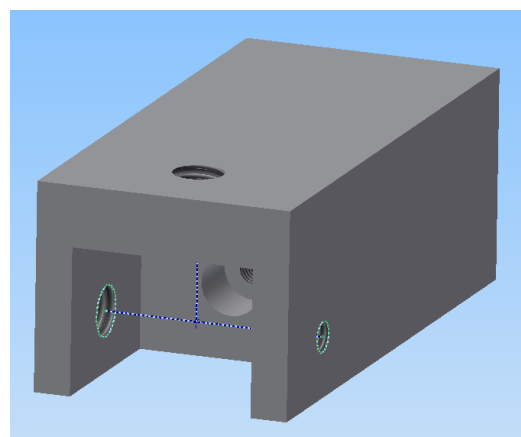


Figure 85: Multi-variant adapter with shared coordinate

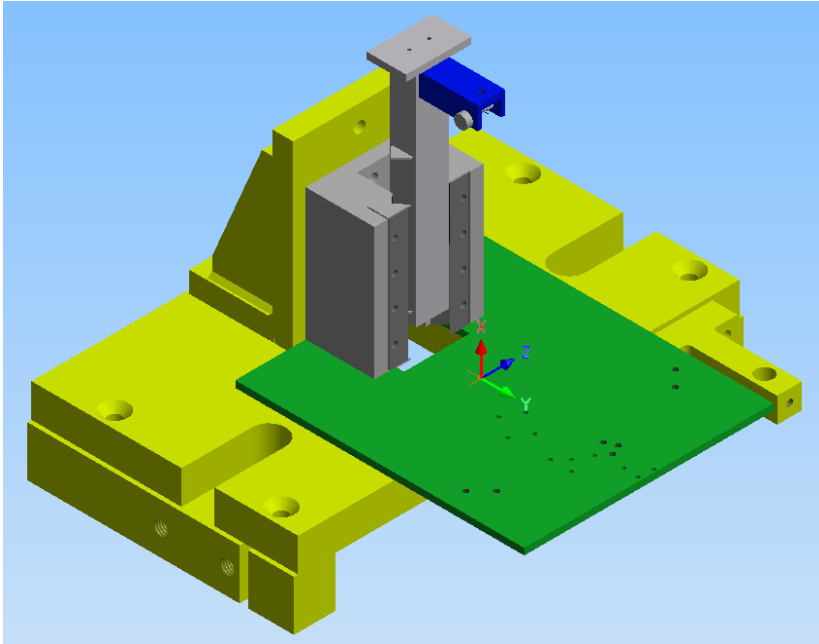


Figure 86: Location of the origin of the Test Coordinate System (TCS)

6.2 Impact conditions

With the movements each IR-TRACC is capable of analyzed, as well as the feasibility of placement in the set-up, it has been decided to subject each IR-TRACC to 2 tests. One test subjects the test-object to a pure vertical displacement, while a second test will subject the 2D and 3D variants to an oblique displacement. Table 13 shows an overview of the impact conditions for vertical displacement per supported model, Table 14 an overview of impact conditions for the oblique displacements per supported model.

These impact conditions were chosen for either maximum displacement for the vertical tests, and optimal similarity with car tests for the oblique tests. With the in-test maximum displacements not expected to exceed 80% of the maximum range of the IR-TRACCs, and angular potentiometers never measuring deflections of more than 30°, verifying the behavior of the IR-TRACCs under these conditions should result in the affirmation of the accuracy of the IR-TRACCs during full scale vehicle tests.

Table 13: Set-up conditions per Model, vertical displacement

Model	Variant	Starting length [mm]	Displacement [mm]	Mounting position	Prescribed drop height [m]	Impact velocity of drop mass at impact [m/s]
6510	1D	125	50		1.64	5.678
IF-362	1D	145	70		3.22	7.95
IF-367	2D	125	70		3.22	7.95
IF-368	2D	125	70		3.22	7.95
IF-372	2D	125	70		3.22	7.95
472-3550; 476-3550	3D	160	80		4.21	9.08
472-3560; 476-3560	3D	160	80		4.21	9.08
472-3570; 476-3570	3D	160	80		4.21	9.08
472-3580; 476-3580	3D	160	80		4.21	9.08
IH-11608	3D	135	60		2.37	6.81
IH-11609	3D	135	60		2.37	6.81
IH-11621	3D	135	60		2.37	6.81
IH-11622	3D	135	60		2.37	6.81
472-4730-1	3D	185	90		5.32	10.22
472-4730-2	3D	185	90		5.32	10.22

Table 14: Impact conditions per IR-TRACC, oblique displacement

Model	Variant	Starting length [mm]	Displacement [mm]	Prescribed drop height [m]	Impact velocity of drop mass at impact [m/s]
IF-367	2D	125	70	3.22	7.95
IF-368	2D	125	70	3.22	7.95
IF-372	2D	125	70	3.22	7.95
472-3550; 476-3550	3D	160	60	2.366	6.81
472-3560; 476-3560	3D	160	60	2.366	6.81
472-3570; 476-3570	3D	160	60	2.366	6.81
472-3580; 476-3580	3D	160	60	2.366	6.81
IH-11608	3D	135	65	2.78	7.38
IH-11609	3D	135	65	2.78	7.38
IH-11621	3D	135	65	2.78	7.38
IH-11622	3D	135	65	2.78	7.38
472-4730-1	3D	185	71.5	3.36	8.12
472-4730-2	3D	185	71.5	3.36	8.12

7. Conclusion

Nr.	Name	Description	Critical value	Validation method	Value in final concept	Reasoning
1	Deceleration	The IR-TRACC needs to be able to experience the same acceleration as if it were used in an actual test	100 G	Calculations	50g	Simulating the set-up showed decelerations of up to 50g do occur, but not up to the specified 100g. This was deemed acceptable since the expected movement closely follows the in-test movement.
2	Impact speed	The impactor of the drop tower with which the test set-up will be used can achieve a certain impact speed. Therefore the test set-up should be capable of withstanding this speed	8 m/s	Calculation based on the required drop height & occurring forces on impact	8 m/s	As Table 13 and Table 14 show, the product will be capable of absorbing the impact fully, without bottoming out
3	IR-TRACC stroke	Due to the impact the IR-TRACC will be displaced. The amount of required displacement will vary with each test and sensor, but the test set-up should be capable of providing a certain range of movement.	100 mm	Measurement in the CAD-model	100 mm	While the initial specifications desired for a displacement of 100 mm minimum, this was later reconsidered. This was done because only the IR-TRACC was capable of the displacement, which it never experienced in tests. In deliberation with the client a maximum displacement of 100 mm was found to be acceptable instead.
4	Compatibility	Humanetics has a wide range of IR-TRACCs, and the test set-up should be compatible with most of these	Yes	Verification of interfacing compatibility by the client	Yes	The adapters specified in Chapter 5 were shown to be capable of mounting all variations of IR-TRACCs.

5	Security	An IR-TRACC is an expensive instrument that requires a lot of time to be calibrated. Therefore it is imperative that any test the IR-TRACC is subjected to does not risk any damage to it.	Yes	Mechanical stop provision	No	While the height of each impact can be increased by 10 cm without endangering the IR-TRACC, a mechanical stop provision only exists at 100mm. Due to the amount of IR-TRACCs involved no simple way of realising a variable mechanical stop provision was found in the time available.
6	Removability	The drop tower will not be used solely for the IR-TRACC verification test. As such the set-up will need to be easily removable from the drop-tower and capable of being stored on a shelf.	Yes	Mass calculation & Analysis of (un)mounting procedures	Yes	The test set-up can be attached and removed from the drop tower with 2 bolts. When not installed the set-up can be placed on a shelf without risk of damage.
7	Durability	The test set-up will be moved and impacted often. In order to preserve the validity of the performed tests the set-up will need to be resistant to bumping and small drops. Also no meaningful deformation may occur between the origin of the IR-TRACCs internal coordinate system and the measured point.	<0.1mm		Yes	The individual components of the set-up are made out of steel and connected by bolts. In order to guarantee accurate placement of each component, dowel pins were used. This provides the design with rigidity comparable to a crash dummy, which is more than adequate for the impacts applied during testing.

8. Recommendations

Short description of what this chapter covers and why it matters.

For future development of a dynamic test set-up, this project advises first and foremost to limit the amount of tests the set-up is to perform. By attempting to make the set-up compatible with both purely vertical displacements, which require a higher displacement and therefore larger spring, and oblique displacements, with no simple way of deriving coordinates from a desired movement, a high amount of time was spent on trying to fully map out these movements. A person with a complete understanding of rotation matrices and access to accessory calculation tools would likely have had more success in this regard.

A different point of discussion that came up during the end of the project is the matter of when the behavior is actually validated. Over the course of this project this was reasoned to be done by subjecting the IR-TRACC to a similar movement as during a test. An alternative way of doing so is to divide the proposed oblique tests into two, where each test would emphasize one rotation over the other.

For the vertical tests it might be possible to simplify the currently mirrored adapters into 1 adapter by putting the existing adapters back-to-back and merging them, but doing so would require a different means of mounting the 1D IR-TRACCs to be found, if desired.

Finally the area behind the displacer could function as a storage for adapters not in use, this would prevent loss of components.

9. Competences

In this chapter the development of the student that executed the project is documented. Due to a lack of relevance to the continuation of the project, this chapter has not been translated into English.

In dit hoofdstuk wordt de ontwikkeling of behoud van competenties van de student verantwoordelijk voor het project gedocumenteerd. Eerst zullen de competenties waarvan aangegeven was dat ze behandeld zouden worden gesommeerd worden. Hierna wordt de ontwikkeling of het behoud van de competenties aangetoond door enkele deelcompetenties te beargumenteren. Voor de beschrijvingen van de deelcompetenties, zie Appendix VII: Competentie-niveaus.

- Competentie 1: Analyseren
Aan te tonen niveau: 3
 - **1a:** Het bezitten van deze deelcompetentie is aangetoond door het opstellen van de onderzoeksvragen in Hoofdstuk 1.5
 - **1c:** Het bezitten van deze deelcompetentie is ingezet bij zowel het opdelen van de hoofdonderzoeksvraag (Hoofdstuk 1.5) als het opstellen en bijwerken van het plan van eisen voor het product (Hoofdstuk 1.6). Zo is bijvoorbeeld de eis van de hoeveelheid verplaatsing van minstens 100 mm bijgesteld naar een maximum van 100 mm. Deze wijziging was geaccepteerd nadat bleek dat een dergelijke verplaatsing niet voorkwam in dummy's. Ook zijn er enkele IR-TRACCs buiten beschouwing gelaten wegens hun unieke eigenschappen en beperkte inzet, en is de eis van de optredende versnellingen aangepast.
 - **1e:** Door het analyseren van het mechanische gedrag van een crash-dummy en deze te benaderen als een massa-veer systeem is het bezitten van deze deelcompetentie aangetoond (Hoofdstuk 3).
- Competentie 2: Ontwerpen
Aan te tonen niveau: 3
 - **2a:** Door aan het eind van het traject bij een eind-concept te arriveren dat gebruikt dient te worden door technici voor onderzoeksdoeleinden en te bevatten is voor mensen met een niet-technische achtergrond is het bezitten van deze competentie aangetoond (Hoofdstuk 6).
 - **2b:** Door het creëren van meerdere adapters waar verschillende IR-TRACCs op gemonteerd moeten worden, met als resultaat dat deze op een opgegeven afstand liggen van een centraal punt, is het bezitten van deze competentie aangetoond.
 - **2c:** Na het ontwerpen van het concept in 0 werd de realisatie gemaakt dat het ontwerp zeer lastig realiseerbaar zou zijn, en daarmee vrij duur voor de eerste versie van een testopstelling. Hierdoor is de keuze gemaakt om die ontwerprichting te laten vervallen, en een ander concept te creëren. Ook is bij onderdelen als de verticale 2D adapter en de veerkoker rekening mee gehouden met een uiteindelijke vervaardiging.
Met deze activiteiten is het bezitten van deze deelcompetentie aangetoond.
- Competentie 8: Professionaliseren
Aan te tonen niveau: 3

- **8a:** Aan het begin van het afstudeertraject is er een Plan van Aanpak opgesteld en zijn er competenties opgesteld met het doel om deze aan te kunnen tonen aan het eind van het afstudeertraject. Gedurende de voortgang van het project zijn deze geherevalueerd op hun relevantie tot het project. Tenslotte is aan het eind van het afstudeertraject teruggeblikt op de ontwikkeling van de student.
Door deze activiteiten is het bezitten van deze deelcompetentie aangetoond.
- **8d:** Tijdens het bedrijfbezoek heb ik een tussenpresentatie gegeven om aan te tonen wat de voortgang in het afstuderen was. Door de feedback na deze presentatie realiseerde ik mij dat ik niet voldoende tijd besteedde aan het duidelijk maken van het onderwerp, doordat ik meer kennis als bekend veronderstelde bij de aanwezigen dan redelijk was. Uit de reacties tijdens en na verdere presentaties heb ik kunnen opmaken dat ik hier verbeteringen heb aangebracht. Dit heb ik ook proberen toe te passen in het schrijven van de scriptie.
Door deze activiteiten is het bezitten van deze deelcompetentie aangetoond.
- **8e:** Gedurende het afstudeertraject zijn er meerdere dagen uitval geweest door depressieve klachten. Alhoewel dit aan het begin al aangegeven was aan Humanetics, heeft dit toch tot vertraging van het traject geleid. Door deze achterstand aan te geven is er na overleg met partijen een verzoek gedaan aan de examencommissie om het eerste inlevermoment van de scriptie te verschuiven naar na de kerstvakantie. Door dit uitstel kreeg de student de mogelijkheid om tijdens de kerstvakantie de achterstand in te halen, zodat deze omstandigheden geen effect hadden op de rest van het afstudeertraject.
Door deze activiteiten is het bezitten van deze deelcompetentie aangetoond.
- **8f:** Het bedrijf waar de afstudeerstage is gelopen is een internationaal bedrijf met werknemers uit onder andere Japan, de Verenigde Staten, Duitsland en Nederland. Hierdoor is de voertaal voor zowel documentatie als communicatie Engels. Dit heeft tot gevolg gehad dat zowel deze scriptie in het Engels is geschreven, als dat communicatie met werknemers in andere landen in het Engels heeft plaatsgevonden. Hierdoor is de kennis van het jargon ook in twee talen gegroeid. Hierdoor wordt het bezitten van deze deelcompetentie als aangetoond beschouwd.

References

- A. McNeill, J. H. (n.d.). CURRENT WORLDWIDE SIDE IMPACT ACTIVITIES – DIVERGENCE VERSUS. <https://pdfs.semanticscholar.org/7c65/05293b51f624dd2b0ee39151c1382ede7474.pdf>.
- Atlas Coevorden. (-). *HVB*. Hengelo: Hengelose Verenfabriek Bakker BV.
- Been, B. (2016). *THOR 3D IR-TRACCs Summary 21MAR16*.
- Beer, J. E. (1996). *Vector equations for engineers: Dynamics (Sixth ed.)*. McGraw Hill.
- Egis-SA. (2018, 9 3). *M AND V GUIDEWAYS | Egis SA*. Retrieved from Egis SA: <http://www.egis-sa.com/en/products/m-and-v-guideways>
- Euro NCAP. (2015, October 7). *Euro NCAP Crash Test of Opel Karl 2015*. Retrieved from Youtube: <https://www.youtube.com/watch?v=GfciJHSYYQo>
- Euro NCAP. (2017, November). *Euro NCAP | Adult Occupant Protection*. Retrieved from Euro NCAP | The European New Car Assessment Programme: <https://www.euroncap.com/en/for-engineers/protocols/adult-occupant-protection/>
- Humanetics ATD. (2018, 8 31). *Infra-Red Telescoping Rod for the Assessment of Chest Compression*. Retrieved from Humanetics ATD main page: <http://www.humaneticsatd.com/instrumentation/ir-tracc>
- Humanetics ATD. (n.d.). *About Us: Humanetics ATD*. Retrieved 9 3, 2018, from Humanetics ATD Web site: <http://www.humaneticsatd.com/about-us>
- ISO. (2015, ISO 6487:2015). *ISO 6487:2015*. Retrieved from Road vehicles -- Measurement techniques in impact tests -- Instrumentation: <https://www.iso.org/standard/64041.html>
- ISO 21002. (n.d.).
- ISO/PRF TS 21476. (n.d.).
- Technical Committee ISO/TC 22. (2018, July 5). *ISO/TR 21002*.
- Wahl, M. (2016). *Evaluation of Alternate Rib Deflection Measurement Technologies*. Friedrichshafen: TRW Automotive.

Appendix I: Original assignment

1. The Assignment: Design of a dynamic IRTACC test setup

1.1 Background

In Crash dummies the deformation of the ribs and the abdomen is commonly measured with an IRTACC (Infra-Red deflection measurement sensor). These sensors are often used in combination with one or two angular potentiometers to obtain 2D or 3D measurements results. Besides the static calibration and the 2D or 3D zero-position verification, there is a need for a dynamic verification test that mimics the in dummy measurement conditions. These voices originate not only from Humanetics, but also from the International Organization for Standardization (ISO). This due to more alternatives to IRTACC entering the market while there are not standards to compare them according to.

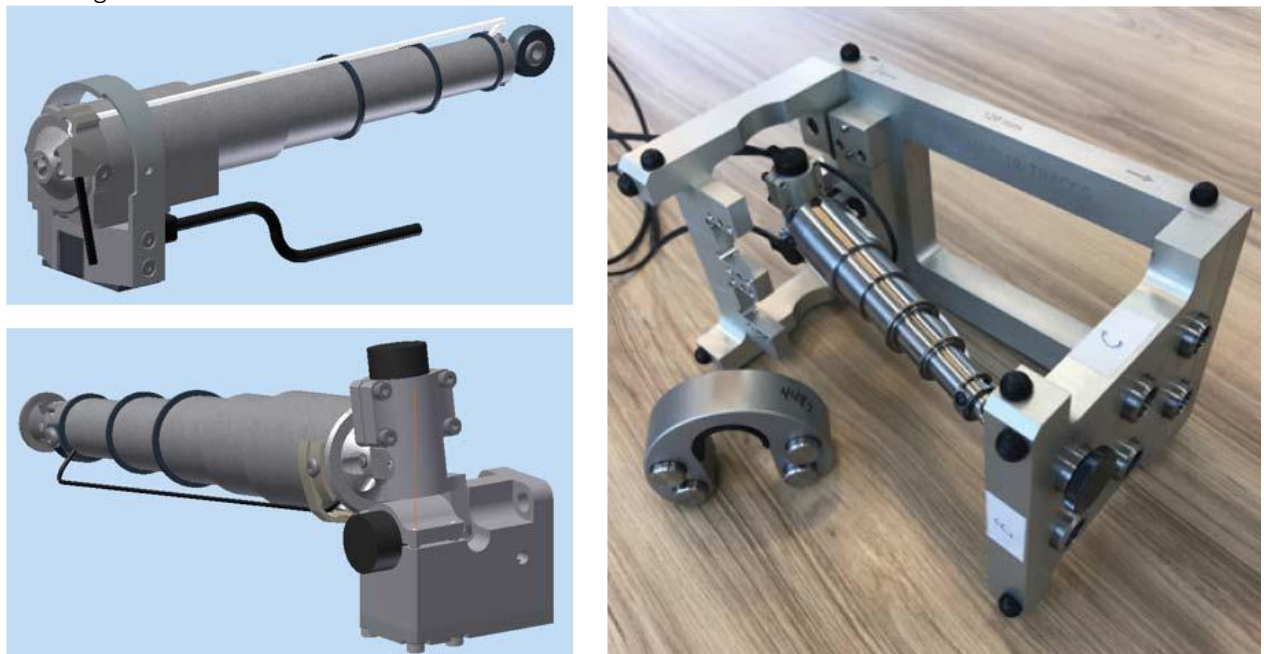


Figure 87: Left top: 2D IRTACC (Infra-Red deflection measurement sensor), Left bottom: 3D IRTACC, Right: Static 3D verification rig suitable for all 3D IRTACCs.

A try-out of the dynamic IRTACC verification test is done by mounting the IRTACCs on a linear guided ES2 rib unit that is impacted with the drop tower with a guided impactor mass (see Figure 3).



Figure 88: Try-out dynamic test set-up, Left: ES2 rib unit with parallel mounted IRTRACC, Right: Drop tower equipment (total height 6.2 m).

The graduate will be the first person to work on this problem, and will be expected to make a detailed analysis of the dynamic forces occurring during a test. The following input is available (in the English language):

- Report on the try-out tests performed with a EuroSID2 rib unit (see Figure 2).
- Information of the IRTRACC mounting interfaces (Inventor models and drawings)
- Information on the drop tower test equipment.

1.2 Thesis objective

The objective of the graduate's task is to design a dynamic test set-up (see the red lined box in Figure 2), that can be used on the drop tower test equipment to test all types of IRTRACCs. The theory behind the impact phenomenon and analysis required to define drop height, impactor mass, obtained accelerations and system stroke are a part of the task. The set-up design should comply with the following (provisional) requirements:

- To be used in combination on the drop tower test equipment (see Figure 2) and later on (if time allows) the E-liner acceleration-deceleration sled test equipment (see Figure 3)
- Suitable for impact up to 8 m/s
- Impactor decelerations up to 200G
- Linear guided stroke of at least 100 mm
- Suitable for all IRTRACC mounting interfaces used on Q-dummies, WorldSID and THOR (uni-axial, 2D and 3D IRTRACCs)
- Damping or ends stop provisions at both stroke ends

If time allows the application on the E-liner test equipment can be detailed.

1.3 Issue and Goal

Issue:	Humanetics has no way of verifying the dynamic behaviour of one of their products: the test-dummies
Goal:	To design a test set-up with which the dynamic behaviour of the test dummies can be tested which can be used in combination with existing test equipment

1.4 Boundaries

The following activities **will** be part of the assignment:

- Visiting and analysing test setup locations
- Creating a complete model of the forces occurring during a typical test, taking into account all (non-negligible) static and dynamic forces that occur during a test
- Generating different ideas to solve the problem
- Creating Proofs-of-Concept and subjecting them to test to determine their viability
- Identifying and investigating existing, relevant norms
- Analysing all information gathered and using it to choose a final concept
- Detailing the final chosen concept
- Documenting all research performed in English

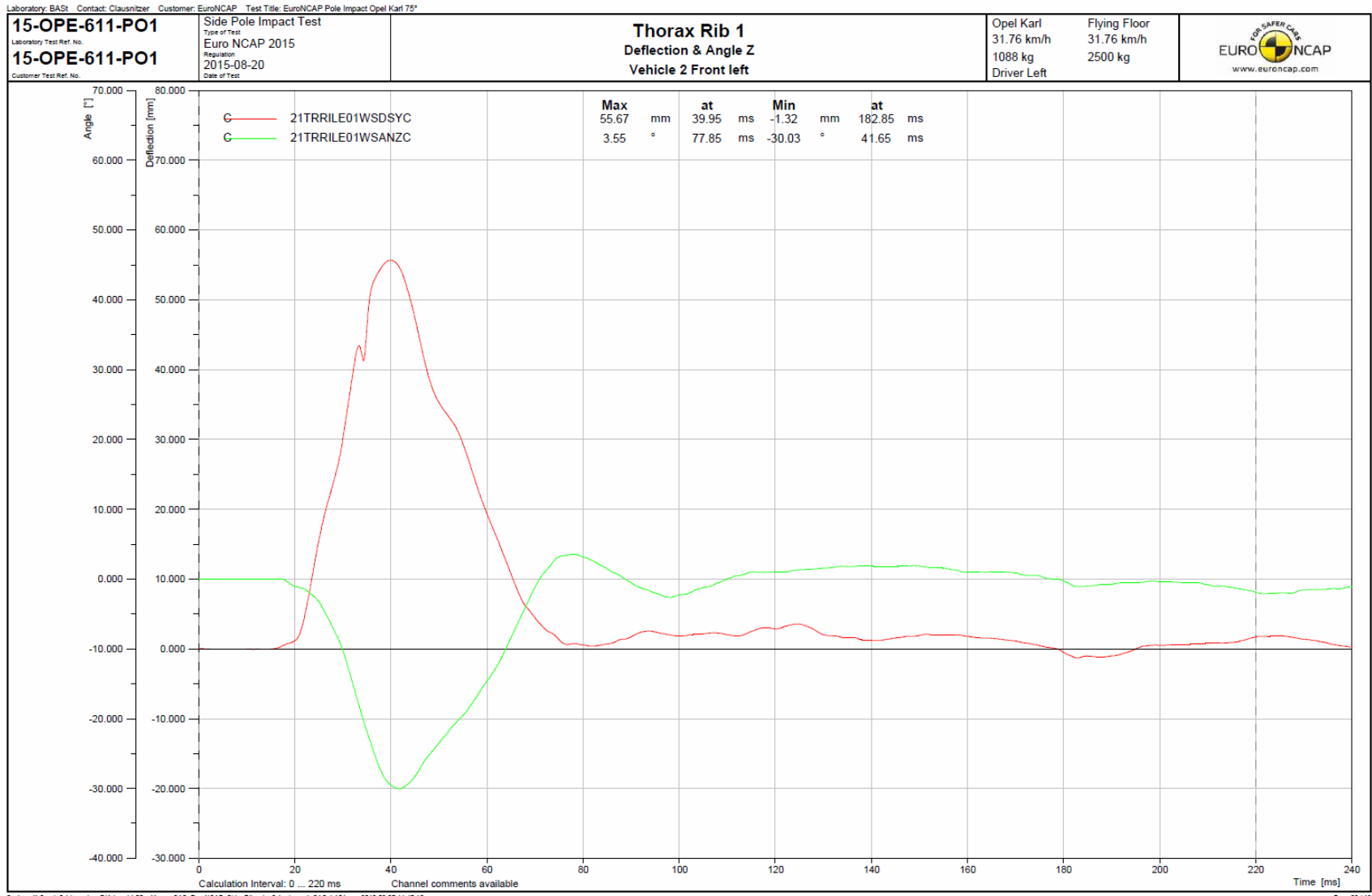
The following **will not** be a part of the assignment:

- Building the complete testing set-up
- Physically verifying whether or not all test equipment is compatible with the final concept
- Communicating with ISO regarding the concept

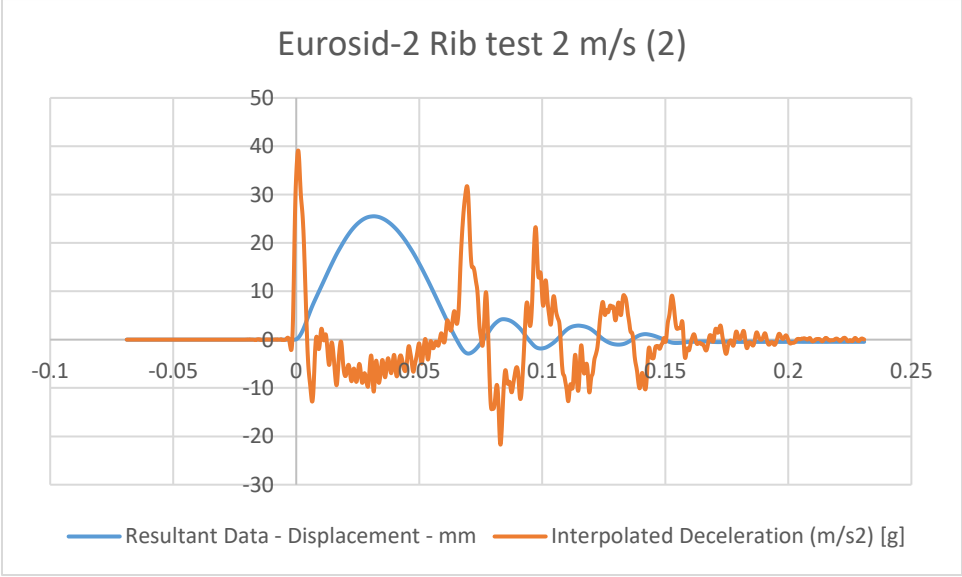
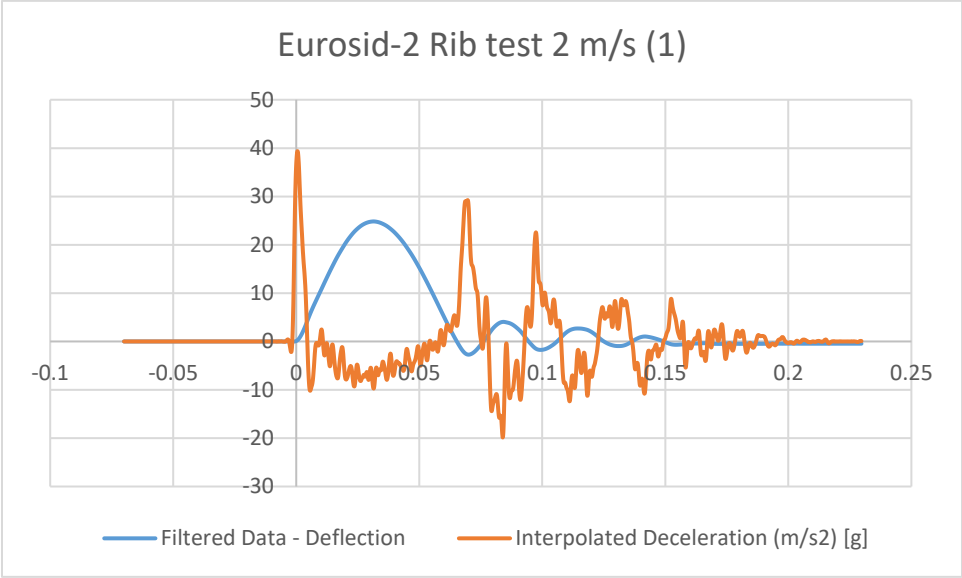
1.5 The final product:

The final product will be a detailed proposal for a research set-up for the purpose of measuring the dynamic behaviour of the rib-units, with at least one part manufactured in the form of a prototype for the purpose of verifying the accuracy of performed simulations.

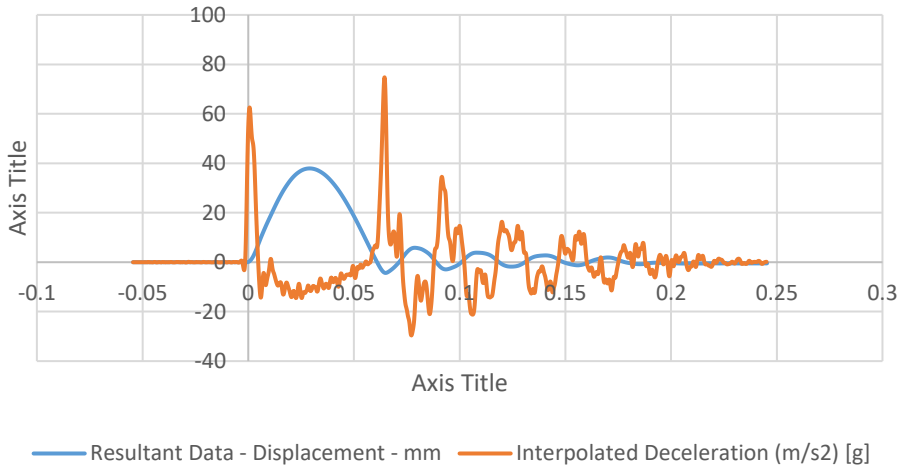
Appendix II: Crash test graph



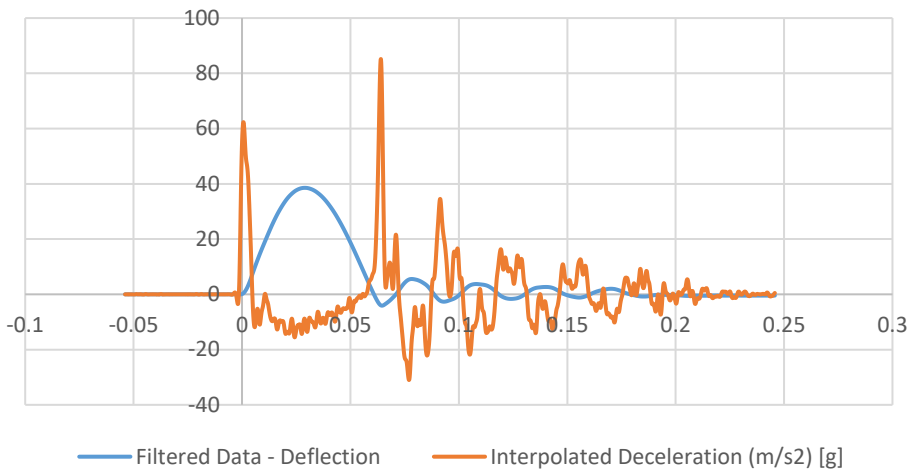
Appendix III: Eurosid-2 test data



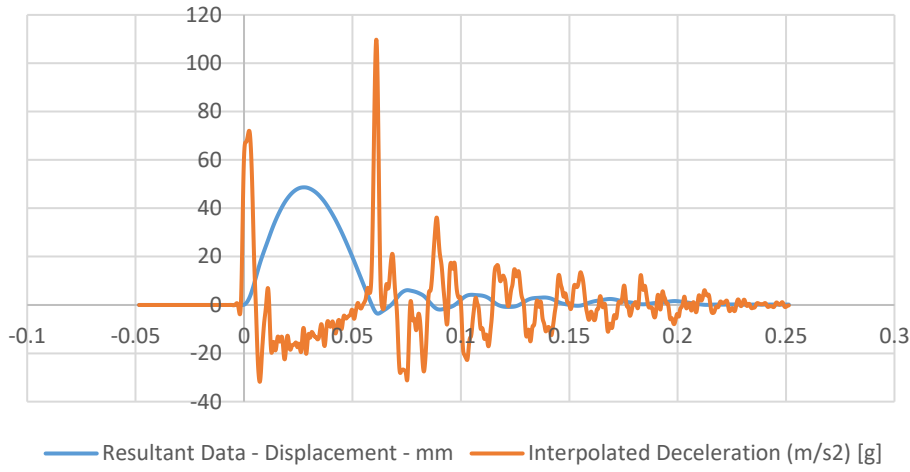
Eurosid-2 Rib test 3 m/s (1)



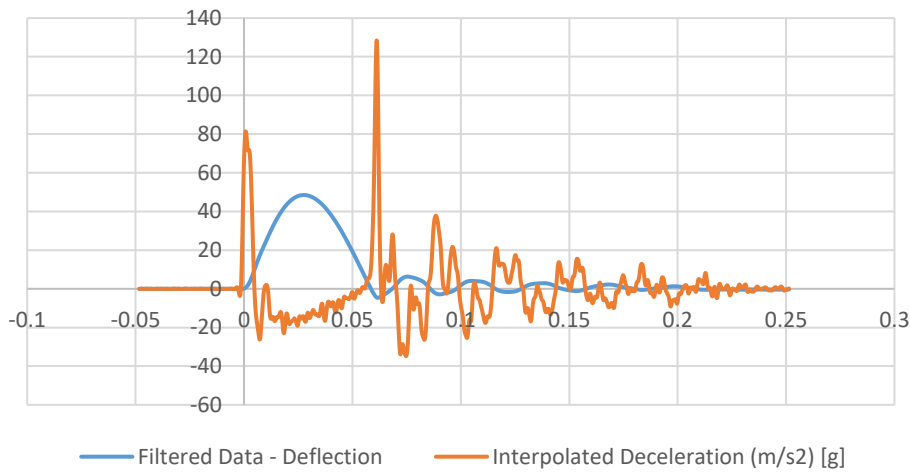
Eurosid-2 Rib test 3 m/s (2)



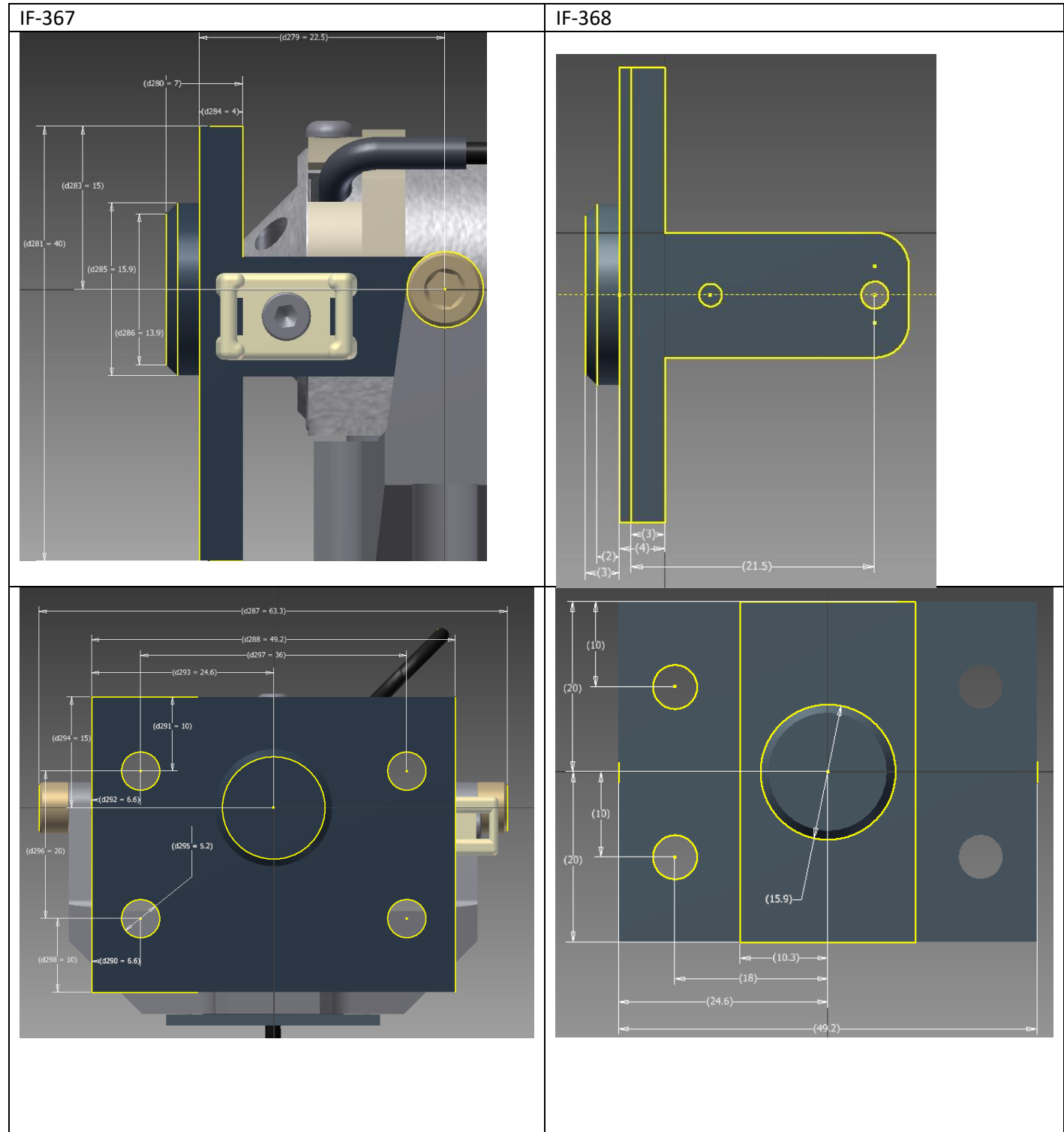
Eurosid-2 Rib test 4 m/s (1)



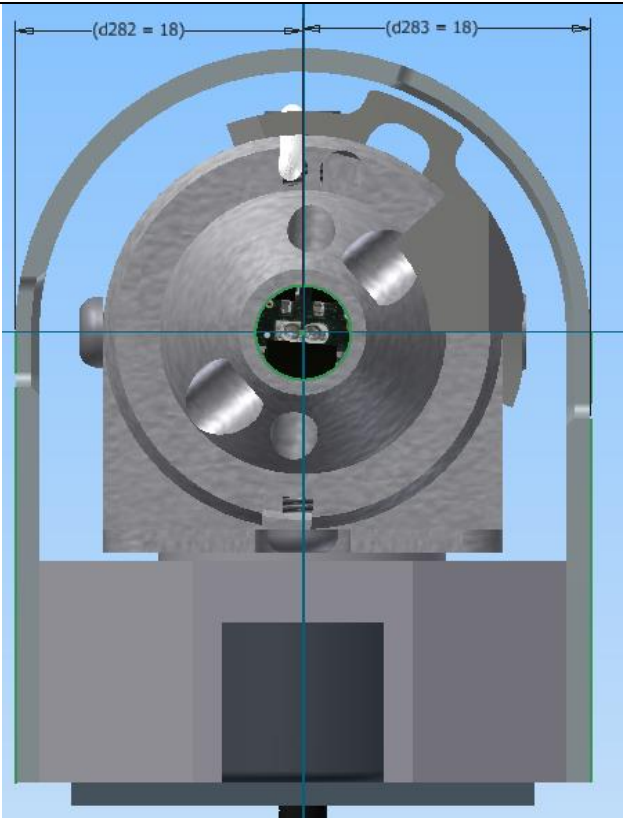
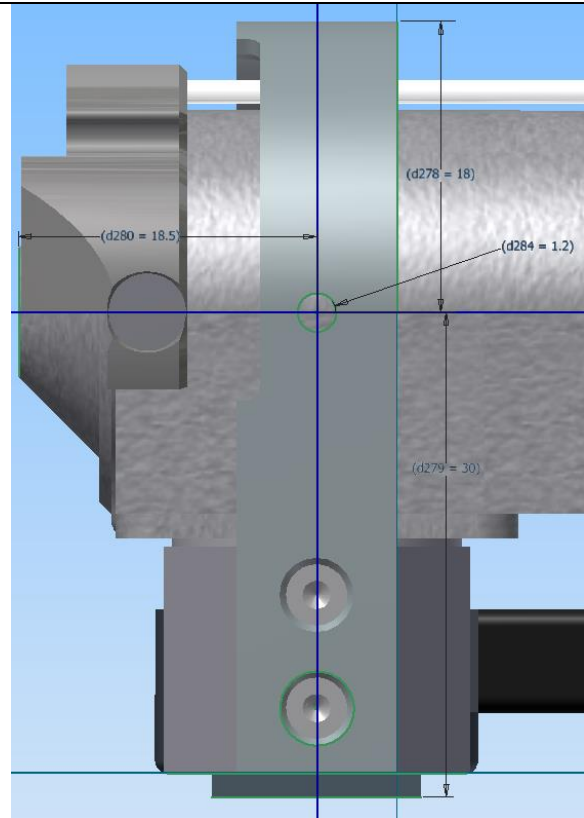
Eurosid-2 Rib test 4 m/s (2)



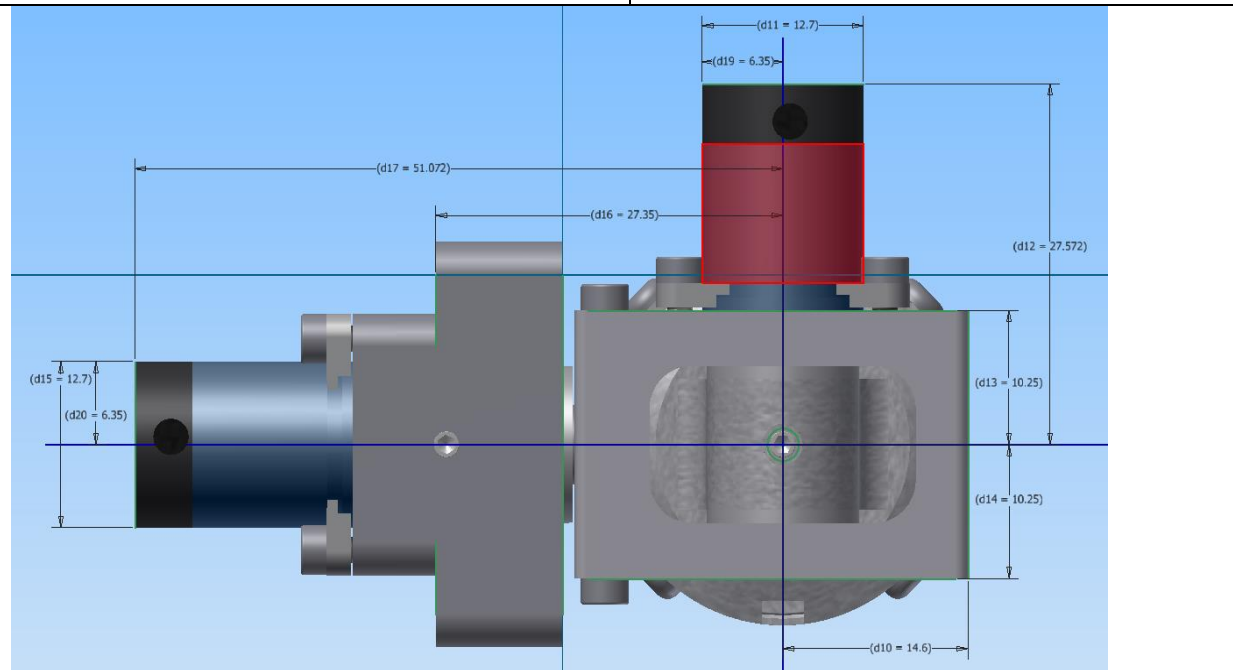
Appendix IV: Mounting dimensions

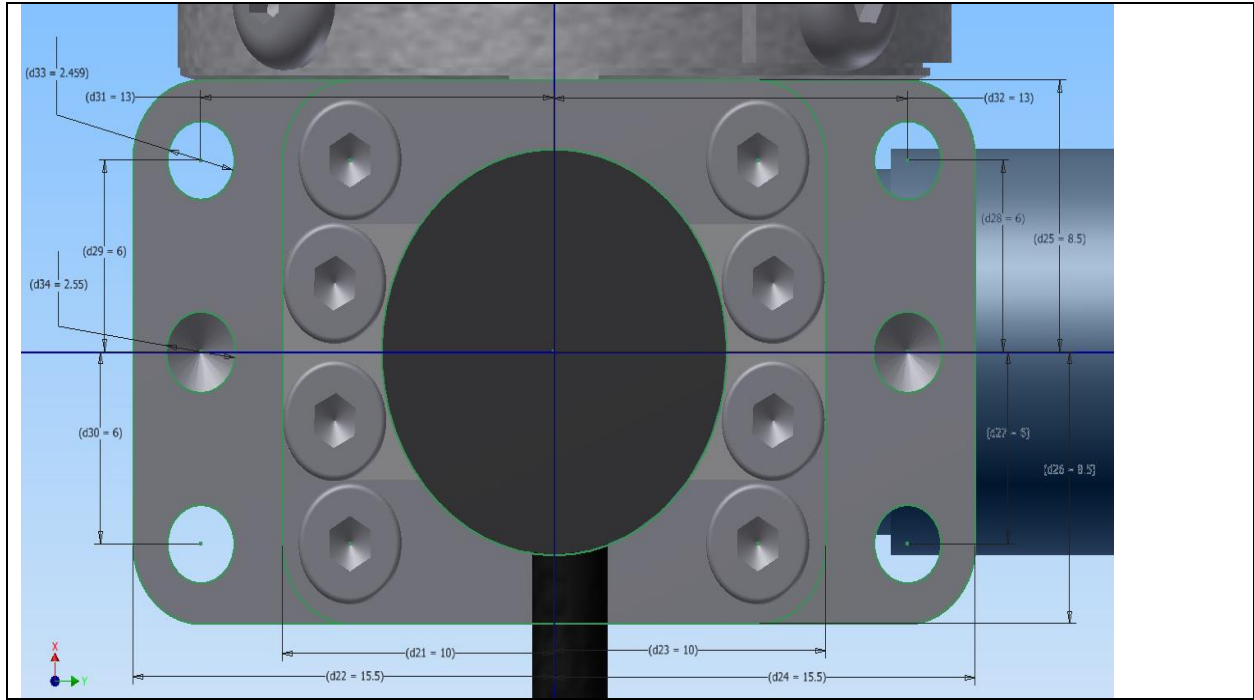


Q10

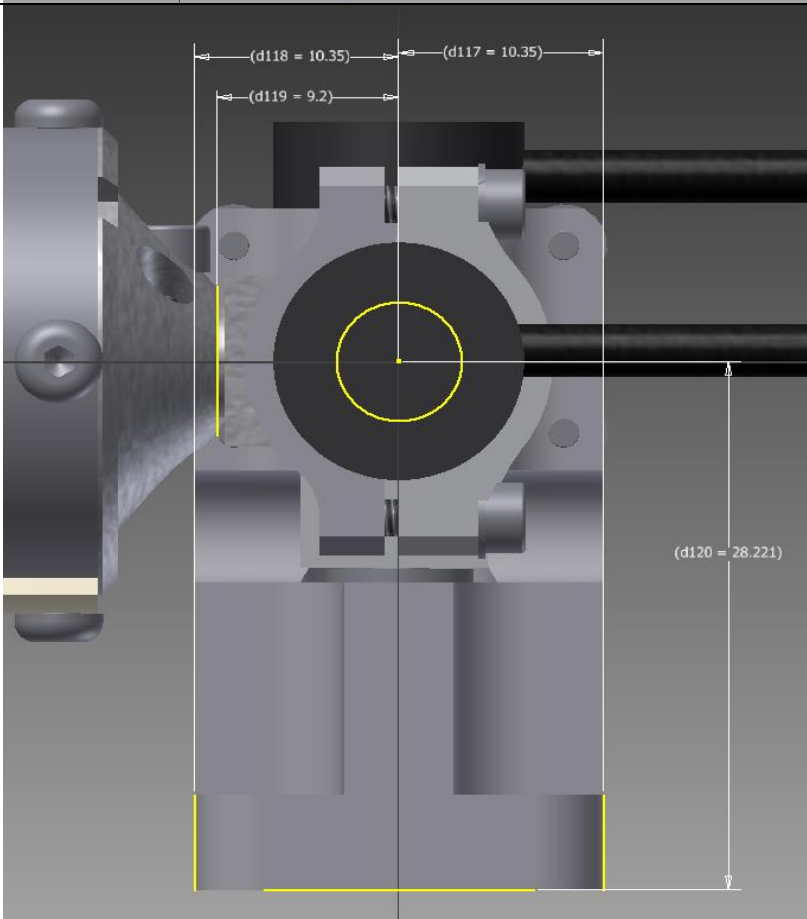
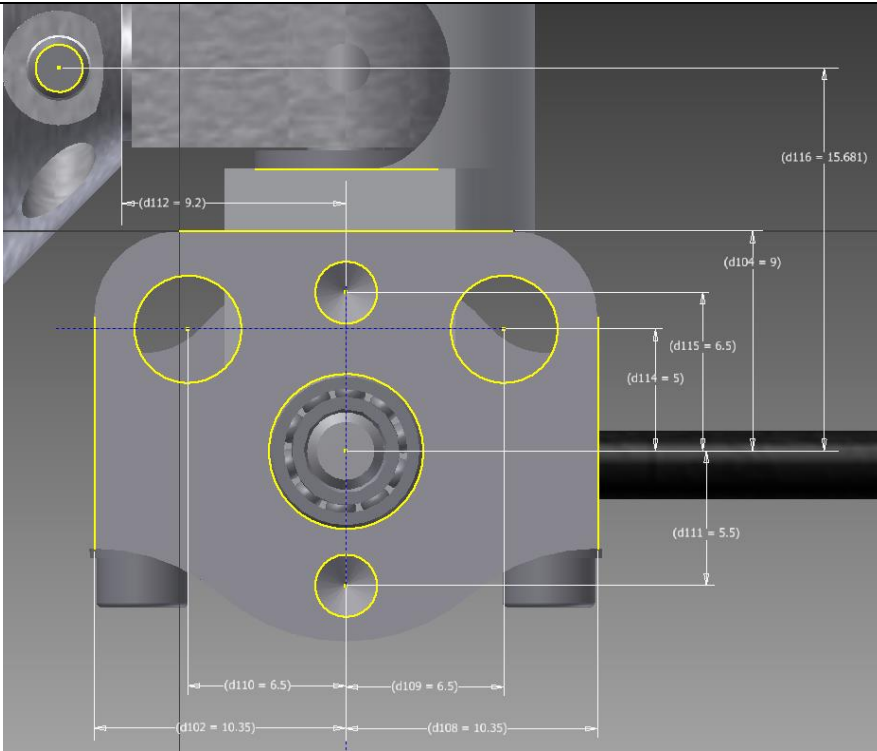


472-4730-1

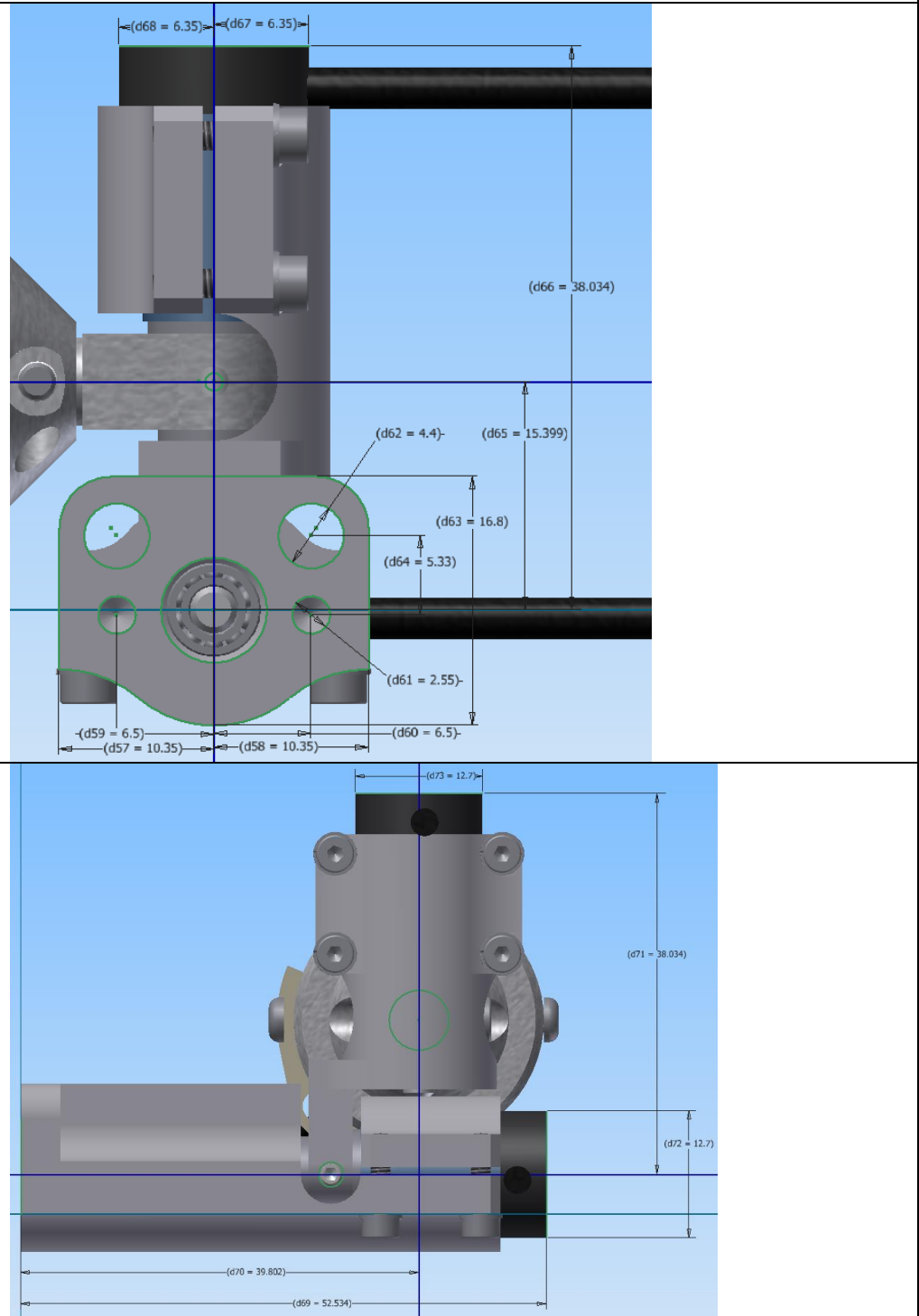




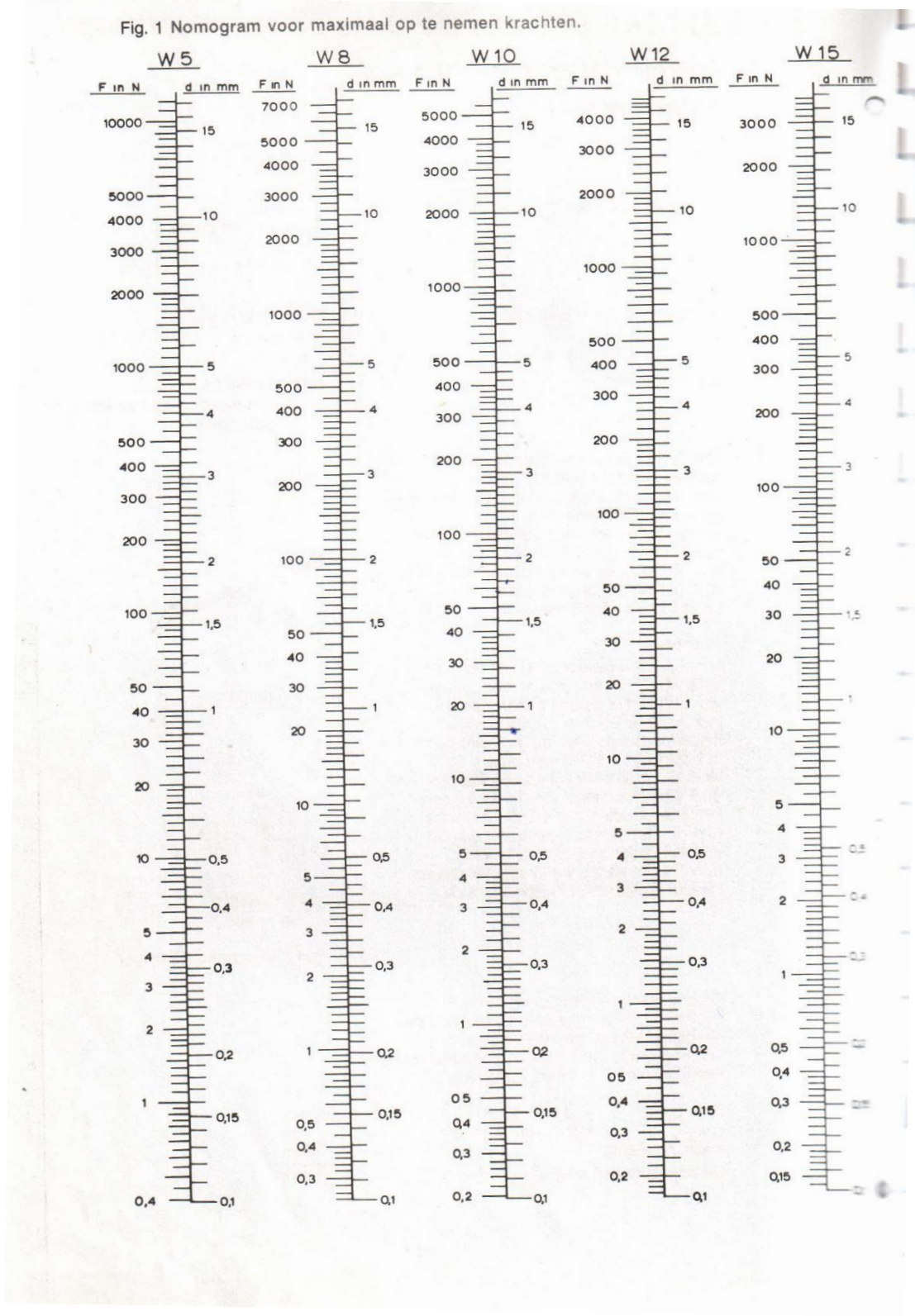
472-3550



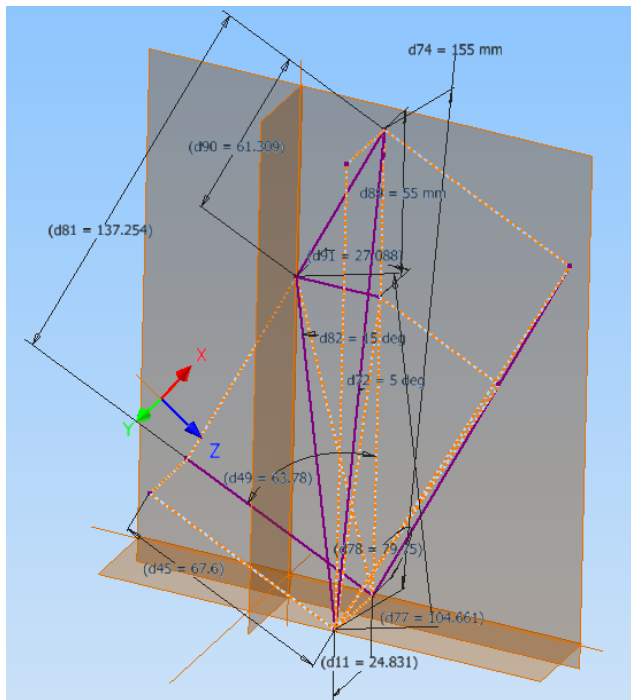
472-3570



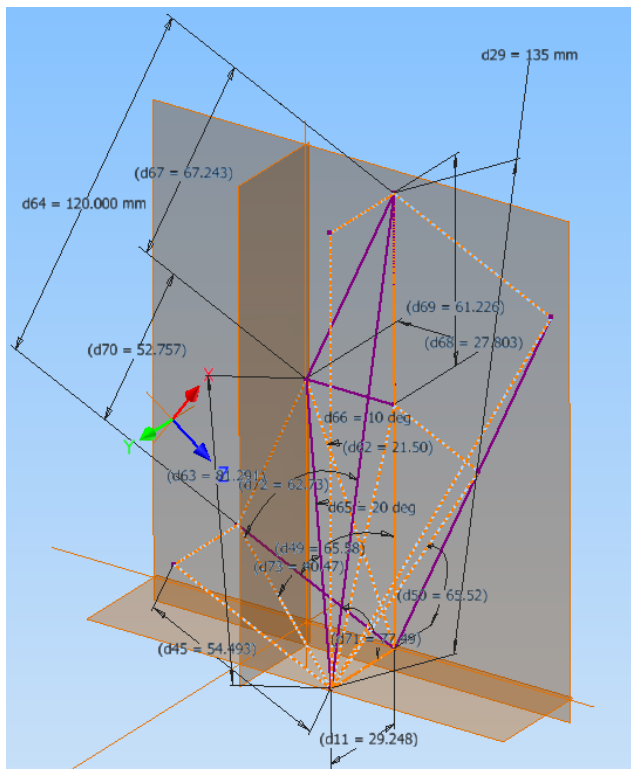
Appendix V: Excerpt from a manual from Atlas Coevoerden



Appendix V: Displacement tools

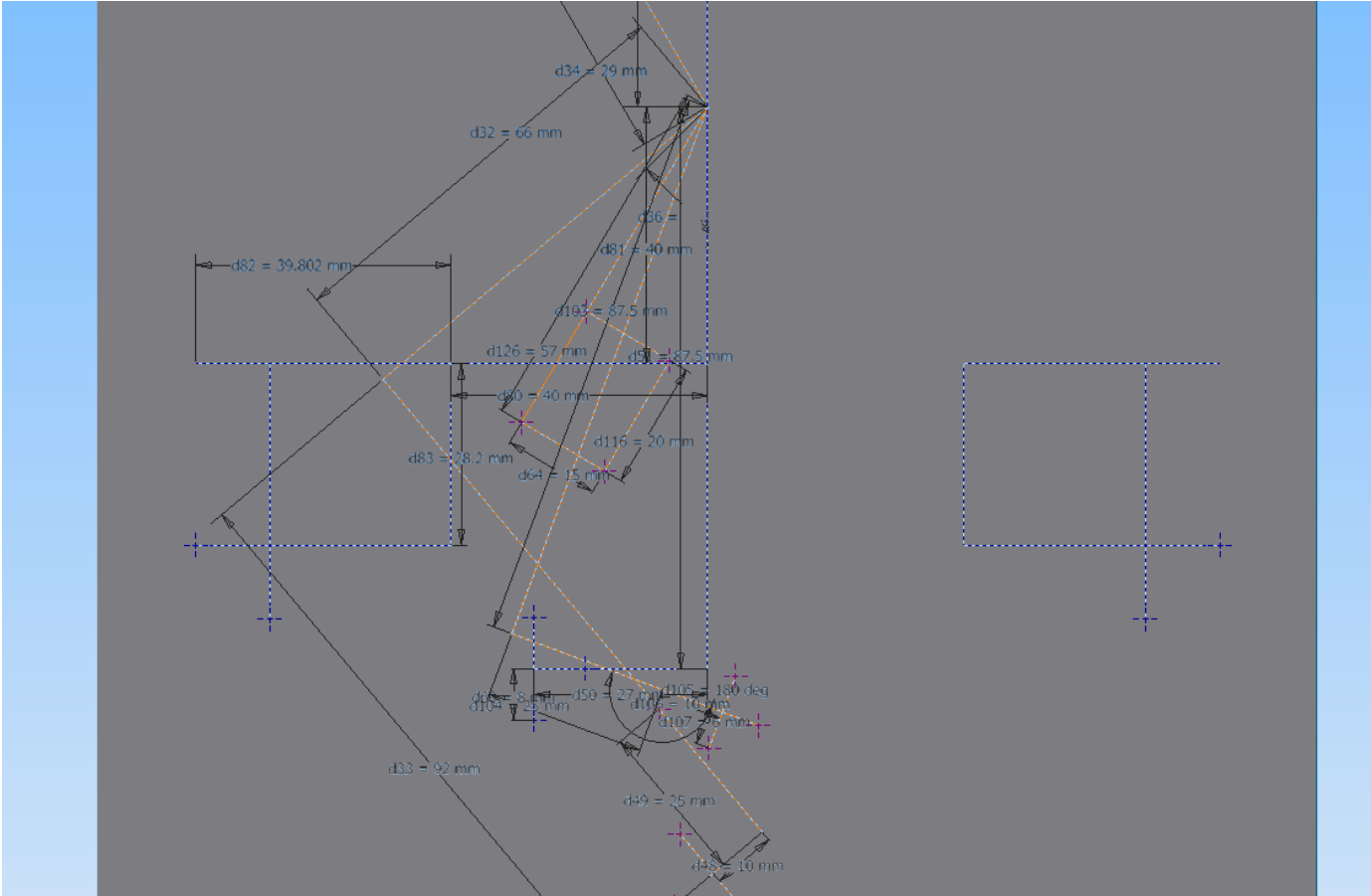


Coordinates for the a Male Thorax IR-TRACC



Coordinates for a Female Thorax IR-TRACC

Appendix VI: IR-TRACC Origin locations



Appendix VII: Competentie-niveaus

1. BoE domeincompetentie Analyseren (minimaal niveau eind major W: 3) (toelichting: deze omschrijving komt uit de Bachelor of Engineering (BoE))

Het analyseren van een engineeringvraagstuk omvat de identificatie van het probleem of klantbehoefte, de afweging van mogelijke ontwerpstrategieën / oplossingsrichtingen en het eenduidig in kaart brengen van de eisen / doelstellingen / randvoorwaarden. Hierbij wordt een scala aan methoden gebruikt, waaronder wiskundige analyses, computermodellen, simulaties en experimenten. Randvoorwaarden op het gebied van o.a. (bedrijfs) economie & commercie, mens & maatschappij, gezondheid, veiligheid, milieu & duurzaamheid worden hierbij meegenomen.

Competentie Werktuigbouwkunde: Analyseren

Competentie-niveaus			
Toelichting op deze tabel	<i>Deze competentieniveaus zijn vastgesteld in de Bachelor of Engineering.</i>		
	Competentie-niveau 1	Competentie-niveau 2	Competentie-niveau 3
Competentie-omschrijving	Analyseren van simpele werktuigbouwkundige functies	Analyseren van lastige WB functies	Analyseren van complexe werktuigbouwkundige functies
Niveau-omschrijving	<p>Aard van de taak: eenvoudig, gestructureerd, past bekende methoden direct toe volgens vaststaande normen</p> <p>Aard van de context: bekend; eenvoudig, monodisciplinair</p> <p>Mate van zelfstandigheid: sturende begeleiding</p>	<p>Aard van de taak: complex, gestructureerd, past bekende methoden aan wisselende situaties aan</p> <p>Aard van de context: bekend; complex, monodisciplinair, in de praktijk onder begeleiding</p> <p>Mate van zelfstandigheid: Begeleiding indien nodig</p>	<p>Aard van de taak: complex, ongestructureerd, verbetert methoden en past normen aan de situaties aan</p> <p>Aard van de context: onbekend; complex, multidisciplinair in de praktijk</p> <p>Mate van zelfstandigheid: zelfstandig</p>

Eisen m.b.t. de leertaken (BoE: gedragskenmerken)			
Toelichting op deze tabel	<i>Omdat de domeincompetentie hierboven zo breed geformuleerd is, is deze hieronder opgesplitst in meerdere deelcompetenties. De onderwijmakers kunnen aan de hand van deze tabel werktuigbouwkundige leertaken ontwerpen. Elke cel correspondeert met één leertaak.</i>		
Toelichting	Deelcompetentie-niveau 1	Deelcompetentie-niveau 2	Deelcompetentie-niveau 3
Deelcompetentie 1a	Begeleid en gestructureerd selecteren van relevante, eenvoudige en bekende aspecten met betrekking tot een simpele vraagstelling	Indien nodig onder begeleiding gestructureerd selecteren van relevante complexe en bekende aspecten met betrekking tot een lastige vraagstelling	Zelfstandig selecteren van relevante complexe en onbekende aspecten uit een ongestructureerde context met betrekking tot de complexe vraagstelling
Deelcompetentie 1b	Begeleid aangeven wat de mogelijke invloed is op eenvoudige en bekende bedrijfseconomische, maatschappelijke en vakgebied gerelateerde aspecten	Indien nodig onder begeleiding gestructureerd aangeven wat de mogelijke invloed is op complexe en bekende bedrijfseconomische, maatschappelijke en vakgebied gerelateerde aspecten	Zelfstandig aangeven wat de mogelijke invloed is op complexe en onbekende bedrijfseconomische, maatschappelijke en vakgebied gerelateerde aspecten in een multidisciplinaire context
Deelcompetentie 1c	Begeleid formuleren van een heldere probleemstelling, doelstelling en opdracht aan de hand van simpele wensen van de klant	Indien nodig onder begeleiding formuleren van een heldere probleemstelling, doelstelling en opdracht aan de hand van bekende, complexe en gestructureerde wensen van de klant	Zelfstandig formuleren van een heldere probleemstelling, doelstelling en opdracht aan de hand van onbekende, complexe en ongestructureerde wensen van de klant in een multidisciplinaire context
Deelcompetentie 1d	Begeleid opstellen van een eenvoudig programma van (bekende technische & niet-technische) eisen voor een bekend probleem en dit vast kunnen leggen	Indien nodig onder begeleiding opstellen van programma van (bekende en complexe technische & niet-technische) eisen en dit vast kunnen leggen	Zelfstandig opstellen van een programma van (onbekende en complexe technische & niet-technische) eisen in een multidisciplinaire context en dit vast kunnen leggen
Deelcompetentie 1e	Begeleid modelleren van een bestaand eenvoudig product, proces of dienst	Indien nodig onder begeleiding modelleren van een bestaand bekend(e) en complex(e) product, proces of dienst	Zelfstandig modelleren van een bestaand onbekend(e) en complex(e) product, proces of dienst in een multidisciplinaire context

2. BoE domeincompetentie Ontwerpen (minimaal niveau eind major W: 3)

Het realiseren van een engineeringontwerp en hierbij kunnen samenwerken met engineers en niet-engineers. Het te realiseren ontwerp kan voor een apparaat, een proces of een methode zijn en kan meer omvatten dan alleen het technisch ontwerp, waarbij de engineer een gevoel heeft voor de impact van zijn ontwerp op de maatschappelijke omgeving, gezondheid, veiligheid, milieu, duurzaamheid (bijv. cradle-to-cradle) en commerciële afwegingen. De engineer maakt bij het opstellen van zijn ontwerp gebruik van zijn kennis van ontwerpmethodieken en weet deze toe te passen. Het te realiseren ontwerp is gebaseerd op het programma van eisen en vormt een volledige en correcte implementatie van alle opgestelde eisen.

Competentie Werktuigbouwkunde: Ontwerpen

	Competentie-niveau 1	Competentie-niveau 2	Competentie-niveau 3
Competentie-omschrijving	Ontwerpen van simpele werktuigbouwkundige functies	Ontwerpen van lastige WB functies	Ontwerpen van complexe werktuigbouwkundige functies
Niveau-omschrijving	<p>I Aard van de taak: eenvoudig, gestructureerd, past bekende methoden direct toe volgens vaststaande normen</p> <p>Aard van de context: bekend; eenvoudig, monodisciplinair</p> <p>Mate van zelfstandigheid: sturende begeleiding</p>	<p>II Aard van de taak: complex, gestructureerd, past bekende methoden aan wisselende situaties aan</p> <p>Aard van de context: bekend; complex, monodisciplinair, in de praktijk onder begeleiding</p> <p>Mate van zelfstandigheid: Begeleiding indien nodig</p>	<p>III Aard van de taak: complex, ongestructureerd, verbetert methoden en past normen aan de situaties aan</p> <p>Aard van de context: onbekend; complex, multidisciplinair in de praktijk</p> <p>Mate van zelfstandigheid: zelfstandig</p>

	Deelcompetentie-niveau 1	Deelcompetentie-niveau 2	Deelcompetentie-niveau 3
2a	Begeleid in staat zijn om vanuit de opgestelde eisen een eenvoudige concept-oplossing (architectuur) te bedenken en te kiezen	Indien nodig onder begeleiding in staat zijn om vanuit de opgestelde eisen een bekende en complexe concept-oplossing (architectuur) te bedenken en te kiezen	Zelfstandig in staat zijn om vanuit de opgestelde eisen een onbekende en complexe concept-oplossing (architectuur) te bedenken en te kiezen in een multidisciplinaire context
2b	Begeleid maken van gedetailleerde eenvoudige ontwerpen aan de hand van de gekozen eenvoudige concept-oplossing (architectuur)	Indien nodig onder begeleiding maken van gedetailleerde complexe ontwerpen aan de hand van de gekozen bekende en complexe concept-oplossing (architectuur)	Maken van gedetailleerde complexe ontwerpen aan de hand van de gekozen onbekende en complexe en concept-oplossing (architectuur) in een multidisciplinaire context
2c	Begeleid rekening kunnen houden met de bekende en eenvoudige maakbaarheid en testbaarheid van het ontwerp	Indien nodig onder begeleiding rekening kunnen houden met de bekende en complexe maakbaarheid en testbaarheid van het ontwerp	Zelfstandig rekening kunnen houden met de onbekende en complexe maakbaarheid en testbaarheid van het ontwerp in een multidisciplinaire context
2d	Het begeleid verifiëren van het eenvoudige ontwerp aan de hand van het eenvoudige programma van eisen	Het indien nodig onder begeleiding verifiëren van het complex ontwerp aan de hand van het complexe programma van eisen	Het zelfstandig verifiëren van het complexe ontwerp aan de hand van het complexe programma van eisen in multidisciplinaire context
2e	Begeleid selecteren van de juiste eenvoudige ontwerp-hulpmiddelen	Indien nodig onder begeleiding selecteren van de juiste bekende en complexe ontwerp-hulpmiddelen	Zelfstandig selecteren van de juiste onbekende en complexe ontwerp-hulpmiddelen in een multidisciplinaire context
2f	Begeleid opstellen van de documentatie ten behoeve van het eenvoudige product, de eenvoudige dienst of het eenvoudige proces	Indien nodig onder begeleiding opstellen van de documentatie ten behoeve van het complexe product, de complexe dienst of het complexe proces	Zelfstandig opstellen van de documentatie ten behoeve van het complexe product, de complexe dienst of het complexe proces in een onbekende of multidisciplinaire context

8.BoE domeincompetentie: Professionaliseren (minimaal niveau eind major W: 2, afstuderen: 3)

Het zich eigen maken en bijhouden van vaardigheden die benodigd zijn om de engineering competenties effectief uit te kunnen voeren. Deze vaardigheden kunnen ook in breder verband van toepassing zijn. Dit omvat onder meer het hebben van een internationale oriëntatie en het kunnen plaatsen van de nieuwste ontwikkelingen, bijvoorbeeld in relatie tot maatschappelijke normen, waarden en ethische dilemma's.

Competentie Werktuigbouwkunde: Professionaliseren

	Competentie-niveau 1	Competentie-niveau 2	Competentie-niveau 3
Competentie-omschrijving	Ontwikkelen van simpele vaardigheden nodig in het werktuigbouwkundige werkveld	Ontwikkelen van lastige vaardigheden nodig in het werktuigbouwkundige werkveld	Ontwikkelen van complexe vaardigheden nodig in het werktuigbouwkundige werkveld
Niveau-omschrijving	<p>I Aard van de taak: eenvoudig, gestructureerd, past bekende methoden direct toe volgens vaststaande normen</p> <p>Aard van de context: bekend; eenvoudig, monodisciplinair</p> <p>Mate van zelfstandigheid: sturende begeleiding</p>	<p>II Aard van de taak: complex, gestructureerd, past bekende methoden aan wisselende situaties aan</p> <p>Aard van de context: bekend; complex, monodisciplinair, in de praktijk onder begeleiding</p> <p>Mate van zelfstandigheid: Begeleiding indien nodig</p>	<p>III Aard van de taak: complex, ongestructureerd, verbetert methoden en past normen aan de situaties aan</p> <p>Aard van de context: onbekend; complex, multidisciplinair in de praktijk</p> <p>Mate van zelfstandigheid: zelfstandig</p>

	Deelcompetentie-niveau 1	Deelcompetentie-niveau 2	Deelcompetentie-niveau 3
8a	Begeleid een eenvoudig leerdoel en leerstrategie bepalen en uitvoeren en het resultaat terugkoppelen naar het leerdoel	Indien nodig onder begeleiding een bekend en complex leerdoel en leerstrategie bepalen en uitvoeren en het resultaat terugkoppelen naar het leerdoel	Op zelfstandige wijze een onbekend en complex leerdoel en leerstrategie bepalen en uitvoeren in een multidisciplinaire context en het resultaat terugkoppelen naar het leerdoel
8b	Zich begeleid flexibel opstellen in uiteenlopende eenvoudige beroepssituaties	Zich indien nodig onder begeleiding flexibel opstellen in uiteenlopende bekende en complexe beroepssituaties	Zich zelfstandig flexibel opstellen in uiteenlopende onbekende en complexe beroepssituaties in een multidisciplinaire context
8c	Bij eenvoudige beroepsmatige en ethische dilemma's begeleid een afweging maken en een besluit nemen, rekening houdend met geaccepteerde normen en waarden	Bij bekende en complexe beroepsmatige en ethische dilemma's indien nodig onder begeleiding een afweging maken en een besluit nemen, rekening houdend met geaccepteerde normen en waarden	Bij onbekende en complexe beroepsmatige en ethische dilemma's een afweging maken en een besluit nemen, rekening houdend met geaccepteerde normen en waarden in een multidisciplinaire context
8d	Op constructieve wijze begeleid eenvoudige feedback kunnen geven en ontvangen, zowel op gedrag als inhoud	Op constructieve wijze indien nodig onder begeleiding bekende en complexe feedback kunnen geven en ontvangen, zowel op gedrag als inhoud	Op constructieve wijze zelfstandig onbekende en complexe feedback kunnen geven en ontvangen, zowel op gedrag als inhoud in een multidisciplinaire context
8e	Begeleid kunnen reflecteren op eigen eenvoudig(e) handelen, denken en resultaten	Begeleid kunnen reflecteren op eigen bekend(e) en complexe handelen, denken en resultaten	Zelfstandig kunnen reflecteren op eigen onbekende en complexe handelen, denken en resultaten in een multidisciplinaire context
8f	Begeleid kunnen gebruiken van diverse eenvoudige communicatievormen en -middelen om effectief te kunnen communiceren in het Nederlands en Engels.	Indien nodig onder begeleiding kunnen gebruiken van diverse bekende en complexe communicatievormen en -middelen om effectief te kunnen communiceren in het Nederlands en Engels.	Zelfstandig kunnen gebruiken van diverse onbekende en complexe communicatievormen en -middelen om effectief te kunnen communiceren in het Nederlands en Engels in een multidisciplinaire context

